VARIABILITY IN HYDRAULIC CONDUCTIVITY AND SOIL SALINITY IN A

FLOOD-IRRIGATED FIELD:

THE LAS NUTRIAS GROUNDWATER PROJECT

by

JEFFREY S. CHAVES

Submitted in Partial Fulfillment of

the Requirements for the Degree of

Master of Science in Hydrology

New Mexico Institute of Mining and Technology

Socorro, NM

May, 1995

ABSTRACT

The Las Nutrias Groundwater Project is designed to quantify the effects of typical agricultural management practices on shallow groundwater in the middle Rio Grande Valley in New Mexico. The field site is a commercial farm located on the floodplain of the Rio Grande near Las Nutrias, New Mexico, characterized by sandy clay loam surface soils with extreme variations in particle size. The farm is equipped with a tile drainage system which has been modified for the purpose of monitoring discharge water. The project goals are to develop a computer model of nutrient and pesticide transport to groundwater and to test the model with data collected at the field site. The current study focuses on characterizing the variability of field-measured hydraulic conductivity and soil salinity utilizing statistical and geostatistical methods.

To achieve this objective, during the summer of 1994, an extensive field infiltration experiment was conducted on a 15-acre portion of a commercial farm. I used a ponded infiltrometer which yielded estimates of saturated hydraulic conductivity at 104 locations and a tension infiltrometer which yielded estimates of unsaturated hydraulic conductivity at preset supply tensions of 3-, 6-, and 15 cm at the same locations. These estimates were later compared to estimates based on water retention data collected in the laboratory from a hanging water column experiment performed on nine undisturbed soil samples collected from the field. From January to May of that same year, monthly salinity surveys were conducted using an electromagnetic induction sensor. Induction measurements are directly related to soil salinity. The measurements were made to depths of 0.75- and 1.5 m depth. Differences between values of the measurements at these two depths were analyzed for their potential as a method of noninvasive model validation.

Significant temporal variation was detected in the hydraulic conductivity measured at saturation and at 3 cm of tension. No significant temporal variation was detected among the measurements at 6- and 15 cm tension. Variogram analyses suggest that the saturated hydraulic conductivity is spatially dependent up to a distance of approximately 12 m, while unsaturated measurements show no spatial dependence. Estimates of unsaturated hydraulic conductivity based on the retention data collected in the laboratory are consistently and significantly higher than the field estimates. The electromagnetic induction measurements displayed a direct relationship to soil salinity based on visual crop observations. Differences between measurements at distinct depths show some promise as a potential method of noninvasive model validation, though more data must be collected and analyzed to verify this. Soil salinity as measured with the electromagnetic induction sensor exhibits spatial dependence up to approximately 100 m.

TABLE OF CONTENTS

LIST OF FIGURES

LIST OF TABLES

LIST OF TABLES (continued)

ACKNOWLEDGEMENTS

I am very grateful to my advisor, Dr. Robert S. Bowman, and committee members Dr. Jan Hendrickx and Dr. Mark Ankeny for their guidance, encouragement and the extra efforts which they made on my behalf.

I would also like to thank my fellow graduate students involved with the project, Tracy Roth and Robert Reedy, for their dedication and hard work as well as Baukje Sijstma for her work during the early stages of the project. All of those fast-food breakfasts on the road to the field site, the hours spent up to our chins in the cold water of the manholes, and the hot afternoons battling the mosquitoes will never be forgotten. Much thanks is due to the undergraduate students who worked on the project, Chris Rossacker and Will Holoman for their long hours of hard work in the field and in the laboratory compiling data for the project. I would also like to thank special friends Colin, Blake, Rocky, Monty, Lance, and Dan whose companionship and antics made the difficult times bearable and especially Bob Mercogliano, whose memory will never fade from those of us here at Tech who loved him most.

1 INTRODUCTION

Sustained agricultural productivity in the United States has long contributed to the nation's economic stability. For the past fifty years, the use of pesticides and fertilizers has played a major roll in this success. Agricultural chemicals and their byproducts often appear in groundwater or are transported via subsurface drains to ditches and streams, threatening these resources and posing potential health risks. Despite the growing concern over contamination, few studies have been conducted to determine the impacts that agriculture may impose on groundwater in New Mexico. Where studies have been conducted on the transport of agricultural chemicals, conditions are often of a tightly controlled research nature rather than on operating commercial farms under typical management practices. The Las Nutrias Groundwater Project is designed to quantify the effects of typical agricultural management practices on shallow groundwater quality in the middle Rio Grande Valley, including the application of pesticides and fertilizers.

To accomplish this goal, the project addresses two specific objectives. First, a computer model describing the various potential flow paths from the soil surface to subsurface drains in two-dimensional, variably-saturated soil profiles will be coupled to a solute transport model which describes the interactions of dissolved chemicals with the soil and with growing plants. The model will be able to account for water uptake by roots, and will employ scaling procedures for the simplification of effects of spatial variability in the unsaturated hydraulic properties as well as the

temperature dependence of such properties. Solute transport will be modeled with

a very general formulation of the convection-dispersion equation in order to include

a variety of interactions among liquid, solid, and gaseous phases within a soil as

well as zero-order production and first-order degradation processes. Finally, the

model will also incorporate provisions which account for heat transport (Proposal

Funded by USDA - CSRS Special Water Quality Grant, "Development and Testing

of a 2-Dimensional Model of Nutrient and Pesticide Transport to Groundwater").

Second, information necessary to validate the model will be collected and analyzed

over at least one complete growing season.

The project field site is located on a sixty-acre commercial farm, situated on

an alluvial floodplain of the Rio Grande, near Las Nutrias, New Mexico (Figure 1).

The climate is arid to semiarid and has a wide range of temperature and rainfall.

Socorro County, where the site is located, receives an annual average rainfall of

210 mm at 1380 meters elevation to 370 mm at 2010 meters elevation (Roybal,

1991). The parent material for the entire valley is alluvium. The field site consists of

sandy clay loam surface soils with extreme variations in particle size, which is

typical for soils along the Rio Grande Valley (Soil survey by Clarence Montoya and

provided by the Socorro office of the Soil Conservation Service, 1992). Specific site

rainfall data was recorded for 1994 and is tabulated in appendix (8.3.4). The farm is

equipped with a subsurface tile-drainage system which has been modified to

measure the rates and quality of irrigation return flow beneath the field. Thus the

project provides data on water quality impacts of nonpoint source pollution relevant

to farming along the entire Rio Grande Valley (Bowman et al., 1992).

Figure 1. General location of Las Nutrias field site in New Mexico.
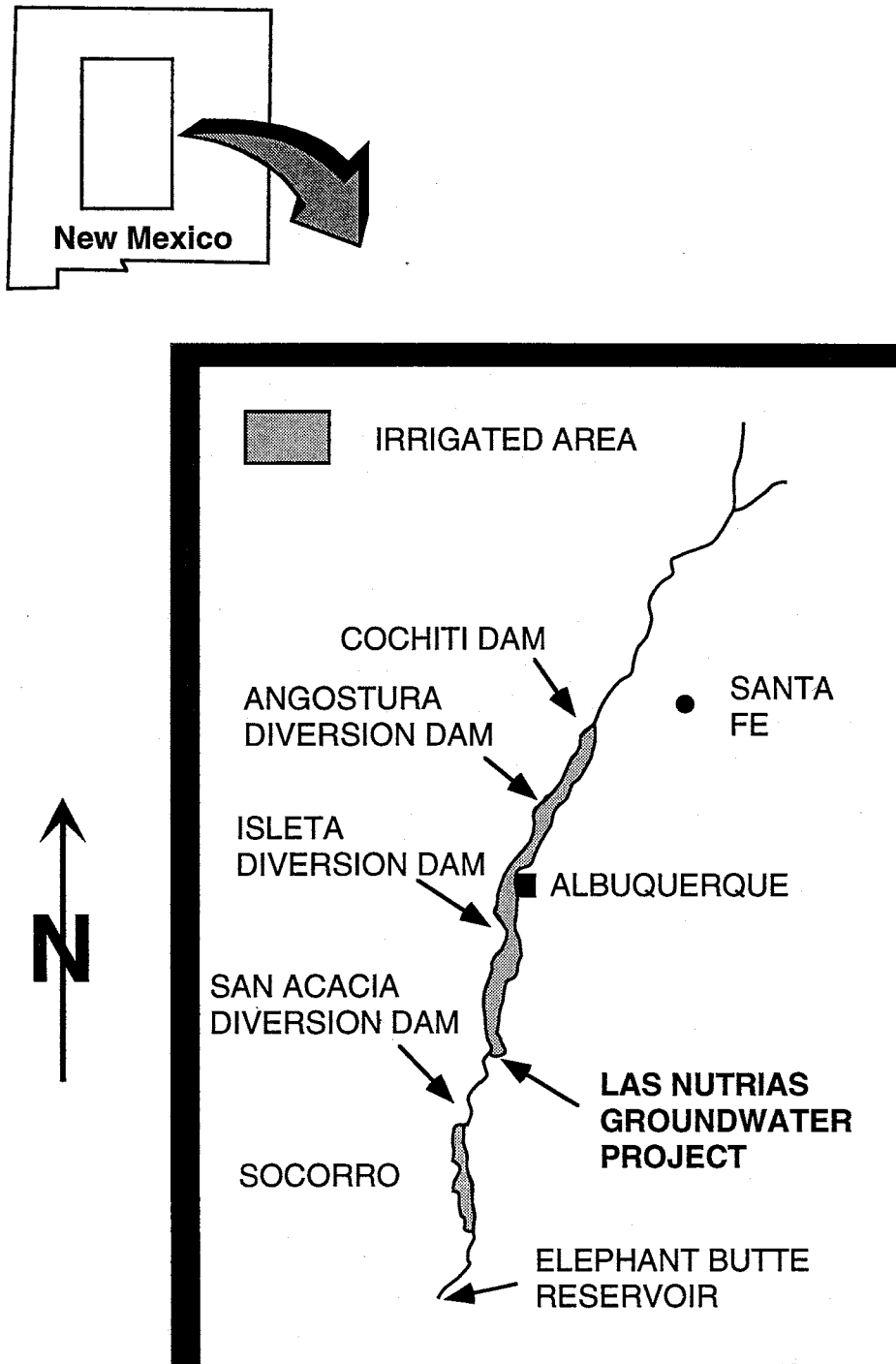
The Las Nutrias field site is divided into three benches - east, west, and center - separated by two berms which trend approximately due north. Alfalfa is the current crop on all three benches, though various crops (corn and others) have been grown in the past. The farm is regularly flood-irrigated from the beginning of March through the end of October. The subsurface tile drainage system consists of four lateral drain lines of perforated plastic pipe which connect to a main line leading to a surface drain (Figure 2). The drain lines are four inches in diameter under the east bench and five inches under the center bench. Under the west bench, which is twice the length of the other two benches, the drain line is five inches under the upstream (eastern) half of the bench and six inches under the downstream (western) half (Figure 2). The main drain line connecting the tile drains (located at the extreme western edge of the field site) is eight inches in diameter and connects to a ten inch diameter pipe which drains into a surface ditch located just west of the study area. The center bench portion of the drainage system has been modified by installing two manholes along a single drain line at the east and west ends of the bench (Figure 2). The drain line intercepted by the manholes is located just south of the middle of the bench. The manholes allow for regular sampling of water entering and leaving that section of drain line. In February and March of 1993, the Socorro office of the U.S. Bureau of Reclamation installed observation wells and piezometers along the perimeters of each of the benches at the field site (Figure 2). The installation was supervised by Baukje Sijtsma, a graduate student from Wageningen Agricultural University in the Netherlands. Sijtsma describes the well installation in detail in an unpublished report entitled "Two-Dimensional Numerical

FIGURE 2. Plan view of the Las Nutrias field site instrumentation

Las Nutrias
Groundwater Project
Socorro County, New Mexico

LEGEND
--- Dirt Road
--- Fence
— Concrete Lined Channel
— Berm
····· Buried Tile Drain Line
● Monitoring Well
○ Piezometer Nest
■ Manhole

West Bench

Center Bench

East Bench

Riverside Drain

5
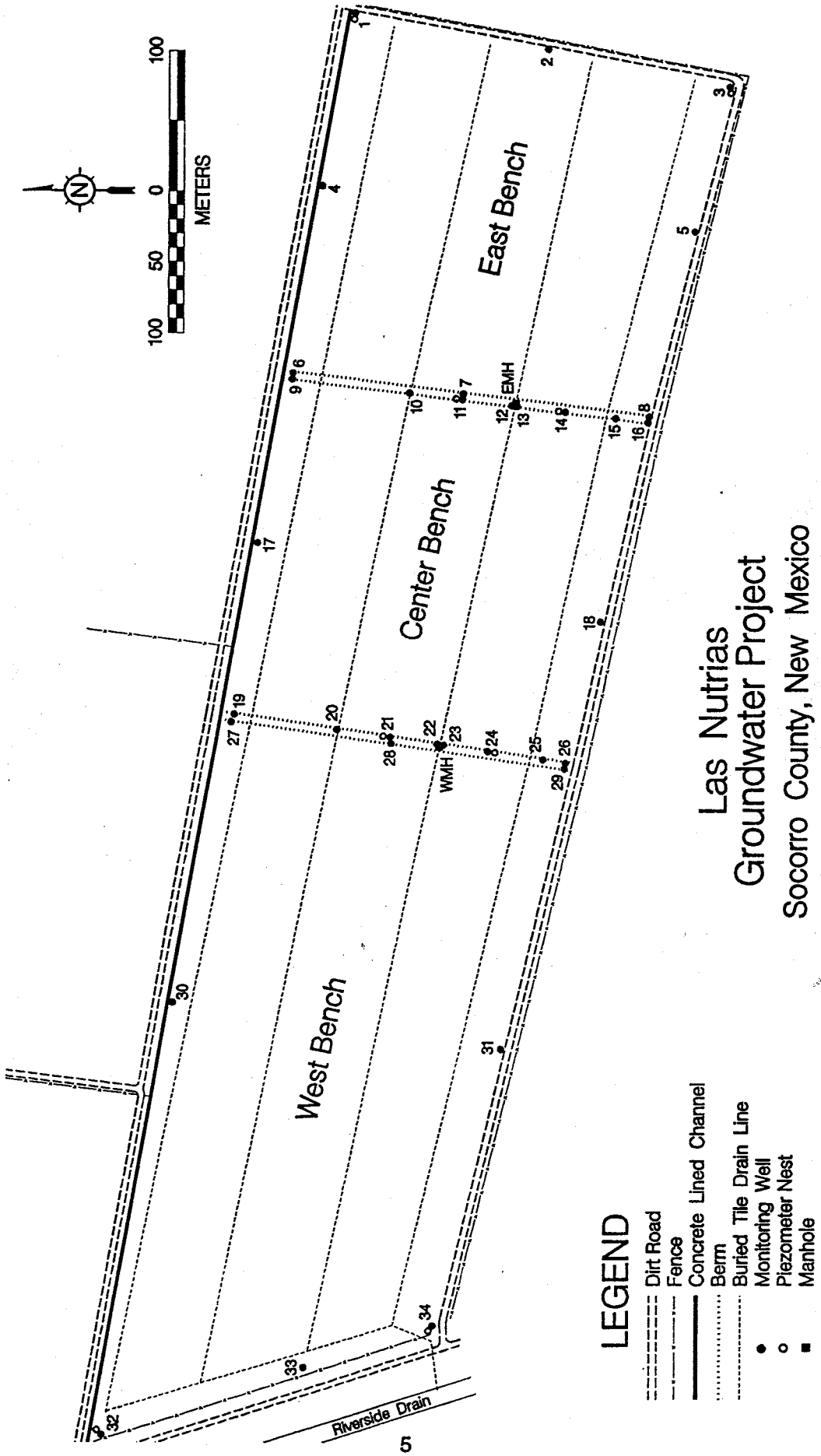
Modeling of a Tile-Drained Field - Field preparation and preliminary model runs".

The observation wells are two-inch inner diameter PVC pipe, perforated along the entire two-meter length of the pipe. The perforations are 1.3 cm diameter holes spaced 5 cm apart. To prevent sedimentation from building up in the bottom of the well, a nylon filter sock was wrapped around the entire screened interval of the well. The observation wells were installed by flushing a 3-inch diameter hole with a jetting-pump and inserting a steel casing. After installing the observation well, the casing was removed and the hole back-filled with sand. A one-to-one mixture of bentonite and soil from the new hole was tamped around the tube from approximately 25 cm below the ground surface and mounded above the ground surface to prevent surface water from short-circuiting into the wells. PVC caps were used to close the top of the wells. The observation wells are sampled regularly for nitrates and electrical conductivity and allow the monitoring of water table fluctuations due to seasonal variations and in response to irrigation and precipitation events. The piezometers are of one-inch inner diameter and are installed to nominal depths of three, five, and seven meters. The piezometers are screened along the lower 20 cm in the same fashion as the observation wells (i.e., 1.3 cm holes at 5 cm intervals). Sijtsma deemed that a bentonite seal was unnecessary for the piezometers due to the coarse sandy nature of the soil. The piezometers allow the piezometric water surface to be measured at specific points in the underlying aquifer, and provide information on vertical pressure gradients below the field as well as vertical gradients in nitrate concentrations. Installing the

wells and piezometers along the perimeter of each bench minimized the impacts of the study on the farmer's ability to produce his crop. Rain gages were located at each of the manholes and at the north central end of the center bench and were read as needed, immediately following individual rainfall events. The gages, purchased from Forestry Suppliers, Inc., Jackson, MS, consist of funnels leading into plastic cylinders with a previously calibrated scale attached for measuring rainfall to a tenth of a millimeter.

Accurate characterization and quantification of variability of hydraulic conductivity, K, are needed to make reasonable estimates of water and chemical recharge to groundwater from agricultural fields. Previous studies have shown that infiltration of water into soil is a strong function of soil macroporosity (Mohanty, et al., 1994). Factors which affect the development of macropores include root development and decomposition (Meek, 1989; Shirmohammadi and Skaggs, 1984; Barley, 1954; Warner and Young, 1991, p. 150 - 159), wetting and drying cycles (Akram and Kemper, 1979), freezing and thawing (Akram and Kemper, 1979; Carter, 1988), earthworm activity (Trojan and Linden, 1992), and tillage and wheel traffic by agricultural machinery (Wager and Denton, 1989; Ankeny et al., 1990). Mohanty et al., (1994) examined the effects of crop rows, interrows, and wheel traffic rows on the spatial variability of soil hydraulic properties.

At the Las Nutrias site, areas of high salinity concentrations have significantly affected the landowner's crop yield. Salinization of soils represents a growing threat to farmers throughout the Rio Grande Valley, where a shallow water table

hinders effective drainage. It was for the purpose of lowering the water table, improving drainage and thereby relieving the salinity problem that the landowner installed the tile drainage system in 1979. Despite this effort, the soil salinity problem persists.

Several investigators have used the EM38, an electromagnetic induction sensor developed by Geonics Limited of Ontario Canada (MacNeill, 1980a) to assess saline environments in New Mexico for various purposes (Hendrickx et al., 1994). In the current study, the EM38 was used to assess the spatial distribution of soil salinity and to check for a relationship between crop productivity and electromagnetic induction measurements. Vertical distributions of salinity are also analyzed as an indication of upward or downward movement of water in the vadose zone, indications which can be compared to computer model predictions based on data collected at the field site.

The specific objectives of the current study focus on the characterization of the variability of hydraulic conductivity and soil salinity measured in situ at the Las Nutrias site. The hydraulic conductivity study provides necessary input parameters for the model. The soil salinity information is also examined for its potential use as a method of noninvasive model validation. Several of the field measurements of unsaturated hydraulic conductivity are compared to calculations based on water retention data obtained from an outflow experiment in the laboratory on undisturbed soil core samples.

2. BACKGROUND

2.1 Tension and Ponded Infiltrometers

The tension infiltrometer (Figure 3) is a compact field instrument used for the in situ measurement of soil hydraulic properties. The design of the instrument evolved from the sorptivity tube designed by Clothier and White (1981) and can also be used to obtain estimates of sorptivity and capillary lengths (White and Perroux, 1987, 1989). In the current study it was used to determine the hydraulic conductivity at preselected tensions of ψ, 3-, 6-, and 15 cm. This particular device was chosen because of its ease of use in the field and for its ability to limit infiltrating flow to macropores of specified diameter which correspond to tensions predicted by the capillary-rise equation. The specified tensions were chosen because of their importance for root growth (Hackett, 1969, pp. 135-145; Russell, 1977) and preferential solute transport (Scotter, 1978).

The ponded infiltrometer (Figure 4) is a simple device, requiring no calibration, and is used to obtain estimates of saturated hydraulic conductivity (i.e., zero tension). Ankeny (1992) reviews the design, calibration, and operation of tension and ponded infiltrometers as well as the analysis of saturated and unsaturated infiltration data obtained from the use of these instruments. A thorough discussion of the historical use of the tension infiltrometer is given by Schmidt-Petersen (1991).

2.2 Geonics EM38

The EM38 ground conductivity meter is an electromagnetic induction sensor developed by Geonics Limited of Ontario, Canada. The lightweight, portable

Figure 3. Schematic diagram of a tension infiltrometer (Ankeny, 1992)

septum

top transducer

tygon tubing

pinch clamp

water level

air entry tube

3-holed rubber stopper

water reservoir

bubbling tube

set screw

bubbling tower

quick coupling

frame

bottom transducer

base

base valve

baseplate
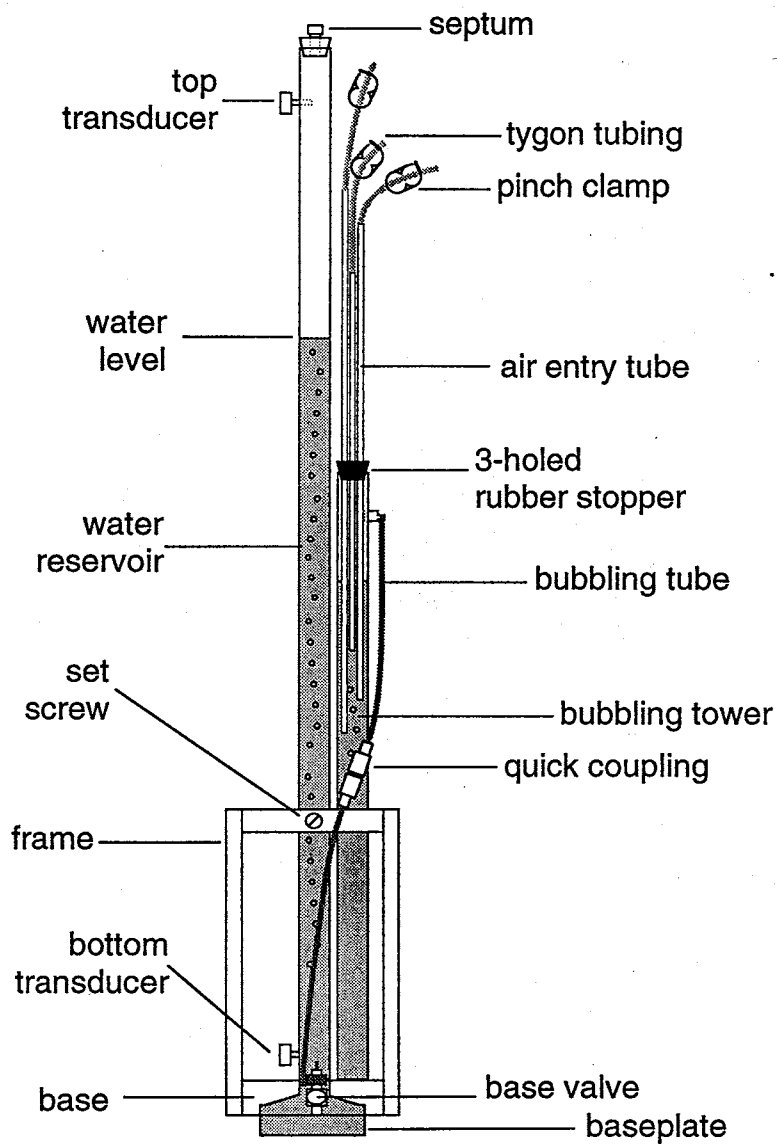
Figure 4. Schematic diagram of a ponded infiltrometer (Ankeny, 1992).
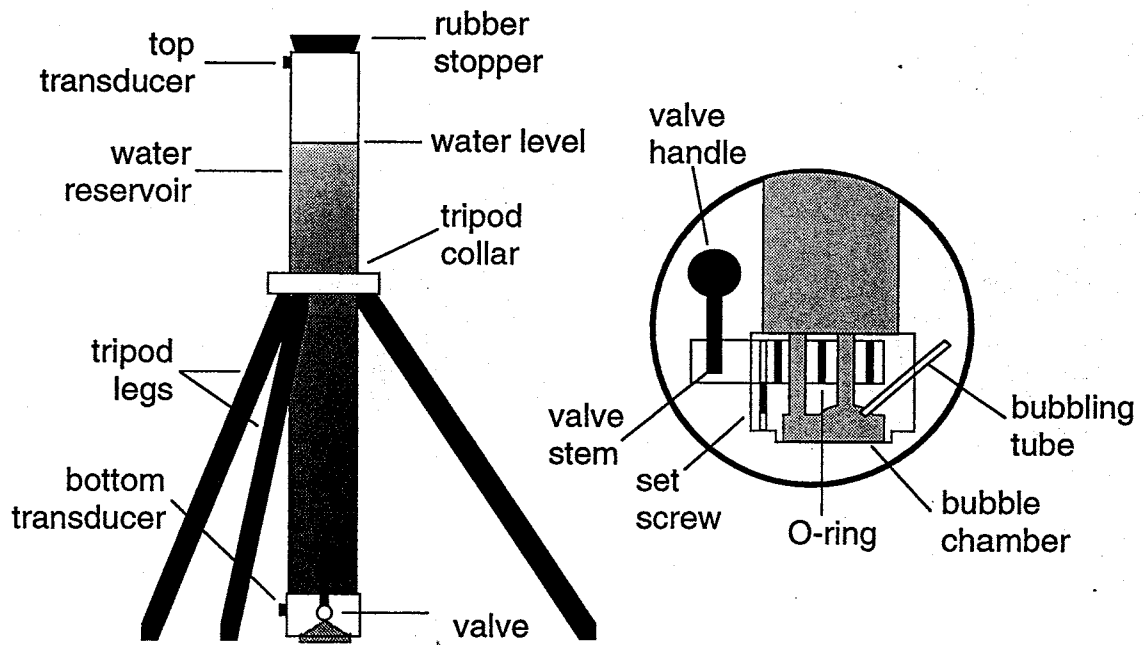
instrument measures the apparent electrical conductivity (EC_a) of a soil directly in the field and has been used to assess a variety of saline environments (Hendrickx et al., 1994). In agriculture, the electromagnetic induction method is widely used for mapping soil salinity for the purpose of crop maintenance. Hendrickx et al. (1992) used the EM38 to characterize the variability and statistical distribution of electromagnetic induction measurements on irrigated land near Faisalabad, Pakistan. Similar studies have also been executed in Canada (de Jong et al., 1979), Senegal (Boivin et al., 1988), Syria (Job et al., 1987), and the United States (Rhoades and Corwin, 1981). The EM38 instruction manual (Geonics, Limited, Ontario, Canada) gives a thorough review of the theory, calibration, and operation of the EM38.

2.3 Spatial Variability and Variogram Theory

The use of geostatistics for the characterization of the spatial variability of the properties of soils is not new. Stemming from mining studies of the spatial variability of ore grades (Journel and Huijbregts, 1978), geostatistics has been applied to various hydrologic studies (Nielsen et al., 1973; Caravallo et al., 1976; Smetten, 1987; Greenholtz et al., 1988) in addition to those listed in the previous section. In the current study, the majority of the statistical analyses and all of the variogram analyses were performed using the software package GEOPACK Version 1.0 (Yates and Yates, 1990).

The variogram satisfies the assumption called the "intrinsic hypothesis". Basically, the hypothesis states that the mean is constant in space and the variance is independent of location. The semivariance is defined as:

$$\gamma(h)= 0.5E[(z(x+h)-z(x))^2] \quad (1)$$

$2\gamma(h)$ is the mean squared difference between two points separated by a lag distance, h. $z(x)$ is the experimental data value at the point x, $z(x+h)$ the experimental data value at a point h distance from x, and h is the lag or separation distance. The variogram estimator, or semivariance, is calculated by the following equation:

$$\gamma'(h)= \sum_{i=1}^{N(h)} \{[(z(x_i+h)-z(x_i))^2]/2N(h)\} \quad (2)$$

where $\gamma'(h)$ is the semivariance, and N(h) is the number of data pairs separated by the lag distance, h. The semivariance will increase as the correlation between observed values decreases from the point of interest. At infinite lag, the semivariance can increase indefinitely or stabilize to a value known as the sill. The sill is the value approximately equal to the variance of the field data plus the nugget. The nugget effect (a term which comes from the mining origins of geostatistics) is a discontinuity at the origin, and is often caused by sampling, handling and data analysis errors. The range is the distance at which the sill is reached. It indicates the extent of spatial dependence of the data. Beyond the range, there is no correlation.

3. EXPERIMENTAL METHODS

3.1 Infiltrometers

Figure 5 illustrates the locations of the transects over which the infiltrometer measurements were taken. The grid center was at the intersection of the north-

Figure 5. Las Nutrias center bench soils series map.

005° (Azimuth)

320°   050°

095°
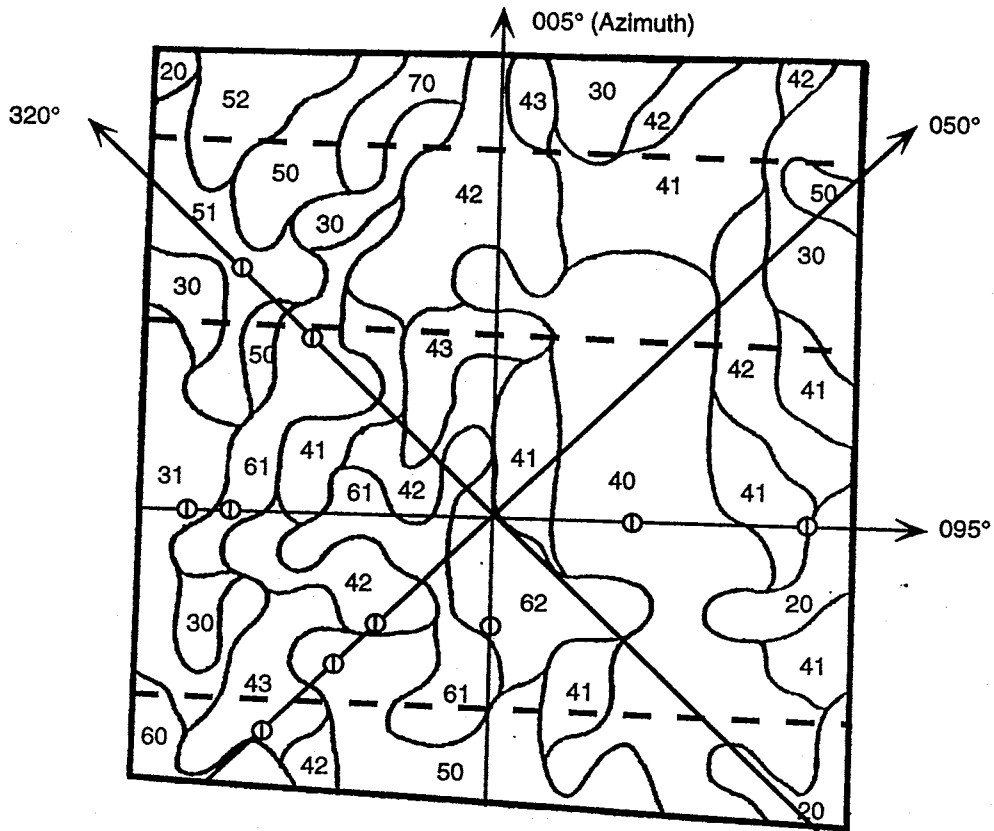
NUMERICAL LEGEND FOR MAP UNITS OF SOIL SERIES PHASES

Symbol	Name
	Anthony sandy clay loam
	Glendale Variant silt loam
	Glendale Variant sandy clay loam
	Saneli clay loam
	Saneli silty clay loam
	Saneli silt loam
	Saneli sandy clay loam
	Harkey silt loam
	Harkey fine sandy loam
	Harkey loamy fine sand
	Glendale sandy clay loam
	Glendale silt loam
	Glendale silty clay loam
	Anthony Variant fine sandy loam

Explanation of Symbols

Φ — Intensive Measurement Sites

——— — Infiltration Measurement Transects

– – – — Tile Drain Lines

Scale 1 cm = 23.90 m

14

south and east-west transects. The measurement sites along each transect were located symmetrically with respect to this center. The north-south transect contained the majority of the measurement locations, 61, and partially bisects the center bench into east and west halves. Along this transect the measurements were taken at the center point, then at 0.5-meter intervals up to 2 m from the center, then at 1.5-meter intervals up to 38 m, and finally at 50 m and 65 m from the center. Each of the remaining transects contained 14 measurement locations. All of the measurements taken along the east-west transect were taken at 15-m intervals. The east-west transect was located directly above the section of tile drain line that is intercepted by the two manholes. Along the diagonal transects measurements were taken at 18-m intervals. The design of the grid had to be such that a sufficient number of measurements could be made for reliable variogram analyses and yet also keep the labor involved at a reasonable level. The spatial discretization of measurement locations was chosen to correspond with the nodes and elements of the model which is to be tested. These nodes are closely spaced near the tile line between the two manholes in order to describe the flow of soil water near the drain with greater accuracy and precision. The spacing between nodes on the east-west and diagonal transects was increased so that large scale heterogeneity may also be analyzed.

The infiltration measurements were recorded in the summer of 1994 during two time frames according to the availability of the infiltrometers. The first set of measurements was recorded during consecutive days from June 14th through the 19th, and again on the 26th and 27th. During these days measurements began

early in the morning (approximately 8:00 am) and ended as late as daylight would allow (approximately 8:30 to 9:00 PM). During this time frame the weather was hot and dry. The soil temperature, measured at ~ 10 cm depth with a soil probe thermometer purchased from Solinst, Inc. in Ontario, Canada, ranged from 24°C to 32°C and the crop (sorghum-sudan cross) was young, with an average height of approximately 25 cm. The second set of measurements was recorded during August of 1994 on the 14th, 19th, 20th, 21st, and 25th. During this time frame the crop was significantly more mature than in June with an average height of approximately 1 m and the weather was warm and humid. Measurements typically began before 8:00 am and lasted throughout daylight hours. The day-time soil temperature ranged from 23°C to 27°C.

The following summary of the typical approach to measurements with the ponded and tension infiltrometers is taken from Ankeny (1992).

1.   Soil surface preparation. The surface crust or top 10 or 20 mm is carefully removed and the prepared surface is leveled.

2.   A sharpened ring is pushed a short distance into the soil to define the area of the infiltration surface, and cheesecloth is placed into the ring.

3.   The ponded infiltrometer is placed over the ring, the valve is opened and the bubbling tube is adjusted to maintain the ponding at a level even with the top of the ring. Ponded infiltration measurements are made.

4. The ponded infiltration measurements are stopped, and the ponded infiltrometer removed.

5. Contact sand is added to fill the inside of the inserted ring and leveled.

6. The tension infiltrometer is centered over the sand-filled ring, and the legs of the device are pushed into the soil until contact is made with the sand.

7. Measurements are made from low to high tension (e.g., from 30-60-150 mm of tension).

For the infiltration experiment at Las Nutrias, a wire barbecue brush worked well for soil surface preparation and appeared to minimize disturbance of the natural pores at the surface. The ring used to define the area of the infiltration surface was of 8.2-cm inner diameter. For ease of use and quickness in the field, cheesecloth was cut into the proper size circles in the office prior to each day of field work. As infiltration was in process, water levels in the instrument reservoirs were recorded at regular time intervals until constant rates were reached. These equilibrium infiltration rates were used to calculate the saturated hydraulic conductivity, (Ksat), under the ponded conditions and the unsaturated hydraulic conductivity, $K(\psi)$, at preset tensions of $\psi = 30$, $\psi = 60$, and $\psi = 150$ mm. Typically, the time necessary to reach equilibrium was 8 to 14 min. with the ponded infiltrometer, 6 to 10 minutes with the tension infiltrometer at 3 cm tension, and six minutes or less at the greater tensions.

In addition, ten sites determined to be representative of the different soil types at the field site were chosen. At those locations infiltration measurements were recorded at several tensions between 0 and 2 cm and at 3-, 6-,and 15 cm and undisturbed soil samples were collected for laboratory measurement of water retention properties. The hydraulic conductivity estimates obtained from this laboratory experiment, which is described in the next chapter, are compared to estimates obtained by measurements in the field.

3.2 Laboratory Measurements of Soil Properties

3.2.1 Bulk Density and Porosity

Soil samples were taken at each of the 104 infiltration measurement sites. Ten points along the transects (labeled in Figure 5) were chosen as representative of the different soil types present at the field site. At those representative points undisturbed soil samples were collected in 103 cm^3 cylindrical stainless steel sleeves for the purpose of determining the soil water characteristic curve, $\theta(\psi)$, and unsaturated hydraulic conductivity in the laboratory. Each of the remaining samples was oven-dried and weighed for the determination of bulk density. The bulk density of each of the ten undisturbed samples was determined after the hanging column experiment was completed. The porosity of each sample was determined by assuming a particle density, ρ_p, of 2.65 g/cm^3 and utilizing the following relationships:

$$\rho_b = m_s/V \quad \text{and} \quad \phi = 1 - \rho_b/\rho_p, \qquad \text{(3) and (4)}$$

where, ρ_b = bulk density, m_s = the mass of the dry soil sample, V = the volume of the soil sample, ϕ = porosity, and ρ_p = particle density.

3.2.2 Water Characteristic Function and Unsaturated Hydraulic Conductivity

The hanging water column used in the laboratory to determine the soil water characteristic function consists of a highly permeable porous ceramic plate contained inside a glass funnel (Jury et al., 1991). One end of a flexible tube is tightly clamped to the narrow end of the funnel. The other end of the flexible tube is securely clamped to a graduated burette with milliliter graduations. The flexible tube and burette are then filled with water until the porous plate is saturated and no air bubbles are visible in the tube or in the portion of the funnel beneath the ceramic plate. The water-filled burette and flexible tube serve together as a manometer. Next, the funnel is inverted and the undisturbed soil sample is placed into the funnel with its bottom surface in direct contact with the porous plate. The porous plate maintains hydraulic continuity between the sample and the hanging column of water. Therefore, it is imperative that the contact between the sample and the ceramic plate is complete (i.e., there is no visible space between the porous plate and the perimeter of the bottom surface of the sample). The manometer is used to control the tension at the interface between the soil sample and the porous plate and to measure the volumes of water drained from the sample during successive increases in soil water tension. The funnel containing the soil sample and the burette are securely fastened to a sturdy and stable rod which is attached to the laboratory floor and ceiling and located within several cm of an unoccupied portion of one of the laboratory walls. This portion of the wall should be covered with graph paper or another length scale with mm precision. Directly behind each hanging column apparatus, the scale should be clearly marked every 5- or 10 cm so that

heights can be easily recorded. So that experimental errors due to evaporation are avoided, a closed system is maintained by sealing the open ends of both the funnel and the burette with rubber stoppers. The rubber stoppers are then pierced and connected to one another by inserting each end of a long section of small diameter flexible tube through the rubber stoppers. Prior to insertion, the ends of the narrow flexible tube should be smeared with vacuum grease to facilitate insertion and to seal the opening. In the current experiment the system was allowed to equilibrate with the water in the manometer at a level coinciding with the interface between the soil sample and the porous plate. This interface was defined as the datum for the experiment. As imbibition of water from the hanging column into the soil sample occurred over a period of several weeks, equilibrium was accomplished by repeatedly raising the burette until the water level in the manometer was at the same height as the top of the porous plate for several consecutive days. After equilibrium was attained at this height - signifying a tension equal to the length of the soil sample - the burette was lowered to 2 cm below datum and again allowed to equilibrate. During this and each successive tension increase, water flowed from the soil samples through the porous plates and into the manometers until the total water potential of each system was constant. Equilibrium measurements were recorded at 3, 4, 6, 10, 15, and 20 cm below datum and then at 10cm intervals down to a final tension of 170 cm below datum. The tension range of the experiment was limited primarily by the space available for lowering the water column.

3.3 EM-38 Surveys

Electromagnetic induction surveys using the Geonics EM38 were executed monthly from January to May of 1994. Measurement sites for the EM38 surveys were located on a square grid encompassing the entire center bench with a uniform square spacing of ten meters. The EM38 has two modes of operation. The horizontal mode measures the soil inductance down to 0.75 meters depth. The vertical mode measures the soil inductance down to 1.5 meters depth. The difference between the horizontal and vertical EM readings indicates the distributions of salinity with depth (e.g., McNeill 1980b). In the current study the difference is defined as the horizontal reading minus the vertical reading. A negative difference indicates increasing salinity with depth. A positive difference indicates decreasing salinity with depth. The data collected over the specified time period was used for the analysis of the spatial variability of soil salinity, which is directly related to induction measurements. The differences between measurements made at each of the modes of operation (to depths of 0.75 and 1.5 m) will be used in the future to validate model predictions of soil water and salinity movement.

An EM38 survey was also conducted during September of 1993 to detect any existing correlation of induction measurements to visual observations of crop productivity. Measurements were taken at 10-m spacings along several parallel transects. Transect locations were chosen so that a wide range of crop productivity would be represented in the data. At each measurement point, a visual salinity

survey based on crop (feed corn at the time of the survey) health was observed and assigned a productivity index according to the following definitions:

3 = Healthy crop; Greater than 2 m height and producing well.

2 = Unhealthy or of questionable health; 1 to 2 m height and

producing marginally.

1 = Very unhealthy crop; Less than 1 m height and not producing.

4. RESULTS AND DISCUSSION

4.1 Infiltrometer Experiment

4.1.1 Infiltration Data Analysis

As discussed in the previous chapter, the data collected in the field with the tension infiltrometer consisted of three dimensional, steady state infiltration rates at preset soil water tensions through a known area of infiltration surface. The analytical method used to calculate hydraulic conductivity values from this infiltration data is discussed in detail in Ankeny et al. (1991) and briefly summarized in this section.

Wooding (1968) proposed a simplified algebraic expression for unconfined (three-dimensional) steady -state water infiltration (zero ponding) into soil from a circular source of radius r described by

$$Q = \pi r^2 K + 4r\phi \qquad (5)$$

where Q (m^3/s) is the steady infiltration rate, K (m/s) is the field-saturated hydraulic conductivity and ϕ (m^2/s) is the matric flux potential (Gardner, 1958). Equation (5)

can be rewritten to show the dependence of K and ϕ on the surface boundary

potential, ψ, resulting in a flux, Q, which is dependent on the surface boundary

potential. Measurement of fluxes $Q(\psi_1)$ and $Q(\psi_2)$ at two potentials (ψ_1 and ψ_2)

yields the following two equations and four unknowns:

$$Q(\psi_1) = \pi r^2 K(\psi_1) + 4r\phi(\psi_1) \qquad (6)$$

$$Q(\psi_2) = \pi r^2 K(\psi_2) + 4r\phi(\psi_2) \qquad (7)$$

A third equation is obtained by assuming a constant $K(\psi)/\phi(\psi)$ ratio

throughout the pressure range from ψ_1 to ψ_2.

$$A = K(\psi)/\phi(\psi) = \text{constant (m}^{-1}) \qquad (8)$$

Support for the use of this assumption can be found in Philip (1985). Thus,

equations (6) and (7) can be rewritten as

$$Q(\psi_1) = [\pi r^2 + 4r/A]K(\psi_1) \qquad (9)$$

$$Q(\psi_2) = [\pi r^2 + 4r/A]K(\psi_2) \qquad (10)$$

Equations (9) and (10) now only contain three unknowns. Elrick et al., (1988, pp.

88-95) developed a numerical approximation for the difference between (ψ_1) and

(ψ_2):

$$\phi(\psi_1) - \phi(\psi_2) = \Delta\psi[K(\psi_1) + K(\psi_2)]/2 \qquad (11)$$

where $\Delta\psi = \psi_1 - \psi_2$. Substituting equation (8) into equation (11) gives

$$[K(\psi_1) - K(\psi_2)]/A = \Delta\psi[K(\psi_1) + K(\psi_2)]/2 \qquad (12)$$

Thus, equations (9), (10), and (12) with three unknowns ($K(\psi_1)$, $K(\psi_2)$, and A)

can be solved simultaneously for hydraulic conductivities for pairs of unconfined

infiltration rates taken at different tensions. In the current study the three

simultaneous equations were solved using 0- and 30-, 30- and 60-, and 60- and

150-mm tensions. A pair of rates yielded estimates of K(ψ) at each tension used. From the three rate pairs, six hydraulic conductivity estimates were obtained and the best estimate was defined as the arithmetic average of available estimates. The following equations demonstrate specifically how K(0), K(30), K(60), and K(150) are estimated:

$$K(0) = K(0)_{0,30} \qquad (13)$$

$$K(30) = [K(30)_{0,30} + K(30)_{30,60}]/2 \qquad (14)$$

$$K(60) = [K(60)_{30,60} + K(60)_{60,150}]/2 \qquad (15)$$

$$K(150) = K(150)_{60,150} \qquad (16)$$

A similar approach was used to estimate the hydraulic conductivities at values equal to 0.3-, 0.5-, 0.7-, 1.0-, 1.3-, 1.5-, 1.8-, and 2.0 m at the intensive measurement locations. To complete this reduction of the infiltration data a FORTRAN code was used which was written by Lance Hughson, a Ph.D. candidate at the New Mexico Institute of Mining and Technology. The code utilizes the Picard method of solving systems of nonlinear equations and is found in appendix 9.4.

4.1.2 Analysis of K(ψ) Variability

Once the infiltration rate data was converted to hydraulic conductivity, a surface plot of the Ksat data was created using Surfer for Windows™, a computer program developed by Golden Software in Golden, Colorado. The surface plot (Figure 6) illustrates what is, arguably, the most revealing aspect of the data set. Depicted by the "valley" trending north-south through the center of the study area is a section of hydraulic conductivity values which are lower than the values throughout the rest of the field. The lower values all appear to be located on the

Figure 6. Surface Plot of ln Ksat
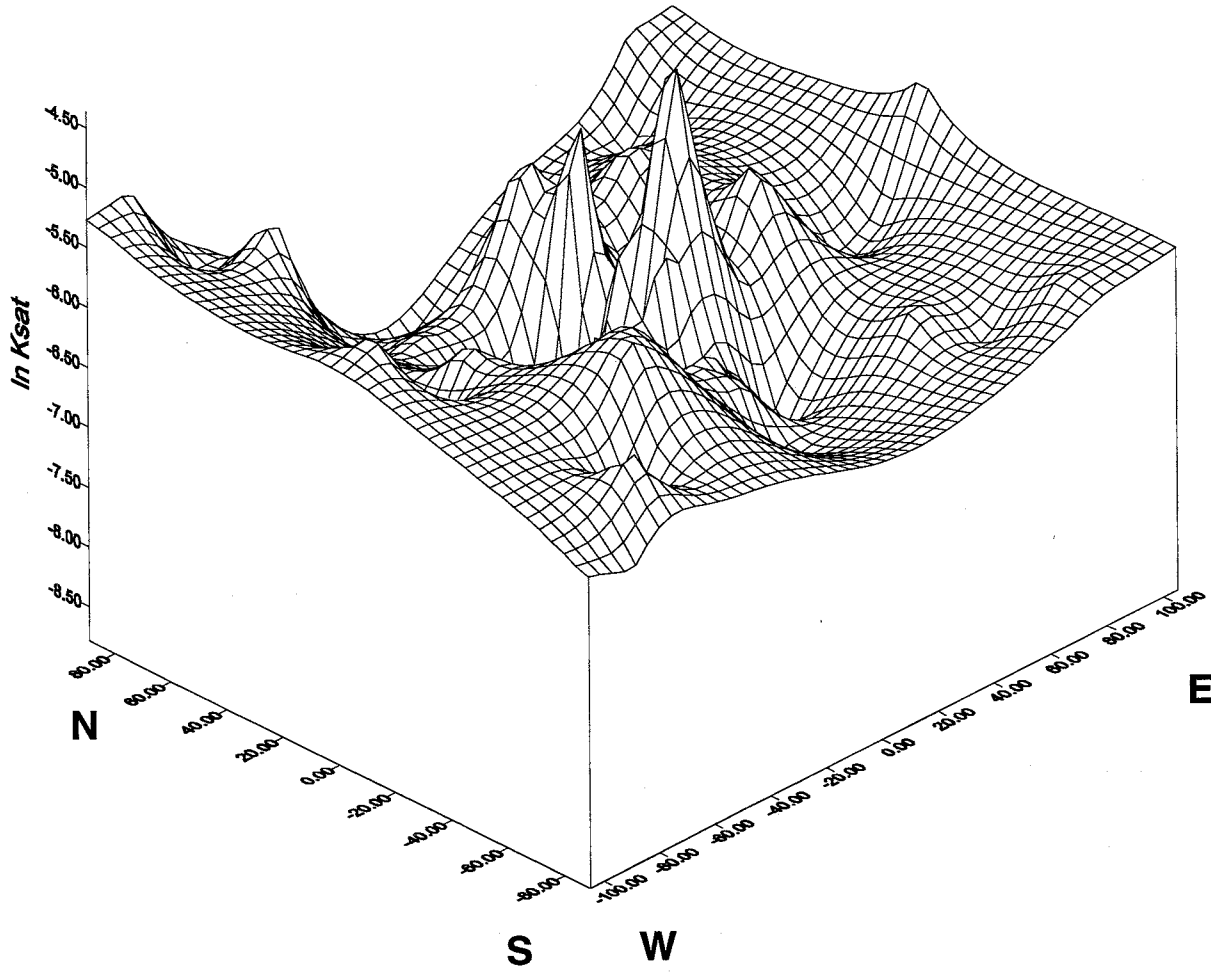
north-south transect. As mentioned in a previous chapter, because of the availability of the instruments, the data was collected in two time periods separated by approximately two months. The first data collection period was in June of 1994 and the second in August. The bimodal character in the Ksat data corresponds to the two time periods of data collection. The bimodal character was also exhibited by the hydraulic conductivity data at 3 cm of tension, though to a lesser degree, and was not present at all in the data at the higher tensions. Therefore it was hypothesized that the observed effect may be due to some phenomenon or combination of phenomena that only affects macropores which drain in the affected tension range (< 6 cm) and not the properties of the bulk soil. The capillary-rise equation predicts that pores of >0.05 cm nominal diameter will drain at tensions <6 cm. A tension of 3 cm corresponds to a nominal pore diameter of 0.1 cm. Such phenomena may include the development of macropores due to root growth or due to wetting and drying cycles during irrigation season. Either cause may explain the observed effect since, between periods of data collection, the field was irrigated three times, experienced several thunder storms, and the crop grew significantly. During the summer of 1994 the crop was a sorghum/sudan cross. Although no literature was found that addresses the effect of root growth of this particular crop on macropores, Shirmohammadi and Skaggs (1984) found that fescue roots loosened the soil and increased the saturated hydraulic conductivity by an average of 40% over soybeans and 80% over bare soil. Warner and Young (1991) also determined that corn roots provided preferential path ways for the movement of water through the top soil. However, results of these studies did not produce

estimates of macropore diameters. Barley (1954) measured intersections of pores on 0.9-mm optical transects and found that soil adjacent to 0.1-mm root channels was compacted and dye tracers were observed to not move preferentially along the edges of these roots. Akram and Kemper (1979) concluded that wetting and drying cycles also contribute to the generation of macropores and significant increases in infiltration rates but, again, do not discuss the pore sizes associated with the increases. Meek et al. (1989) found that while infiltration rates in loose soils decreased in response to flood irrigation, in soils slightly compacted (as due to traffic) infiltration rates increased in response to flood irrigation.

4.1.2.1 Stationarity of K(ψ) with Respect to Time

Descriptive statistics were calculated for both the June and August data sets separately and are listed in Tables 1 and 2. These statistics show a significant difference between the mean values for the saturated and 3 cm tension data from June to August. A t-test was performed on each of the data sets at each tension in order to determine if the observed differences in the means were significant or if the two samples came from the same population and the differences were random. In the current study, the t-tests were executed using the data analysis package within the Excel™ spreadsheet developed by the Microsoft Corporation® of Redmond, Washington. The type of t-test used is not a paired test, therefore the two samples under comparison need not be of equal size. The classical assumptions for the validity t-tests are (1) normality, (2) equality of variance, and (3) statistical independence (Scheffé, 1959, p.331). According to Kolomogorov-Smirnoff tests for

Table 1

Descriptive Statistics for the June, 1994 Sample of ln K(ψ) Estimates.

ln K0			ln K3	
Mean	-6.19		Mean	-7.57
Standard Error	0.11		Standard Error	0.050
Median	-6.14		Median	-7.57
Mode	-6.51		Mode	-8.03
Standard Deviation	0.86		Standard Deviation	0.39
Sample Variance	0.75		Sample Variance	0.15
Kurtosis	2.66		Kurtosis	-0.13
Skewness	-0.55		Skewness	0.13
Range	5.44		Range	1.81
Minimum	-9.41		Minimum	-8.41
Maximum	-3.96		Maximum	-6.60
Significance level, α	0.05		Significance level, α	0.05
ln K6			ln K15	
Mean	-8.47		Mean	-9.36
Standard Error	0.06		Standard Error	0.056
Median	-8.47		Median	-9.37
Mode	-8.31		Mode	-9.09
Standard Deviation	0.45		Standard Deviation	0.45
Sample Variance	0.199		Sample Variance	0.21
Kurtosis	0.83		Kurtosis	-0.014
Skewness	0.10		Skewness	-0.13
Range	2.44		Range	2.23
Minimum	-9.64		Minimum	-10.61
Maximum	-7.19		Maximum	-8.38
Significance level, α	0.05		Significance level, α	0.05

Table 2

Descriptive Statistics for the August, 1994 Sample of ln K(ψ) Estimates.

ln K0			ln K3	
Mean	-4.91		Mean	-7.34
Standard Error	0.09		Standard Error	0.049
Median	-4.93		Median	-7.32
Mode	-5.06		Mode	-7.21
Standard Deviation	0.57		Standard Deviation	0.29
Sample Variance	0.32		Sample Variance	0.087
Kurtosis	-0.40		Kurtosis	0.28
Skewness	-0.11		Skewness	0.37
Range	2.31		Range	1.31
Minimum	-6.24		Minimum	-7.87
Maximum	-3.93		Maximum	-6.56
Significance level, α	0.05		Significance level, α	0.05
ln K6			ln K15	
Mean	-8.46		Mean	-9.29
Standard Error	0.053		Standard Error	0.058
Median	-8.44		Median	-9.17
Mode	-8.31		Mode	-9.17
Standard Deviation	0.32		Standard Deviation	0.35
Sample Variance	0.10		Sample Variance	0.13
Kurtosis	-0.47		Kurtosis	-0.18
Skewness	-0.025		Skewness	-0.70
Range	1.26		Range	1.32
Minimum	-8.98		Minimum	-10.0
Maximum	-7.73		Maximum	-8.70
Significance level, α	0.05		Significance level, α	0.05

normality performed with GEOPACK, each of the K(ψ) data sets are normally
distributed at a significance level of 0.1 or less. Bradley (1980, pp. 275-278)
examined the robustness of the regular t-test to differing variances (an effect that
the method employed in the current study attempts to take into account). Bradley
found that if the sample sizes are not equal and the larger variance is associated
with the smaller sample size, there is a significant probability of a false-positive
result if the variance ratio is 4 or more. The t-test is justified in the current study
because the larger variance is associated with the larger sample size and the
variance ratios are approximately 2 for the Ksat and K(3 cm) samples. McNichols
and Davis (1988, pp. 135-150) found that if values are correlated (e.g. due to spatial
or temporal correlation) the t-tests for differences should not be strongly affected in
the case where the observations are normally distributed. Based on these
justifications the t-tests were executed and the results of these tests, found in
Tables 3,4,5, and 6, indicate that the mean differences for both the saturated and 3
cm tension data sets are indeed significant.

Table 3
Results of t-test for means of June and August samples of ln Ksat data.

t-Test: Two-Sample Assuming Unequal Variances		
	August	June
Mean	-4.91	-6.19
Variance	0.320	0.746
Observations	37	62
Hypothesized Mean Difference	0	
df	96	
t Stat	8.92	
t Critical two-tail	1.98	
Significance level, α	0.05	

Table 4
Results of t-test for means of June and August samples of ln K(3cm) data.

t-Test: Two-Sample Assuming Unequal Variances		
	August	June
Mean	-7.34	-7.59
Variance	0.0869	0.150
Observations	36	57
Hypothesized Mean Difference	0	
df	88	
t Stat	3.50	
t Critical two-tail	1.99	
Significance level, α	0.05	

Table 5

Results of t-tests for means of June and August samples of ln K(6) data.

t-Test: Two-Sample Assuming Unequal Variances		
	August	June
Mean	-8.46	-8.47
Variance	0.100	0.200
Observations	36	63
Hypothesized Mean Difference	0	
df	92	
t Stat	0.161	
t Critical two-tail	1.99	
Significance level, α	0.05	

Table 6

Results of t-tests for means of June and August samples of ln K(15) data.

t-Test: Two-Sample Assuming Unequal Variances		
	August	June
Mean	-9.29	-9.36
Variance	0.125	0.206
Observations	37	65
Hypothesized Mean Difference	0	
df	90	
t Stat	0.794	
t Critical two-tail	1.99	
Significance level, α	0.05	

The results also show that no such significant distinction exists between the two data sets at the higher tensions. Prior to proceeding with the variogram analysis, the mean difference between the June and August data sets was eliminated by subtracting the magnitude of the difference from the values recorded in August, which were greater than the values recorded in June. This step is a simple normalization similar to subtracting the mean from a sample in order to center the distribution at zero without affecting the variability in the sample. This is a valid step because the current study involves variogram analyses and is only concerned with data variability (Ross, 1987, p. 50).

Since salinity is often an effect of poor drainage and because plants, and therefore roots, do not grow where ECa values are high, a study of the correlation of Ksat to ECa was executed with the hope that such information might provide evidence pertaining to the hypothesis that root growth contributed to the increase in Ksat with time. Correlation coefficients were calculated for the June (based on 11 coinciding measurement points) and August (based on 18 coinciding measurement points) data sets, $r_{June} = -0.362$ and $r_{August} = 0.214$. Surprisingly, r_{August} did not indicate a strong negative correlation as might be expected, but rather a weak positive correlation. Therefore this information could not be used to either support or to negate the root growth hypothesis.

4.1.2.2 Spatial Variability of K(ψ)

With the exception of a spatial correlation up to approximately 12 meters for the saturated data set, variograms for the data sets at each tension display a pure

nugget effect (Figures 7 - 10). The pure nugget effect corresponds to a total absence of spatial correlation between the two variables z(x) and z(x + h), at least for all available lag distances, and is equivalent to the well-known phenomenon of "white noise" in physics. In so far as geostatistics is concerned with second-order moments, a pure nugget effect will be interpreted as spatial independence (Journel and Huijbregts, 1978, p. 153). At every point, the best estimator of the hydraulic conductivity is the mean value of the measurements. The means and other descriptive statistics for the adjusted data sets are listed in Table 7.

Figure 7 - Variogram for ln (K_0)
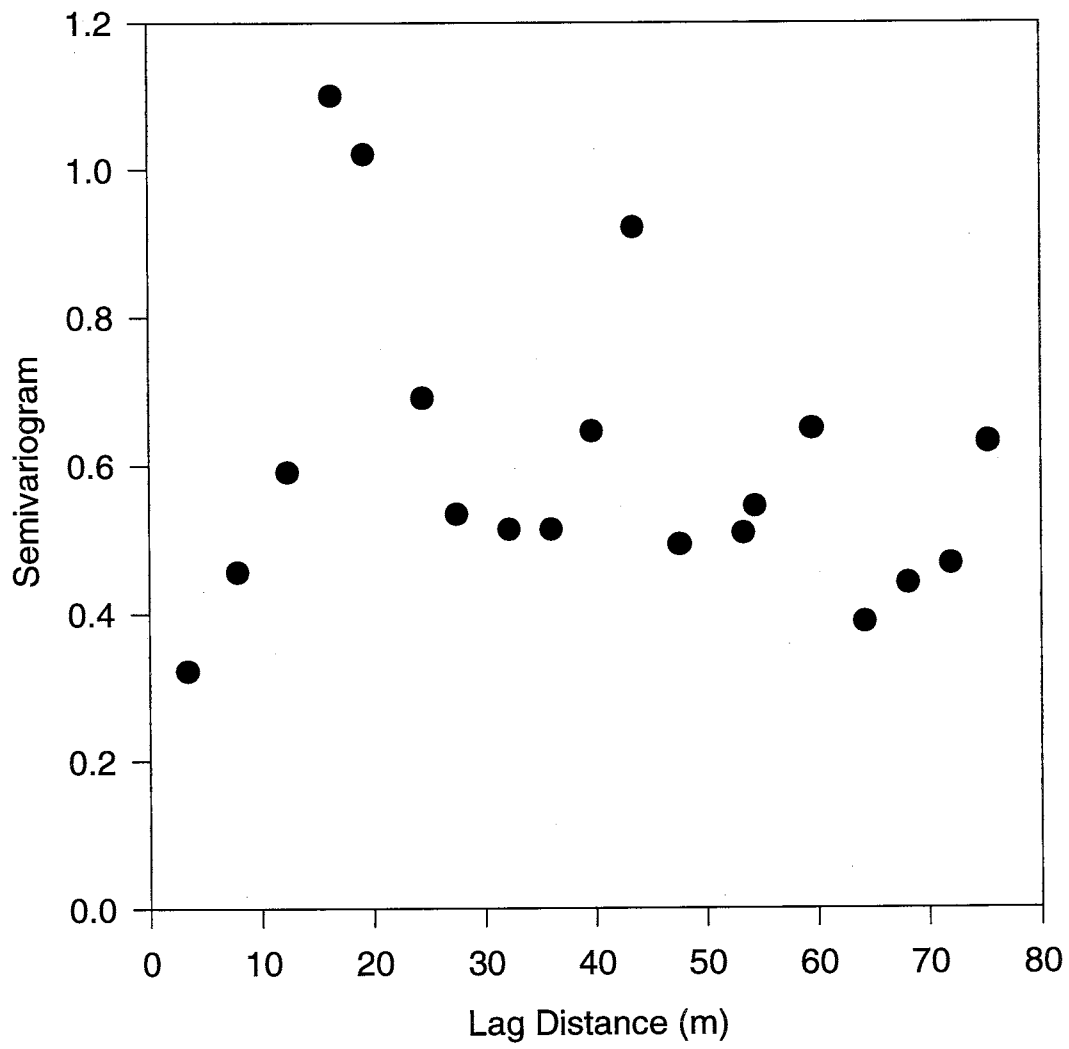
Figure 8 - Variogram for ln (K₃)
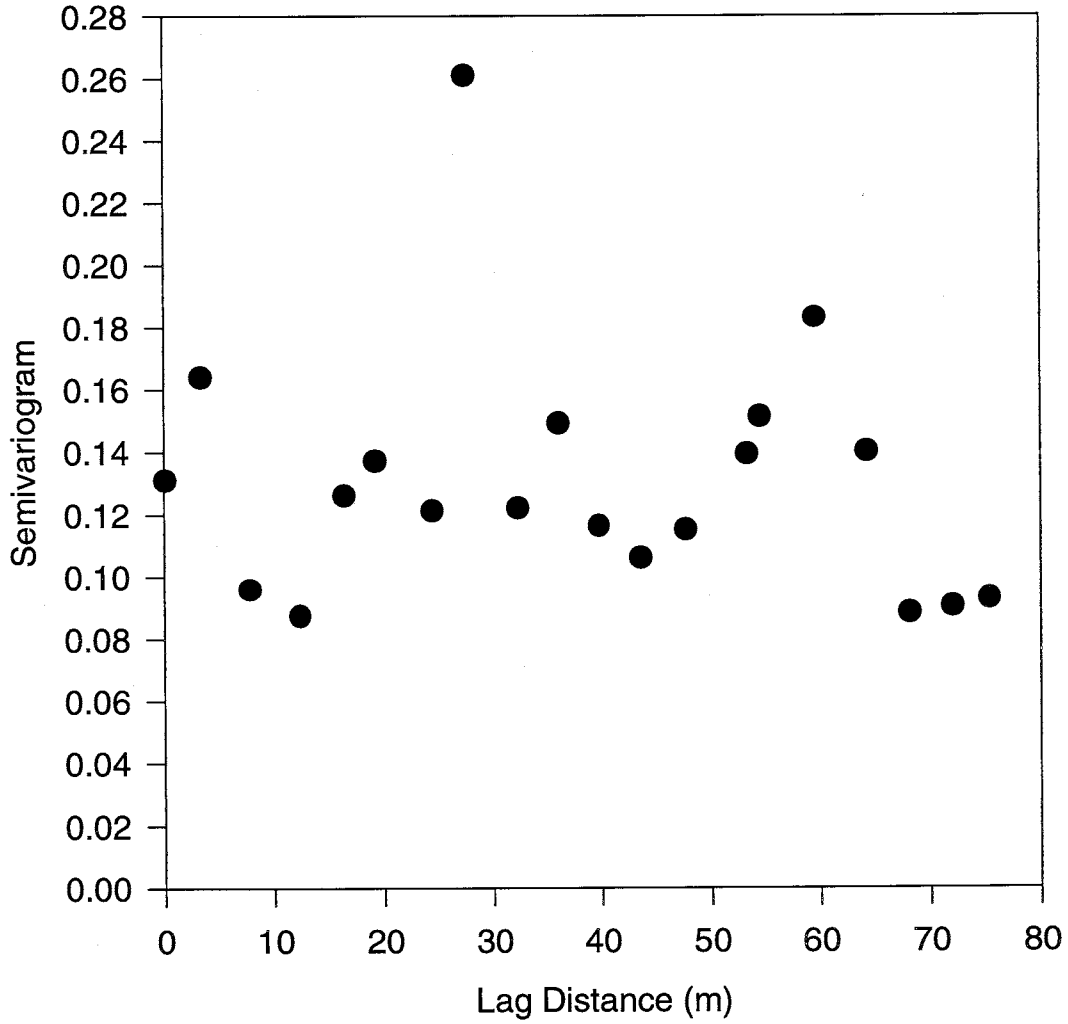
Figure 9 - Variogram for ln (K$_6$)
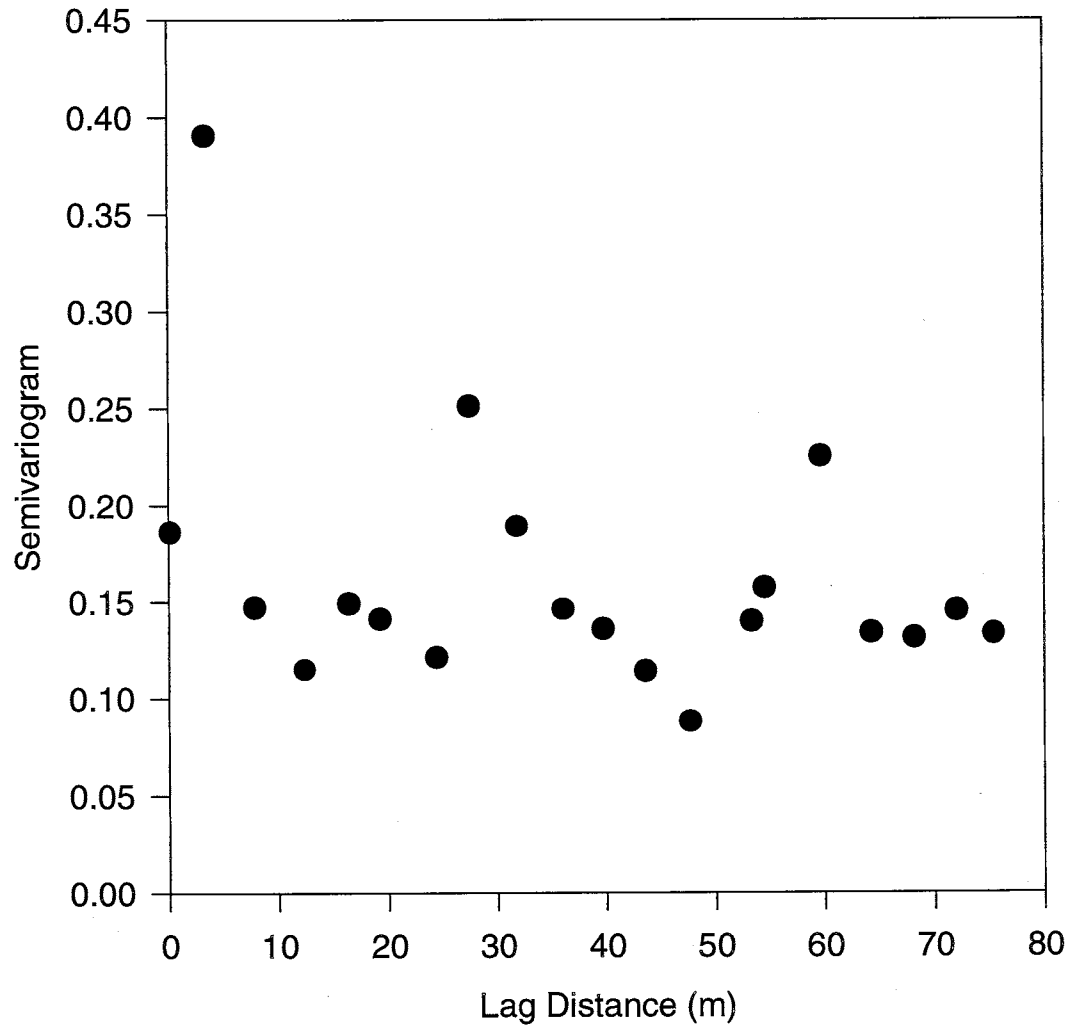
Figure 10 - Variogram for In (K$_{15}$)
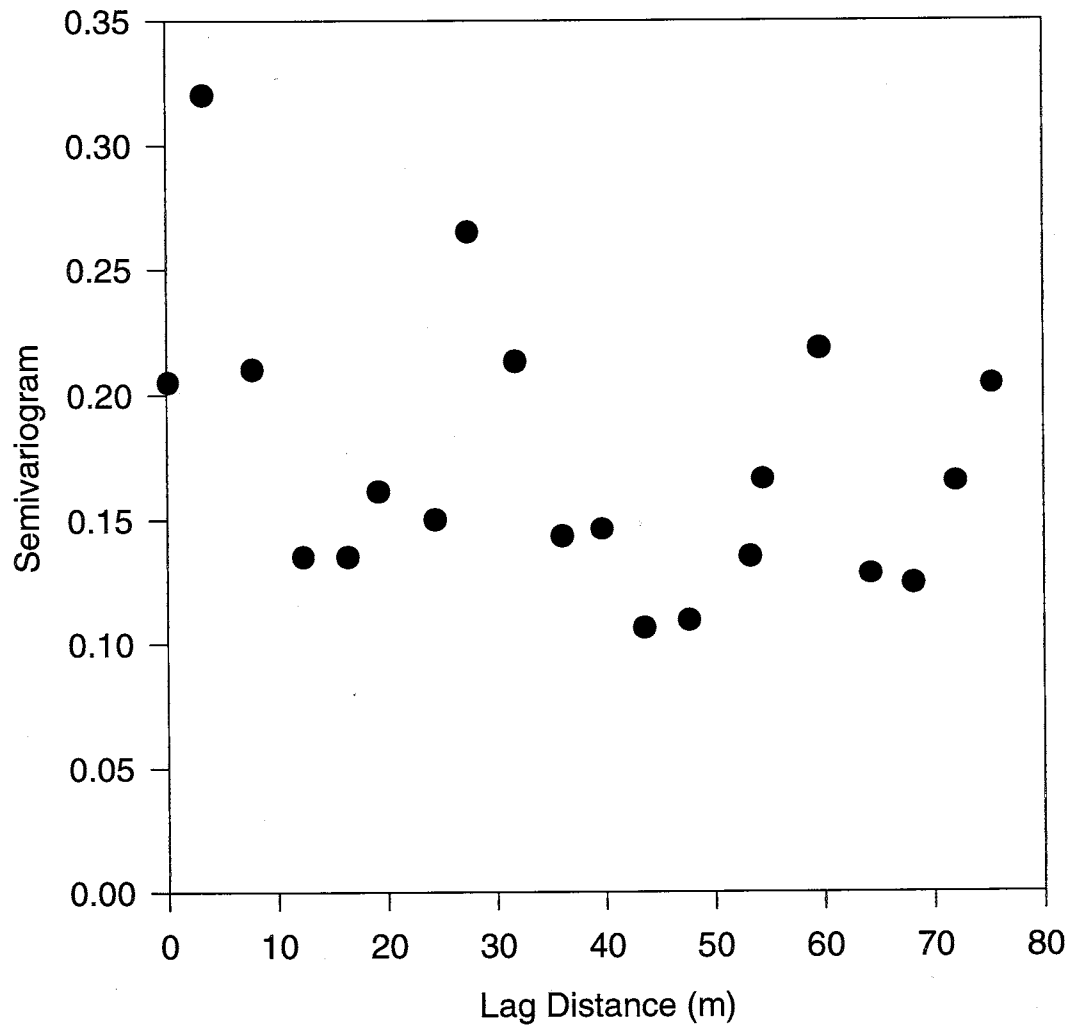
Table 7

Descriptive Statistics for Entire Sample of Adjusted In K(ψ) Data.

Adjusted In Ksat			Adjusted In K(3cm)	
Mean	-6.19		Mean	-7.57
Standard Error	0.0767		Standard Error	0.0361
Median	-6.20		Median	-7.56
Mode	-6.51		Mode	-8.03
Standard Deviation	0.763		Standard Deviation	0.355
Sample Variance	0.582		Sample Variance	0.126
Kurtosis	2.93		Kurtosis	0.0694
Skewness	-0.505		Skewness	0.175
Range	5.44		Range	1.81
Minimum	-9.41		Minimum	-8.41
Maximum	-3.96		Maximum	-6.60
Significance level, α	0.05		Significance level, α	0.05
Adjusted In K(6cm)			Adjusted In K(15cm)	
Mean	-8.47		Mean	-9.34
Standard Error	0.0405		Standard Error	0.0416
Median	-8.47		Median	-9.29
Mode	-8.31		Mode	-9.17
Standard Deviation	0.403		Standard Deviation	0.420
Sample Variance	0.162		Sample Variance	0.176
Kurtosis	0.932		Kurtosis	0.0273
Skewness	0.0653		Skewness	-0.294
Range	2.44		Range	2.23
Minimum	-9.64		Minimum	-10.6
Maximum	-7.19		Maximum	-8.38
Significance level, α	0.05		Significance level, α	0.05

4.2 Estimation of The Unsaturated Hydraulic Conductivity Function From Observed Soil Water Retention Data

The soil water characteristic curves were determined for the undisturbed soil samples using the hanging column and porous plate apparatus described in the previous chapter. The wet end of each curve was measured and the dry end of each curve was extrapolated from the wet data using the parameter estimation computer program RETC developed by the U. S. Environmental Protection Agency (van Genuchten et al., 1991b). The program was used to quantify the unsaturated hydraulic functions of the soil samples employing van Genuchten's parametric soil water retention model (van Genuchten, 1980),

$$(\theta - \theta_r)/(\theta_s - \theta_r) = S_e = [1+(\alpha\psi)^n]^{-m} \qquad (17)$$

where θ is the volumetric water content, θ_r and θ_s are the residual and saturated water contents, respectively, S_e is the effective saturation, and α, n, and m are empirical constants affecting the shape of the retention curve. As an attempt to avoid uniqueness problems in the parameter estimation process associated with a lack of data in the low water content range, m and n were not allowed to vary independently. Instead, a restriction was applied according to the following:

$$m = 1 - 1/n. \qquad (18)$$

The decision to restrict m and n was also based on the consideration that the form of the equation for predicting the unsaturated hydraulic conductivity in the variable m, n case is very complicated when combined with one of the statistical pore-size distribution models (van Genuchten et al., 1991a). In the current study, van Genuchten's water retention model was combined with the model of Mualem (1976) for predicting the hydraulic conductivity as a function of the soil water tension, $K(\psi)$:

$$K(\psi) = K_s\{1 - (\alpha\psi)^{mn}[1 + (\alpha\psi)^n]^{-m}\}^2/[1 + (\alpha\psi)^n]^{ml} \qquad (19)$$

where the two additional parameters, K_s and l, are the saturated hydraulic conductivity and the pore-connectivity parameter respectively and, again, m is restricted according to (18). Mualem (1976) estimated l to be about 0.5 on average for a wide variety of soil types. During the parameter estimation process in the current study, values for K_s were fixed according to the estimates obtained from field measurements with the ponded infiltrometer. Following the recommendation of Mualem (1976), l was fixed at a constant value of 0.5. Preliminary parameter estimation results from RETC indicated unrealistic values for both θ_r and n, again, due to the lack of data in the low water content (i.e., high soil water tension) range. When θ_r was fixed at a constant value of zero, fitted estimates for n resulted in reasonable values. These restrictions left three parameters to be estimated by the RETC program - θ_s, α, and n. Though available independent calculations of porosity may have been used as estimates for θ_s, such estimates would not have accounted for trapped air bubbles and/or immobile water. Therefore it was decided

to fit θ_s using the computer program. The soil hydraulic parameter estimates for each of the samples are summarized in Table 8.

Table 8

Soil hydraulic parameters for nine soil types at
Las Nutrias. Parameters fitted with the RETC computer program indicated by *.
SSQ is the sum of squares of differences between observed and fitted values and
R^2 is the absolute value of the correlation coefficient between observed and fitted
values. Both are measures of the goodness of the fit to the observed values.

Sample	SSQ	R^2	θ_r	θ_s*	α*	n*	m*(=1-1/n)	K_S (cm)	L
2-SW54.0	0.00194	0.980	0	0.440	0.0114	1.65	0.394	0.016	0.500
3-W90.0	0.00046	0.997	0	0.481	0.015	1.61	0.379	0.017	0.500
4-SW108.0	0.00236	0.975	0	0.517	0.0486	1.21	0.174	0.013	0.500
5-SW72.0	0.00079	0.991	0	0.424	0.00874	1.97	0.492	0.018	0.500
6-NW90.0	0.00187	0.960	0	0.494	0.0291	1.18	0.153	0.016	0.500
7-S38.0	0.00705	0.894	0	0.506	0.00647	1.83	0.454	0.0021	0.500
8-E45.0	0.00881	0.930	0	0.505	0.00642	3.27	0.694	0.015	0.500
9-W105.0	0.0005	0.997	0	0.445	0.0137	1.84	0.457	0.015	0.500
10-E105.0	0.00188	0.986	0	0.534	0.0206	1.39	0.281	0.014	0.500

Utilizing the parameters summarized in Table 8, $K(\psi)$ was calculated for each of the samples listed at values of soil water tension that correspond to the tensions used with the tension infiltrometer measurements in the field, namely, ψ = 3-, 6-, and 15 cm. These calculated values are listed in Table 9.

4.3 Comparison of Estimates of Unsaturated Hydraulic Conductivity Based on Field and Laboratory Methods

A summary of all of the $K(\psi)$ data collected throughout the summer of 1994 is catalogged in Appendix 8.1.1. A subset of that data set is found in Table 10 and includes the field estimates of $K(\psi)$ measured with the tension infiltrometer at the

Table 9

K(ψ) estimates based on water retention data collected in the laboratory.

Sample	K(ψ=3cm) (cm/s)	K(ψ=6cm) (cm/s)	K(ψ=15cm) (cm/s)
2-SW54.0	1.26E-02	1.09E-02	7.52E-03
3-W90.0	1.23E-02	1.01E-02	6.23E-03
4-SW108.0	1.52E-03	8.29E-04	2.61E-04
5-SW72.0	1.70E-02	1.60E-02	1.33E-02
6-NW90.0	2.07E-03	1.27E-03	5.03E-04
7-S38.0	1.94E-03	1.83E-03	1.54E-03
8-E45.0	1.50E-02	1.50E-02	1.49E-02
9-W105.0	1.30E-02	1.15E-02	8.15E-03
10-E105.0	6.16E-03	4.42E-03	2.17E-03

Table 10

K(ψ) estimates based on field measurements with the tension infiltrometer.

Sample	K(ψ=3cm) (cm/s)	K(ψ=6cm) (cm/s)	K(ψ=15cm) (cm/s)
2-SW54.0	1.06E-03	3.38E-04	1.53E-04
3-W90.0	7.06E-04	2.28E-04	1.67E-04
4-SW108.0	6.20E-04	1.48E-04	5.03E-05
5-SW72.0	7.29E-04	2.49E-04	1.36E-04
6-NW90.0	8.47E-04	2.28E-04	9.17E-05
7-S38.0	7.40E-04	2.41E-04	8.55E-05
8-E45.0	6.23E-04	2.10E-04	1.05E-04
9-W105.0	7.40E-04	2.46E-04	1.05E-04
10-E105.0	7.40E-04	2.46E-04	1.05E-04

exact locations where the undisturbed soil samples were collected for laboratory

determination of K(ψ). Figures 11, 12, and 13 illustrate the relationship between the

field and laboratory methods of determining K(ψ) at ψ = 3-, 6-, and 15 cm.

Figure 11. Laboratory vs. Field Estimates of ln K(3cm)
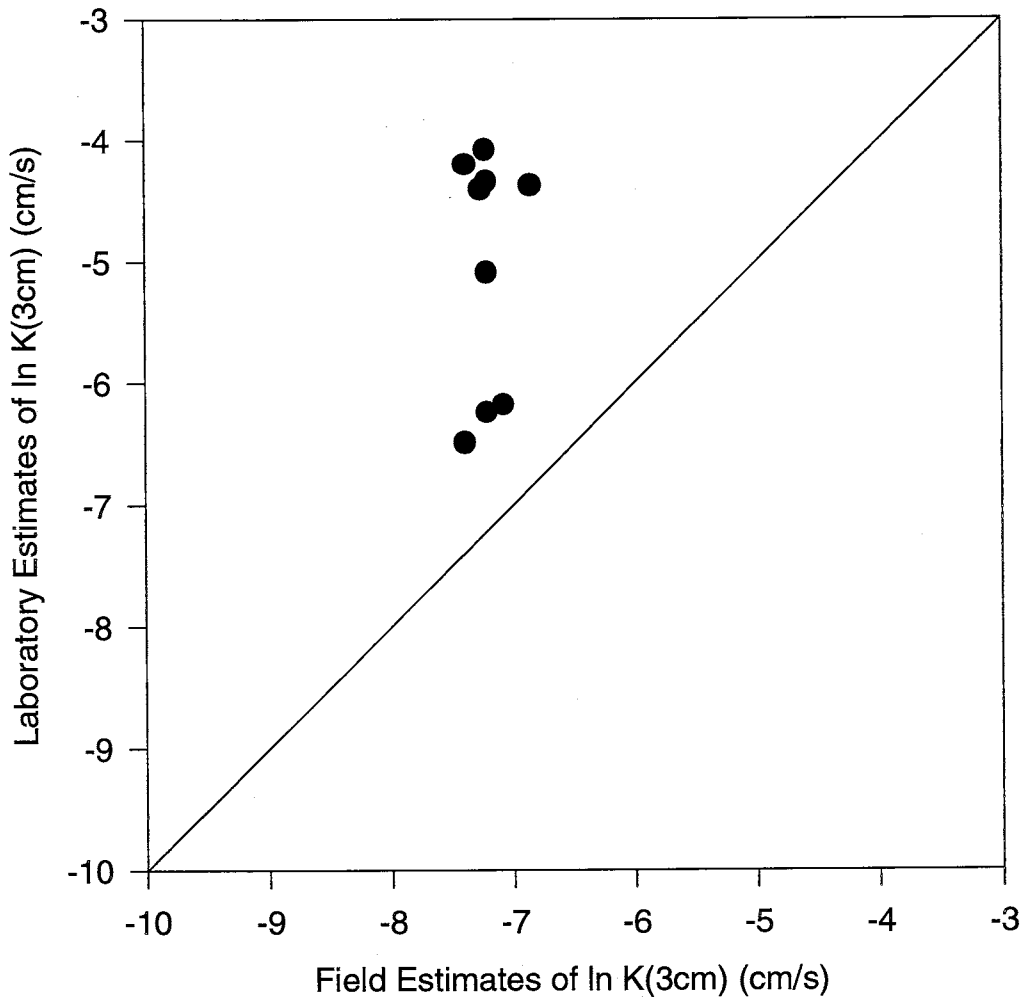
Figure 12. Laboratory vs. Field Estimates of ln K(6cm)
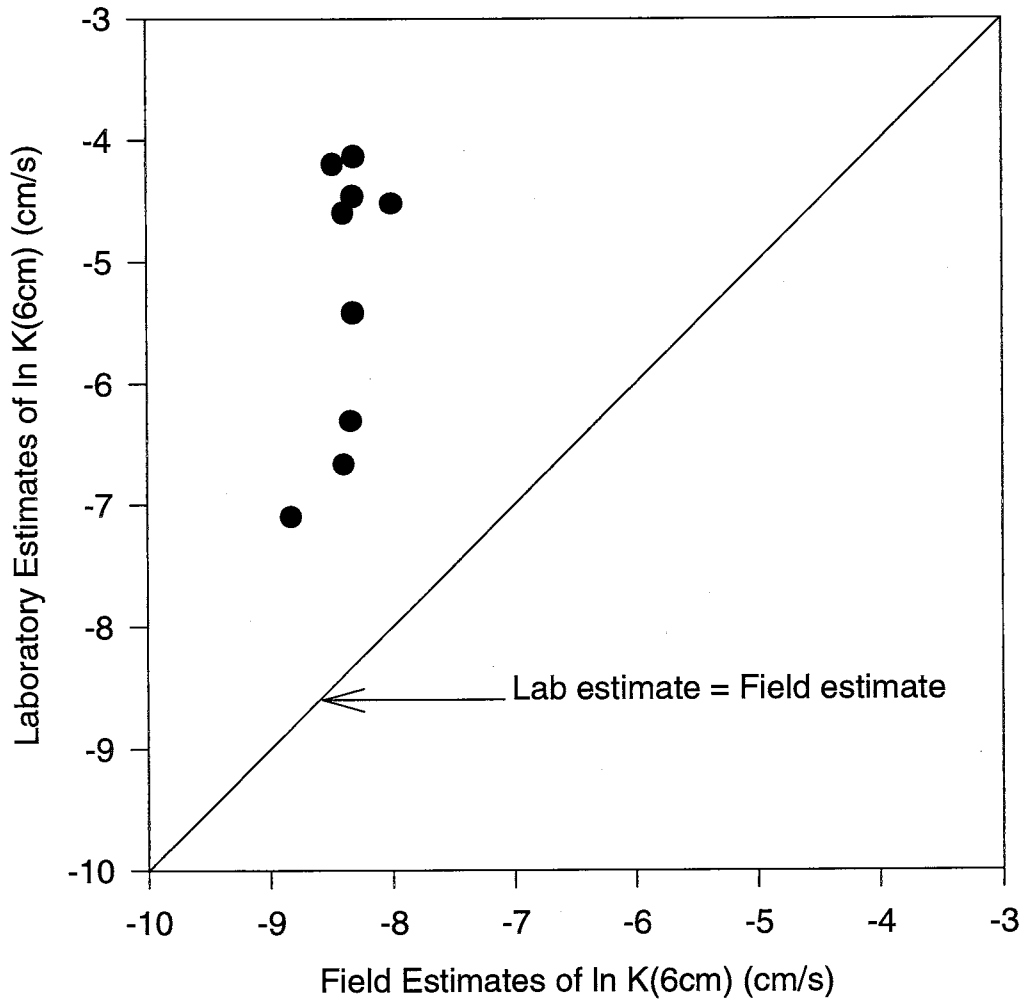
Figure 13. Laboratory vs. Field Estimates of In K(15cm)
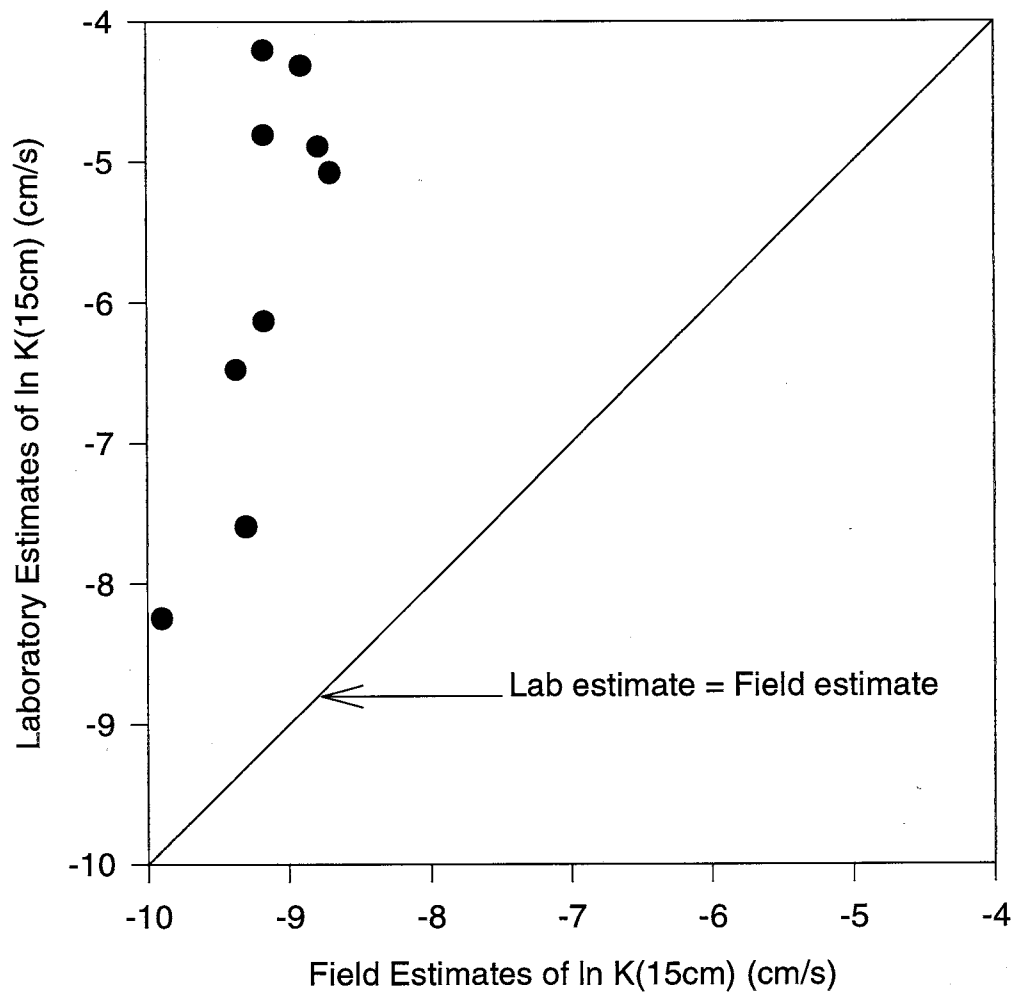
Figures 11 - 13 clearly indicate that the estimates of $K(\psi)$ obtained from the water retention data observed in the laboratory are consistently higher than those measured in the field. This result differs significantly from those of Ankeny et al. (1991) who found that on similar graphs of unconfined versus confined infiltration rates, field estimates were usually slightly greater than lab estimates. The result in their study was attributed to the fact that the field estimates, based on measurements of unconfined, three-dimensional infiltration rates should be greater than the estimates based on confined, one-dimensional flow because the unconfined rates consist of both gravitational and matrix flow components while the confined rates consist only of a gravitational component of flow. In the current study, the lab estimates of $K(\psi)$ are not based on infiltration rates, but rather on hydraulic parameter estimates fitted to water retention observations. As van Genuchten et al. (1991) point out, the accuracy of these estimates may be suspect near saturation (the range of the current comparison is near saturation) because K near saturation is determined by a few very large pores and/or cracks which may have only a minor relation to the bulk pore-size distribution which determines the general shape of the fitted curve at intermediate soil water tensions.

4.4   EM-38 Surveys

4.4.1 Electromagnetic Induction Measurement Changes with Depth as Indicators of Water Flow Direction in the Vadose Zone

Hendrickx et al. (1992) state that negative and positive differences between horizontal and vertical readings are good indicators of whether the main water and salt movement in the soil profile is typified by leaching or capillary rise, respectively. The differences determined in this study are listed in Appendix 9.1.4. As water in

the vadose zone flows downward, salts are transported in that direction as well. Similarly, as water moves upward in the vadose zone the salts are transported upward. Thus, distributions of salinity with depth can be used as indicators of the direction of water movement in the vadose zone within the depth range of induction measurements. The data presented in Appendix 9.1.4 and illustrated in Figures 14a - 14e seem to indicate water movement that is very nonuniform in the prescribed range. In other words, distributions of salinity with depth at adjacent measurement locations indicate water moving in opposite directions. Also, the data indicate that the flow direction often changes from month to month at several measurement locations. This is not surprising, considering the measurements vary in time with respect to irrigation and rainfall events. All of this may imply that the flow regime between 0.75 m and 1.5 m is very complex - changing frequently with respect to both space and time.

4.4.2 Correlation of Electromagnetic Induction Measurements to Crop Productivity

Salinity surveys based on visual agronomic observations and electromagnetic induction measurements clearly indicate a very strong correlation between the two survey methods. In Figure 15a productivity indices, defined in the previous chapter, and induction measurements are plotted along a transect of the center bench. This particular transect is located on the EM grid (refer to section 3.3) at x = 40 m and measurements were recorded at 15-m intervals starting at y = 0 m and ending with y = 225 m. Similar graphs were created for each of the transects surveyed. Some of these graphs illustrate the correlation quite distinctly while others do not show the correlation so clearly. Figure 15b shows the range of

Figure 14a - Contour map of differences between EM38 measurements made in January at 0.75m and 1.5m depth. White indicates higher salinity near the surface, gray indicates higher salinity at depth.
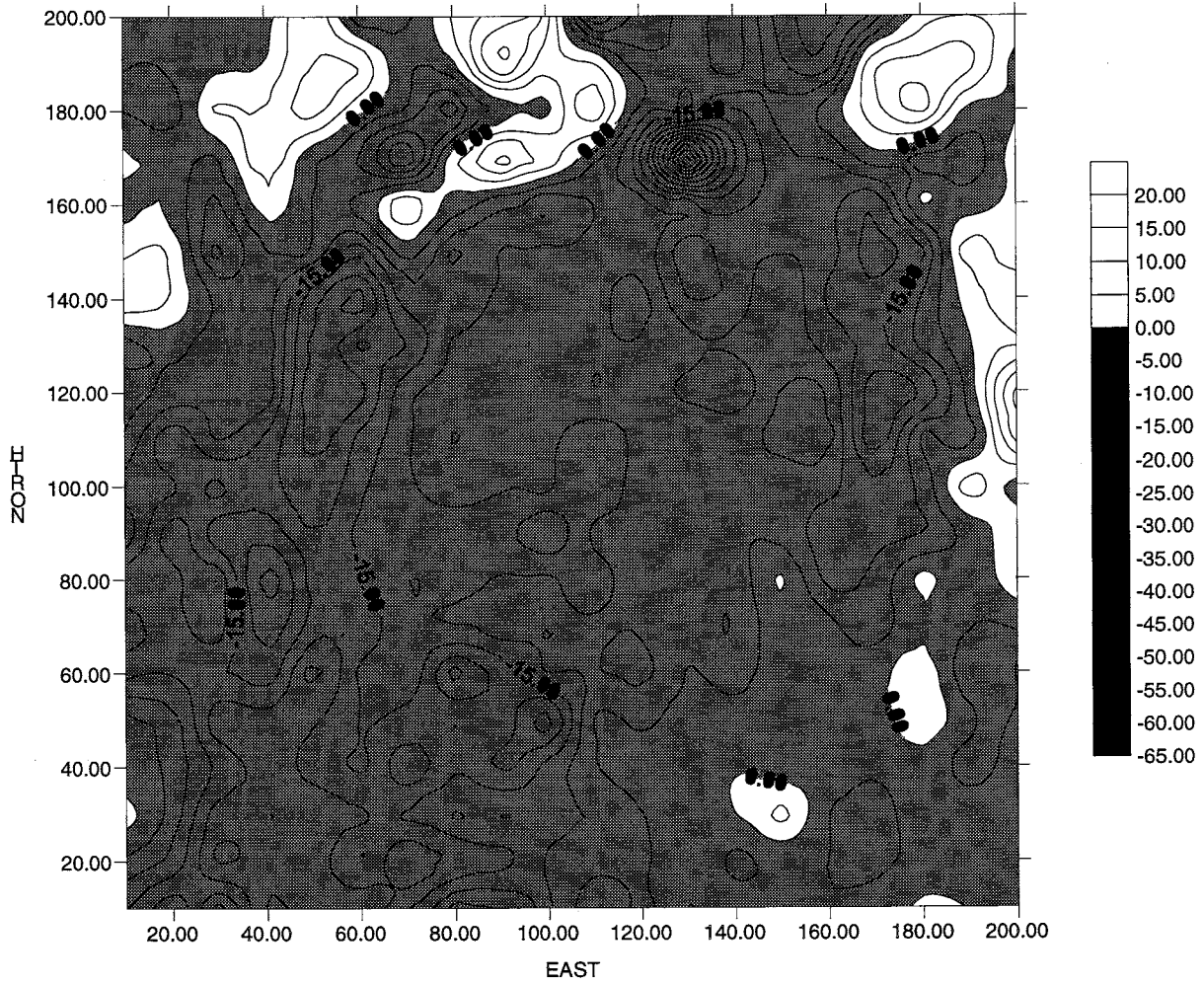
Figure 14b - Contour map of differences between EM38
made in february at 0.75m and 1.5m depth. White indicates
higher salinity near the surface, gray indicates higher
saliniy at depth.
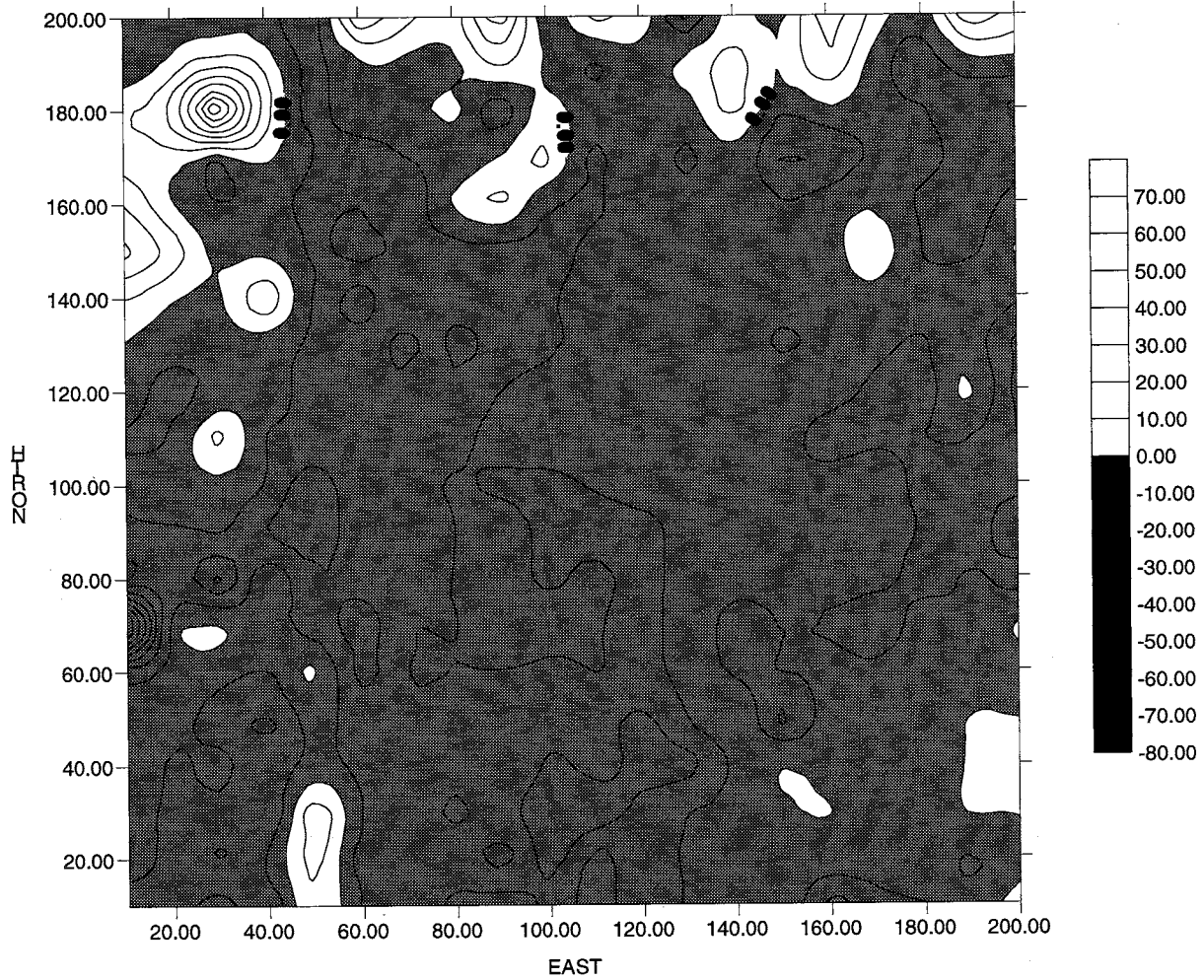
Figure 14c - Contour map of differences between EM38 measurements made in March at 0.75m and 1.5m depth. White indicates higher salinity near the surface, gray indicates higher salinity at depth.
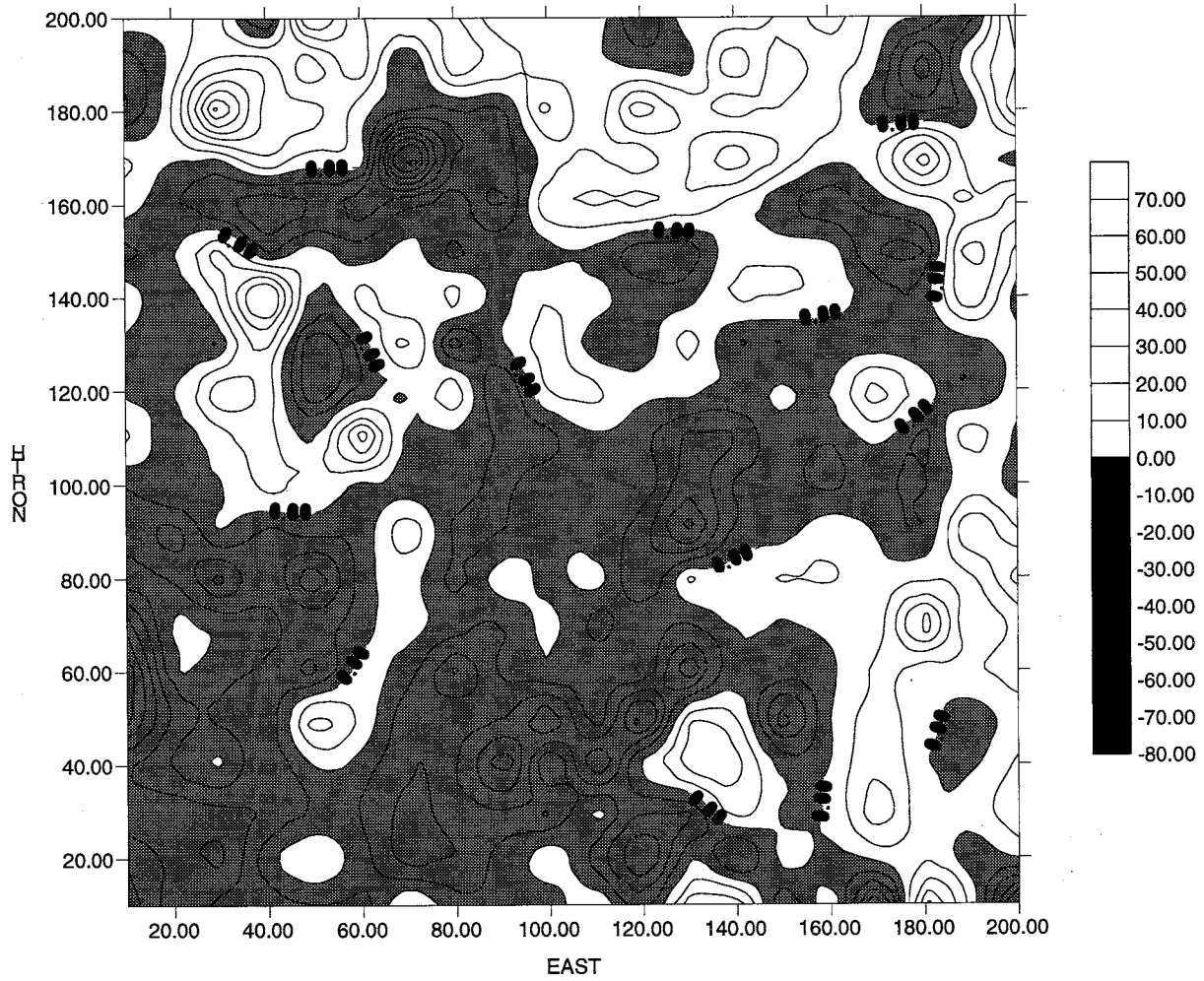
Figure 14d - Contour map of differences between EM38 made in April at 0.75m and 1.5m depth. White indicates higher salinity near the surface, gray indicates higher salinity at depth.
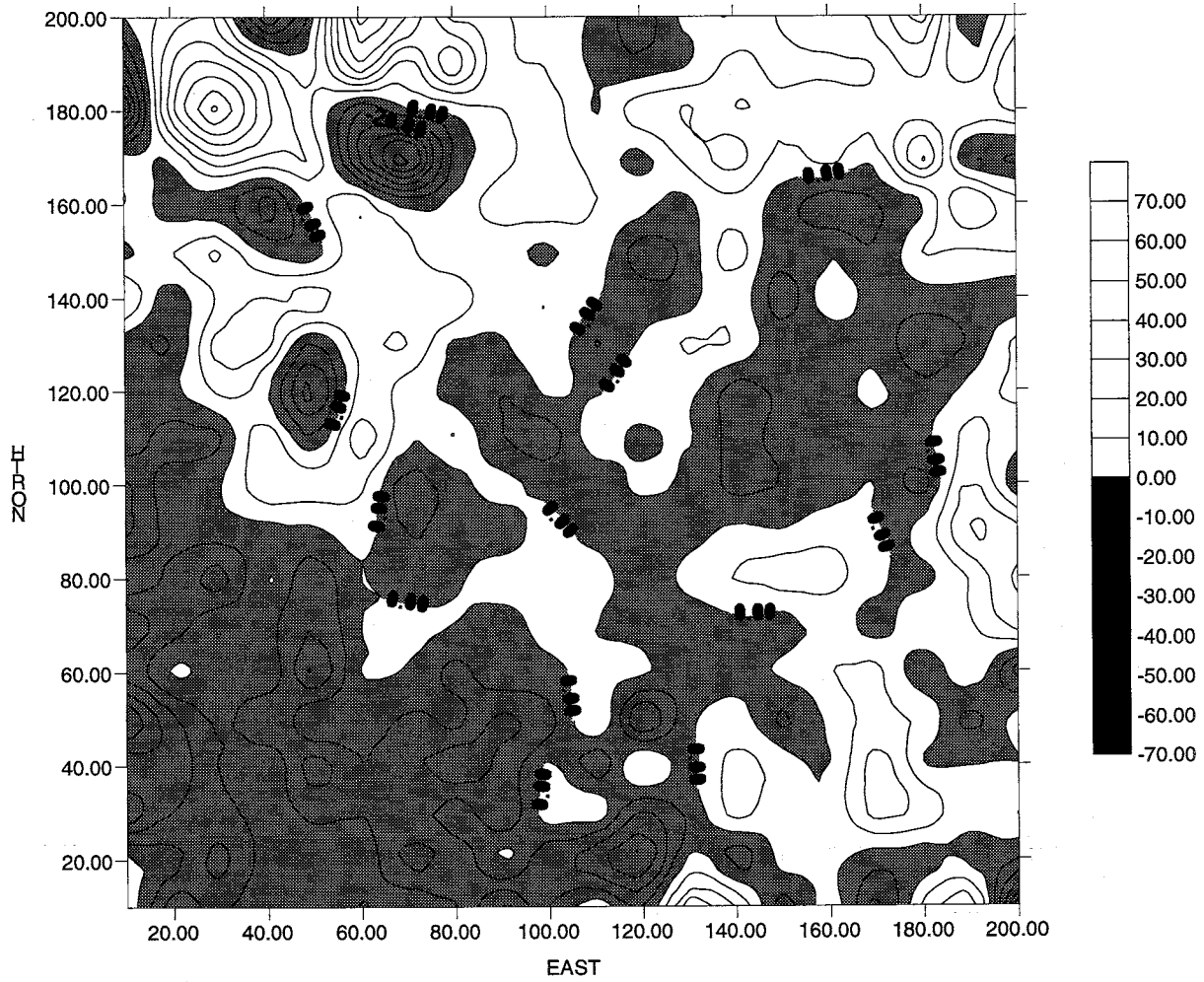
Figure 14e - Contour map of differences between EM38 measurements made in May at 0.75m and 1.5m depth. White indicates higher salinity near the surface, gray indicates higher salinity at depth.
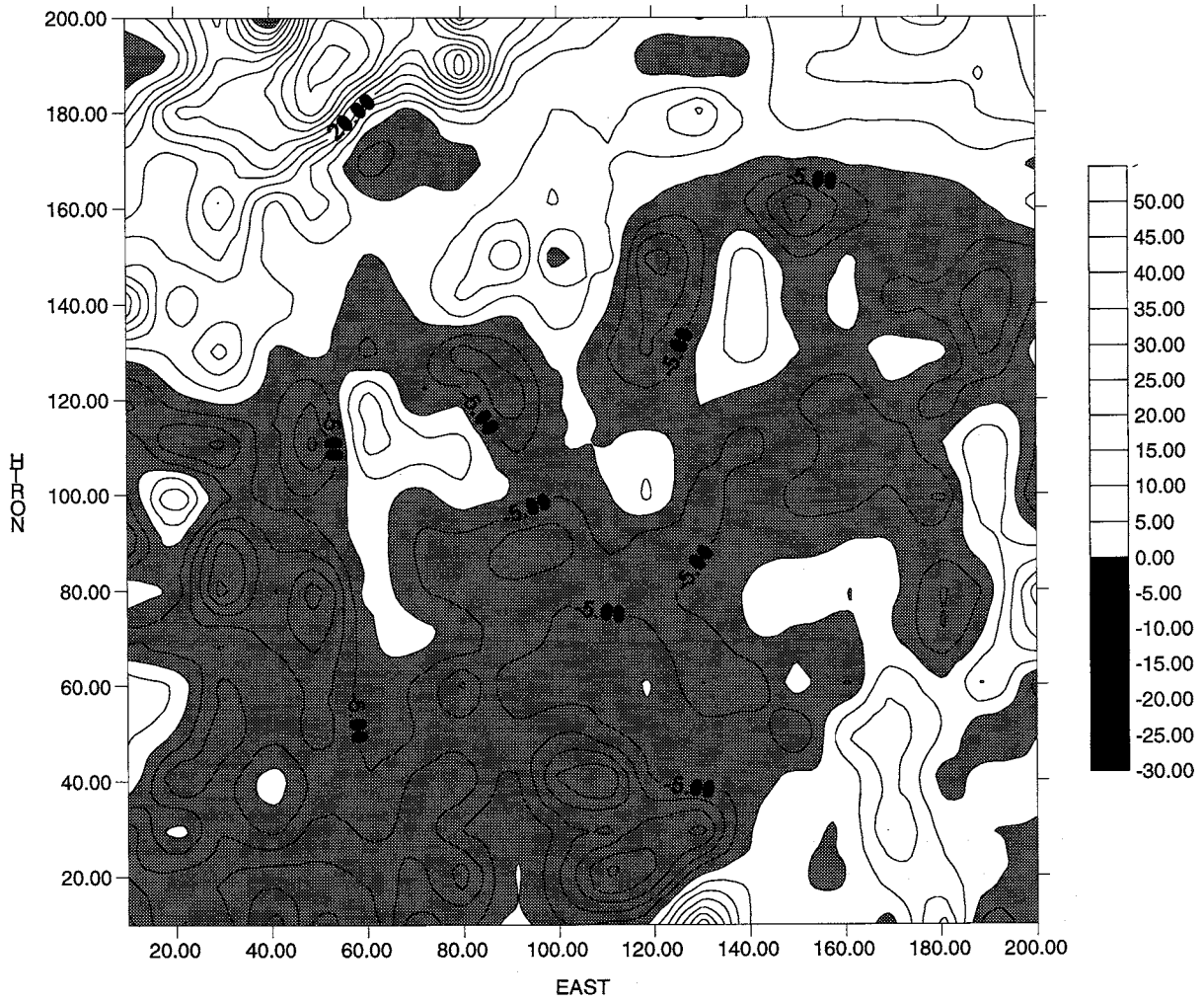
Figure 15a. EM Measurements and Crop Productivity Along a Transect
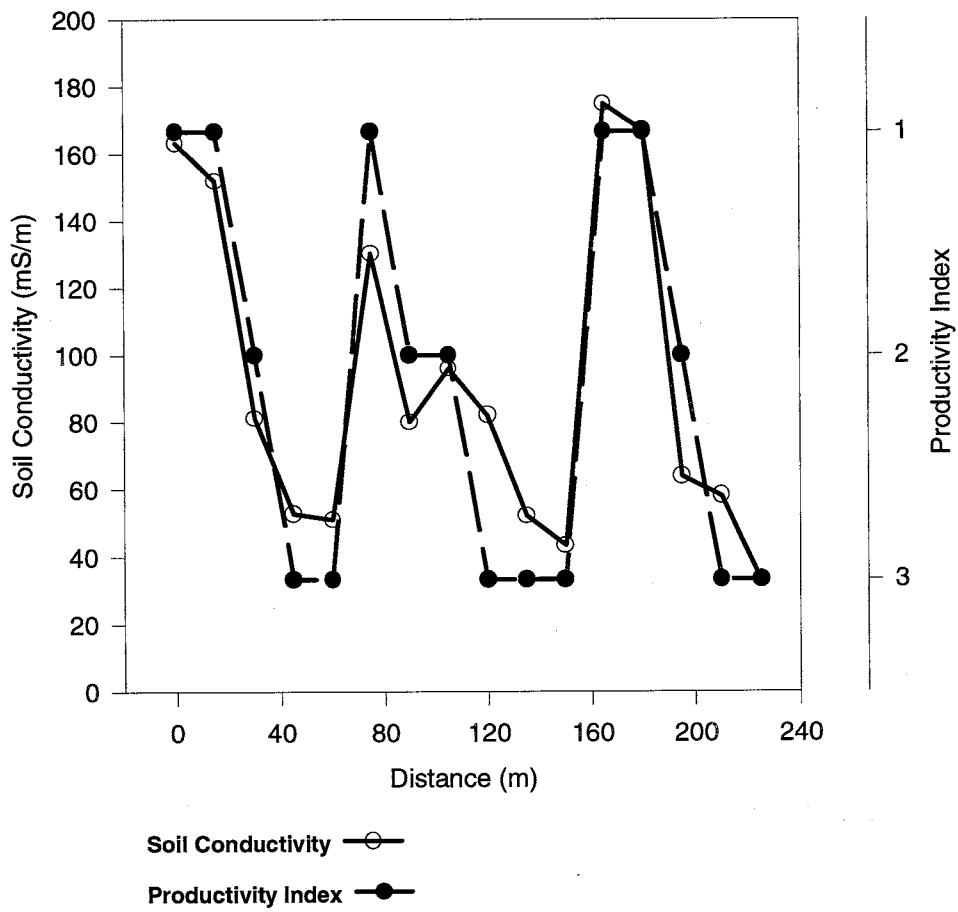
Figure 15b - EM38 Measurements & Crop Productivity
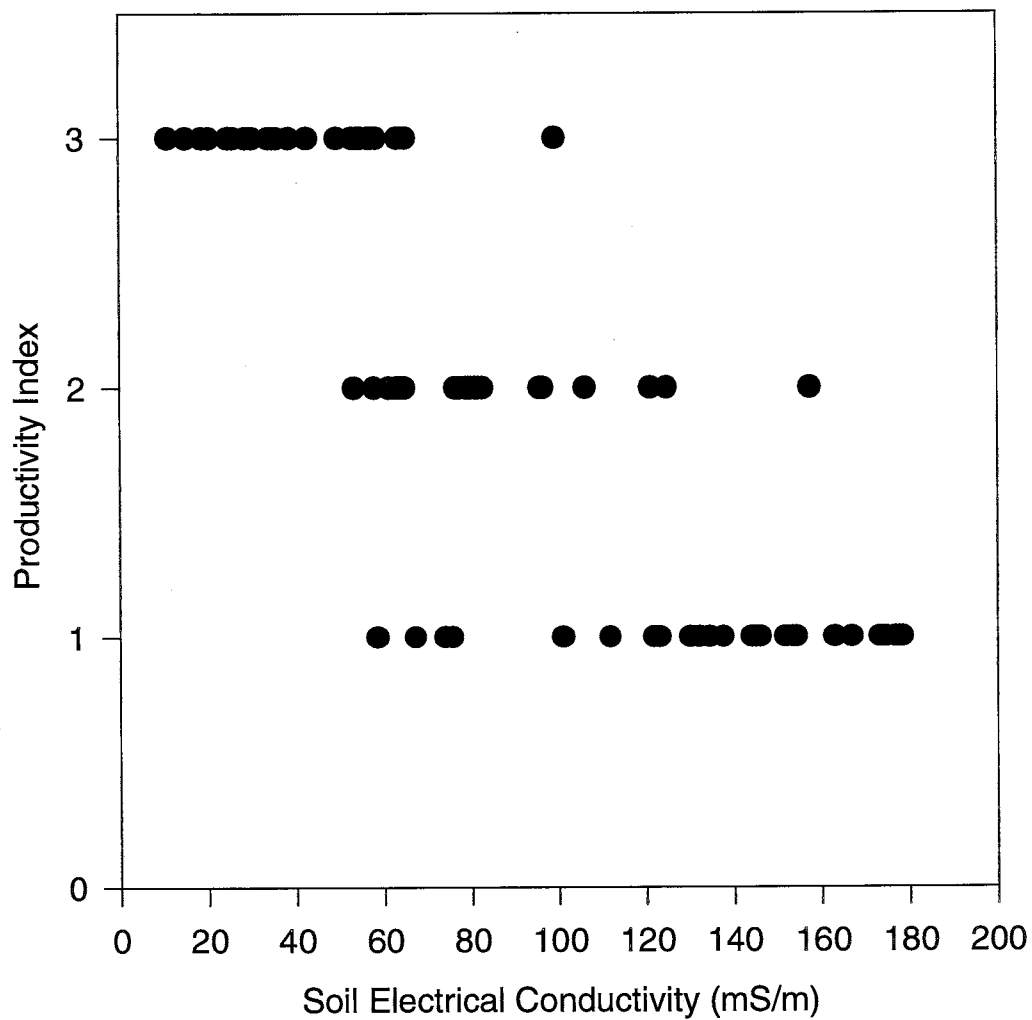
induction measurements for each of the productivity indices and, because it includes all of the data from the entire survey, it is an improved illustration of the correlation of the two survey methods. The correlation is further illustrated by making a visual comparison of a photograph taken from above the surveyed field and contour maps of induction measurements at 0.75 m and 1.5 m depths. The photograph and contour maps, presented in Figures 16a, b, and c indicate that areas of high electrical conductivity correspond to areas on the bench where the crop has been most severely affected. The comparison of the photograph with the 1.5-m depth measurements also serves to illustrate that the correlation at this depth is not obscured by the water table since the water table is rarely deeper than 1.5 m beneath the soil surface.

A convenient feature of the electromagnetic induction method is the relatively simple method employed to convert EC_a measurements into average root zone salinities, EC_e. Historically, many laboratory analyses were required for each soil unit in order to establish the calibration relationship for the conversion (Hendrickx, 1992). Recently, however, Rhoades et al. (1988,1990) have demonstrated that adequate soil salinity assessments can be obtained from electromagnetic induction measurements combined with field estimates of clay and soil water content. Estimates of EC_e have been calculated from a set of EC_a data recorded in May, 1994 and are found in Appendix 8.1.5. In the current study analyses have been executed on the EC_a values which have been shown herein to be directly related to soil salinity.

Figure 16a. Contour Map of May 30,1994 EM38 Measurements at 0.75 m Depth.

North
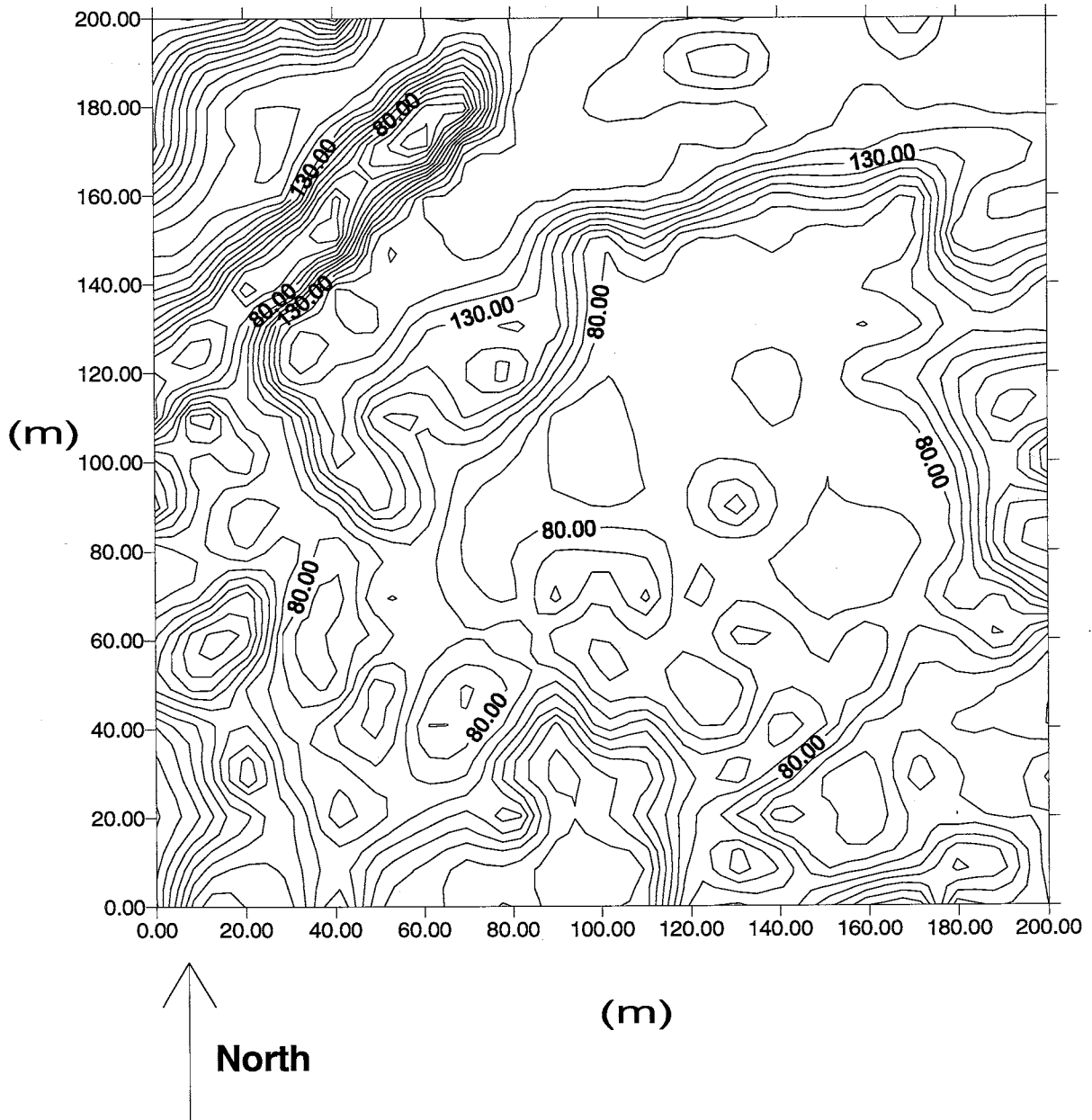
Figure 16b. Contour Map of May 13, 1994 EM38 Measurements at 1.5 m Depth.

North
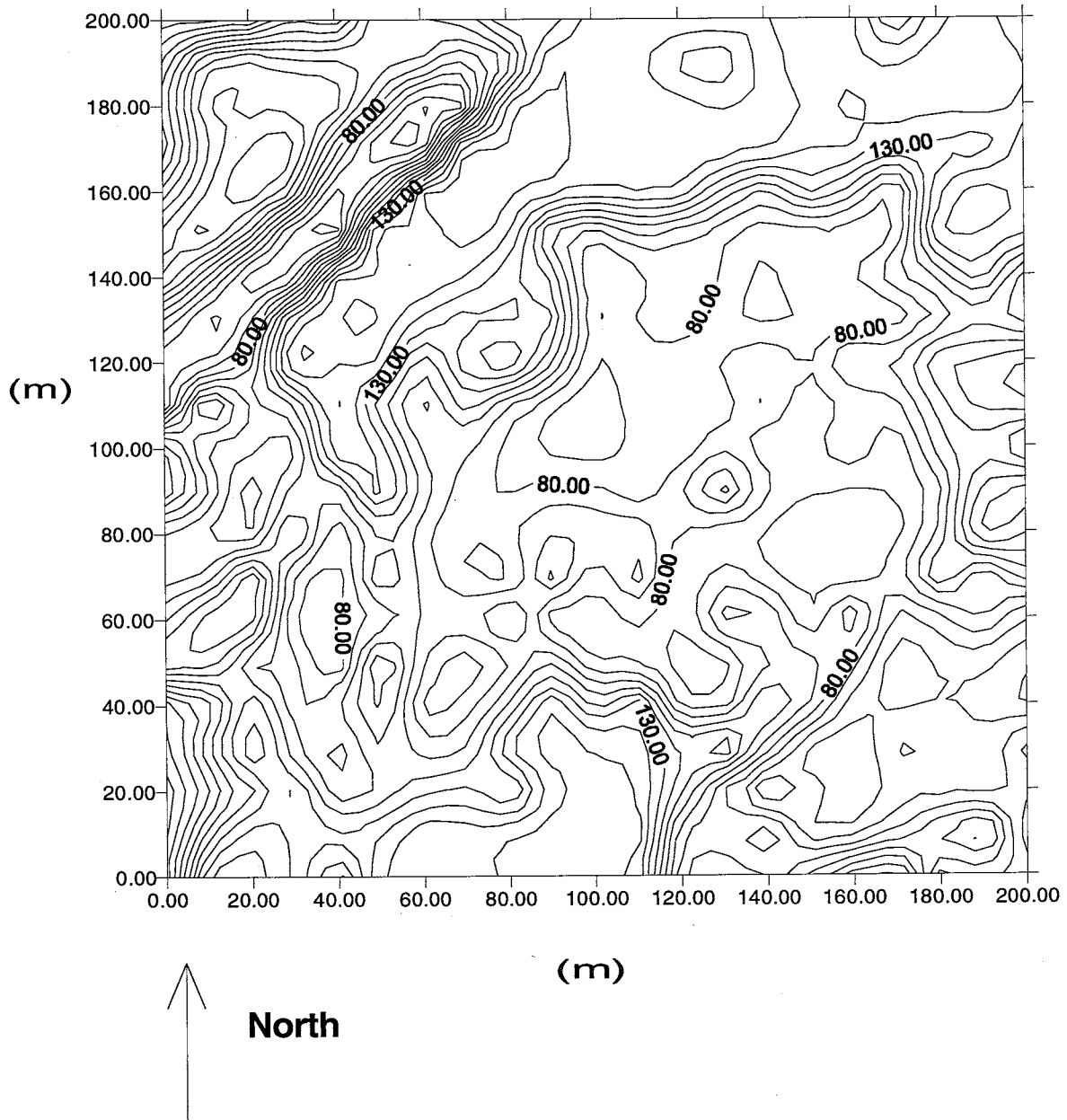
4.4.3 Spatial Variability of Electromagnetic Induction Measurements

In contrast to the hydraulic conductivity measurements, the electromagnetic induction measurements at 0.75 m depth exhibit a very high degree of spatial correlation. The variograms of the induction measurements are presented in Figures 17 - 21. The horizontal lines in these graphs indicate the variances of the measurements. Descriptive statistics for each of the monthly surveys are presented in Tables 11 and 12. Where the value of the semivariogram equals the variance, spatial dependency no longer exists. The variograms, therefore, indicate that the maximum distance of spatial dependency of the electromagnetic inductance data is approximately 100 meters. This is on the order of about half the size of the survey grid. A map of the various soil types encountered throughout the surveyed field (Figure 5) indicates that the variation of soil types is on a significantly smaller scale than the variation of salinity as determined by the spatial analysis of the inductance measurements. This verifies the well-known fact that irrigation and soil management in flat irrigated lands determine the spatial variability of salinity to a much greater extent than the prevalent soil characteristics (Hendrickx et al., 1992; Raats, 1975).

Figure 17 - Variogram for EM38 Data at 0.75 m Depth - Jan. 13, 1994
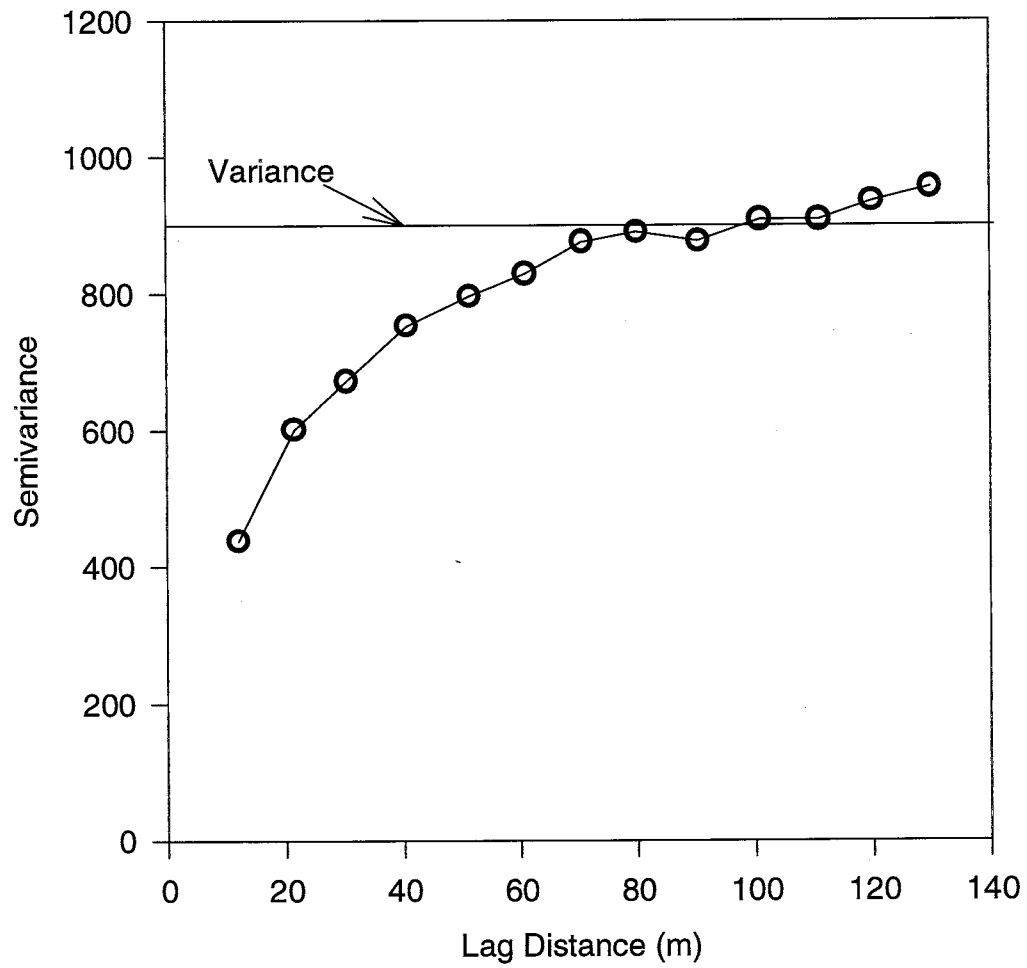
Figure 18. Variogram for EM38 at 0.75 m Depth Data - Feb. 27, 1994
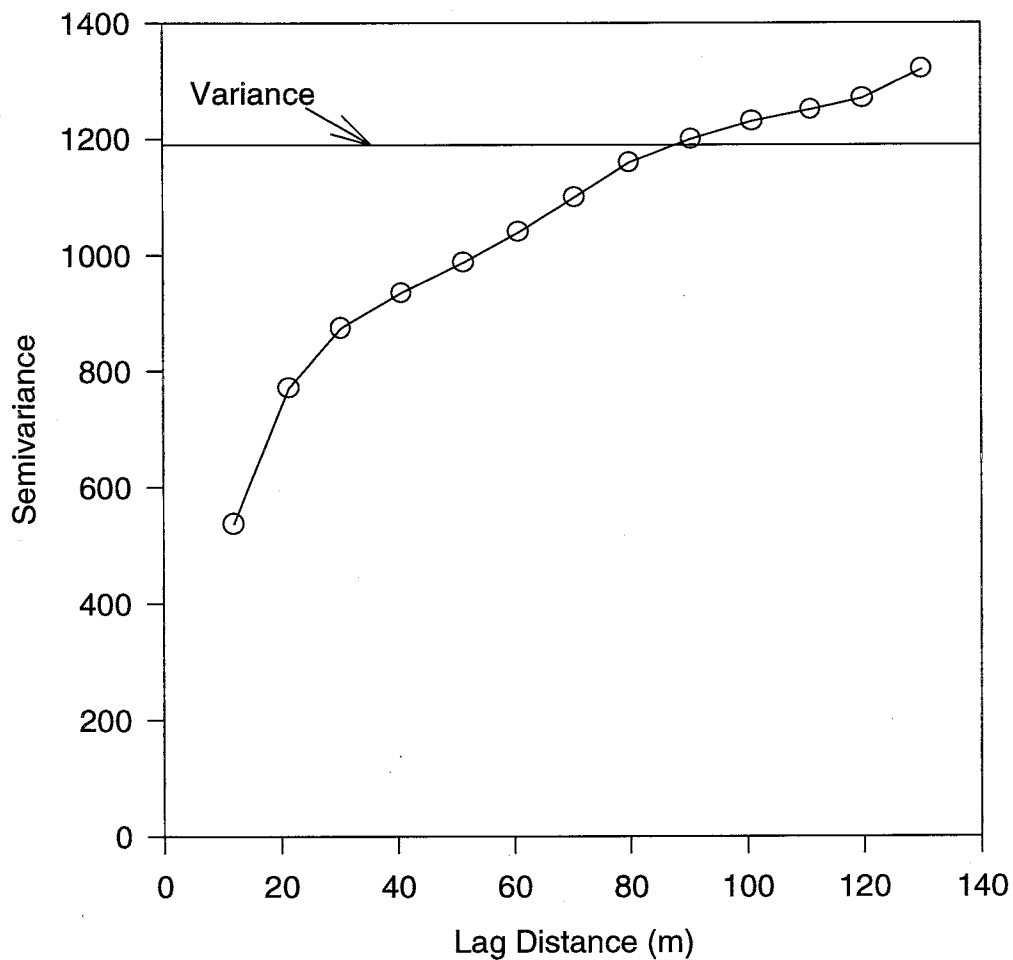
Figure 19. Variogram for EM38 Data at 0.75m Depth-Mar. 22, 1994
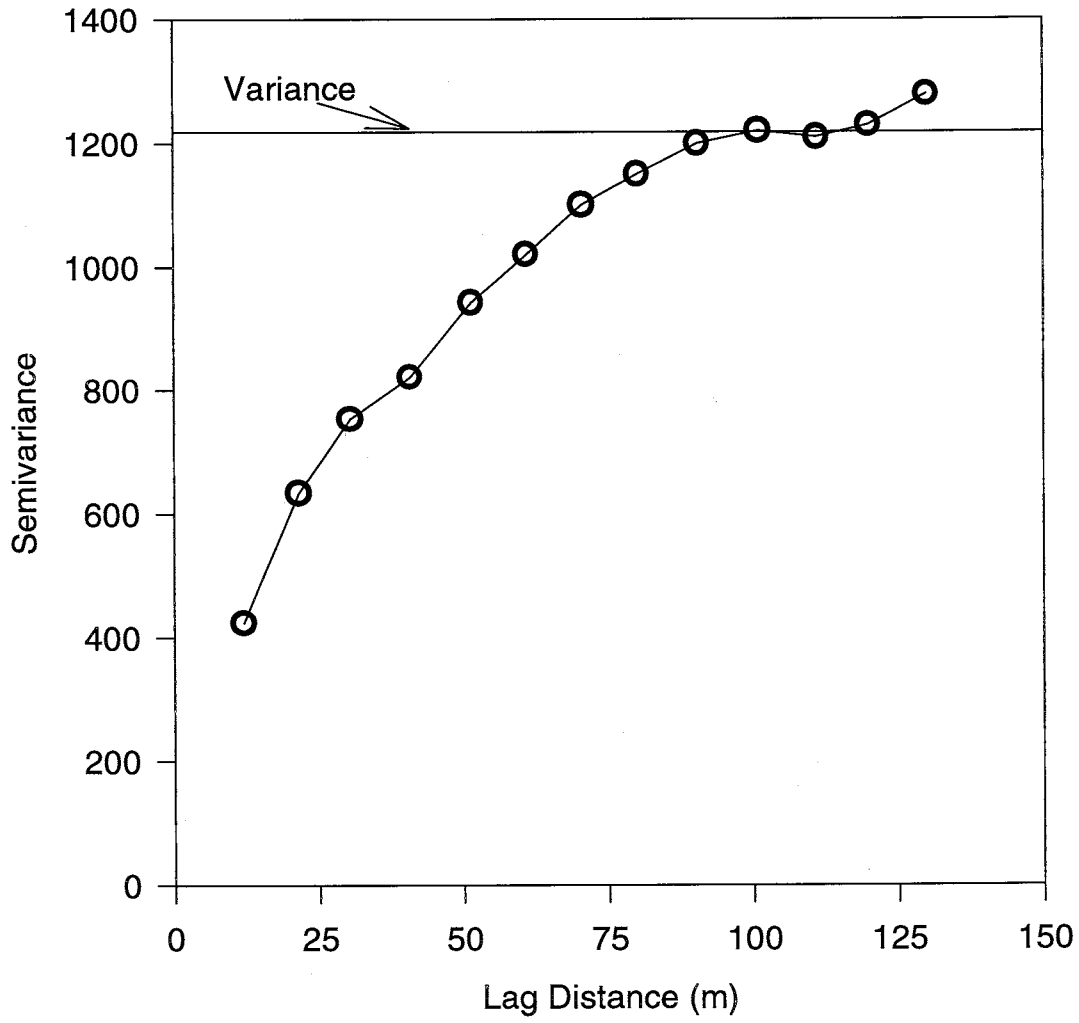
Figure 20. Variogram for EM38 Data at 0.75m-April 29, 1994
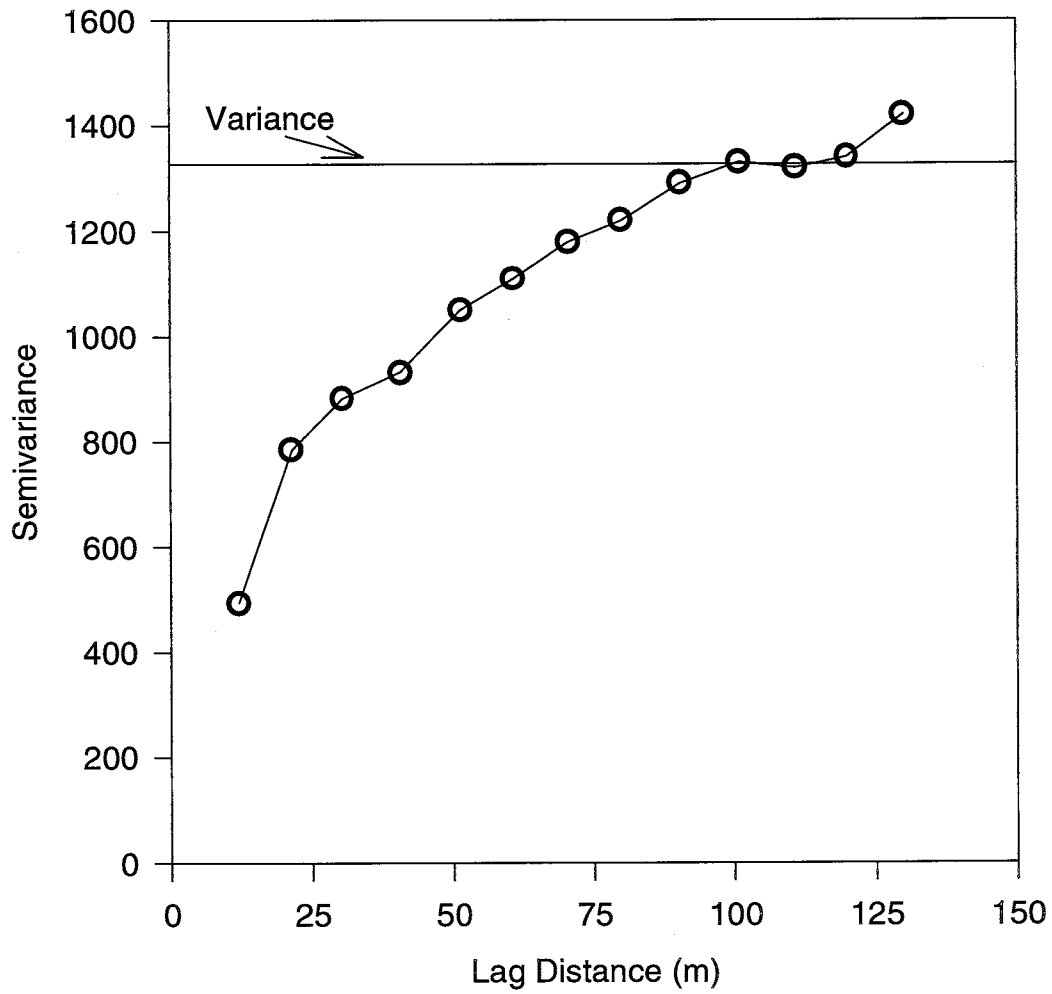
Figure 21. Variogram for EM38 Data at 0.75m Depth-May 30, 1994
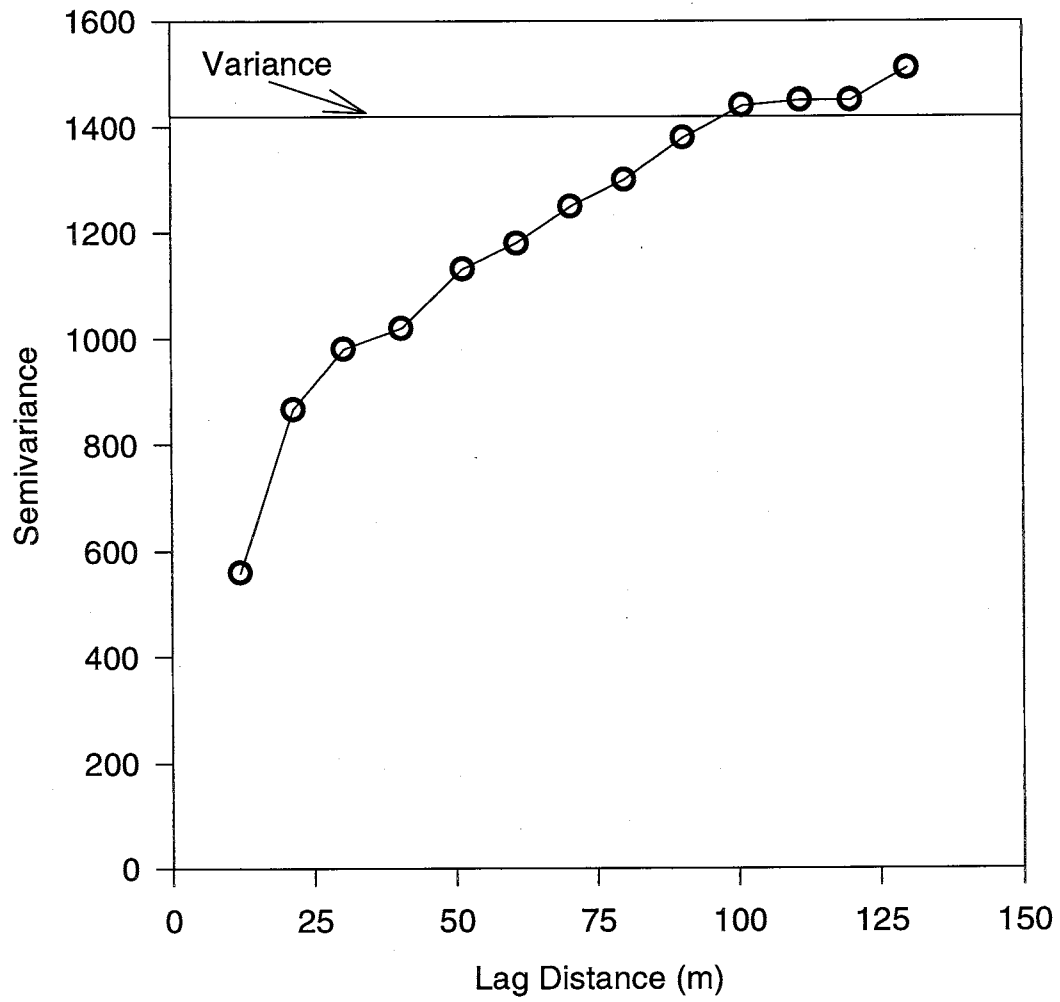
Table 11

Descriptive Statistics for EM38 Measurements to 0.75 m Depth

	January	February	March	April	May
Mean	59.9	72.6	91.8	98.3	104.4
Standard Error	1.51	1.73	1.75	1.82	1.79
Median	53.2	61.5	80.8	89.5	95.9
Mode	51.3	46.8	77.3	69.4	98.9
Standard Deviation	30.2	34.5	34.9	36.4	37.6
Sample Variance	912	1190	1220	1330	1410
Kurtosis	-0.182	-0.172	-0.770	-1.02	-1.27
Skewness	0.633	0.811	0.463	0.315	0.165
Range	150	159	161	149	143
Minimum	10.2	17.6	14.3	19.7	25.2
Maximum	160	177	175	168	168
Significance level, α	0.05	0.05	0.05	0.05	0.05

Table 12

Descriptive Statistics for EM38 Measurements to 1.5 m Depth

	January	February	March	April	May
Mean	68.0	79.8	93.0	97.6	104.0
Standard Error	1.57	1.72	1.64	1.62	1.70
Median	62.3	71.3	88.5	92.6	100.3
Mode	50.3	71.3	74.2	81.4	130
Standard Deviation	31.4	34.4	32.8	32.5	35.6
Sample Variance	987	1180	1080	1060	1270
Kurtosis	-0.558	-0.358	-0.795	-0.906	-1.17
Skewness	0.406	0.594	0.302	0.171	0.0213
Range	151	156	150	141	138
Minimum	13.7	21.1	18.4	27.9	28.8
Maximum	165	177	168	169	166
Significance level, α	0.05	0.05	0.05	0.05	0.05

5. CONCLUSIONS

5.1 Infiltrometer Experiment

The results of the infiltrometer experiment are very strong evidence of the existence of a complex system of macropores which are highly variable both with respect to time and space. Therefore, the model under development should include a preferential flow component. The lack of spatial structure among the hydraulic conductivity measurements indicates that the variability among K values is random with respect to location. In other words, it is very difficult to predict K based on measured values. The hydraulic conductivity at tensions less than 6 cm is subject to significant temporal changes. Since the temporal variability was only observed at low tensions, the process(es) involved are clearly only affecting the soil macropores. This effect has been attributed to macropore development due to root growth and to the wetting and drying cycles of flood irrigation practices.

5.2 Laboratory Measurements

The tension range of the hanging water column experiment executed in the laboratory was limited to values between 0- and 170 cm due to the short space available for lowering the water column. This limitation necessitated that a very large portion of the $\theta(\psi)$ and $K(\psi)$ functions be extrapolated, leading to significant uncertainty regarding the estimates of $K(\psi)$ provided by these functions. The large values of these estimates may also imply that they of suspect accuracy. Measurements of K or θ in the high soil water tension range should be obtained in

order to constrain the fitting of hydraulic parameters thus leading to greater accuracy of the hydraulic functions.

5.3 EM-38 Surveys

A strong correlation exists between electromagnetic induction measurements and salinity surveys based on visual observations of crop productivity. The determination of this correlation was possible because the crop, corn at the time of the survey, was highly affected by the saline conditions of the soil. However, now that the correlation has been established, surveys can be made even in the absence of a crop and may aid the farmer in decisions regarding which sections of his land are suitable for planting.

Differences between induction measurements at 0.75 m and 1.5 m are highly variable both with respect to time and to space, changing from positive to negative at adjacent measurement locations and at the same locations from month to month. This implies that the distribution of salts within the measurable depth range as well as the manner with which soil water is moving is very complex.

The spatial analysis of the induction measurements indicates a very high degree of structure. This structure is significant to a distance of approximately 100 m. Over the time period from January to May of 1994 there appears to be very little change in measured values of the EC_a and little or no change in the variability and distribution of the measurements in space. Generally, EM measurements are affected by porosity, amount and composition of clays and colloidal particles, moisture content, dissolved salt concentration, and the temperature and phase of the pore water. While it is not likely that the porosity or the clay composition of the

67

soil at the field site experienced significant changes during the time frame of the EM surveys, changes in salinity, moisture content, and pore water temperature are likely. McNeill (1980a) has attempted to quantify the effects of each of these properties. While the expressions he developed to account for these effects individually are relatively simple, accounting for the combined effects remains largely uncertain. The increase in the mean of values with respect to time may be caused by the increase of soil temperature associated with the onset of spring. However, this can not be verified in the current study since the temperature of the soil was not recorded during the surveys. Though no soil moisture content data is available, it is very likely that water contents in the soil profile are significantly variable. In the winter months the water table is at its deepest level of the year and begins to rise during spring. Undoubtedly, the soil salinity distribution also exhibits variation as salts are transported with changing moisture profiles. However, without more information regarding soil temperature and moisture content, it remains extremely difficult to resolve how much of the observed changes are due to changes in the salinity of the pore water.

6. RECOMMENDATIONS

To better understand the nature of the temporal variation in hydraulic conductivity measured at low tensions, infiltrometer measurements should be made at regular time intervals throughout the year, particularly during the growing season when the effects of irrigation and root development. It is impractical to repeatedly make the measurements at all of the locations measured in the current study.

These measurements should be recorded at as many locations as can be accomplished in one to two days (approximately 10 - 20). If this becomes too labor-intensive, measurements at fewer locations may still provide enough information to further analyze the temporal variation of $K(\psi)$ assuming the measurements are recorded regularly. Particular attention should be given to measured values before and after irrigation events to better quantify the effects that wetting and drying cycles may have on these measurements. The crop is no longer the sorghum/sudan cross that was present at the time the measurements were recorded for this study. Therefore, the effect of root growth seen in the data presented in the current study will be difficult to further analyze. However, effects that alfalfa root systems have on the temporal variability of macropore flow could be observed more closely. This might be accomplished by carefully removing small sections of the crop and measuring the diameters of the roots as they develop throughout the growing season. These measurements could then be compared to any changes in infiltrometer measurements which may be observed.

The EM38 measurements are currently made on a fine grid. The high degree of spatial correlation of the measurements may indicate that the grid spacing could be increased to reduce the time needed for each survey. Also, for future surveys, soil temperature variations must be monitored so that appropriate corrections can be executed. Information regarding the changes in the soil moisture content combined with temperature data will aid greatly in resolving the effects of variable soil salinity on the induction measurements. In the current study, analyses were made of EM data collected over a few months and very little data was collected

during the growing season. Since it is unnecessary to execute the surveys on such a fine grid, the measurements should be executed more frequently on a coarser grid, thereby obtaining more information regarding the temporal variability of the induction measurements. Differences between the horizontal and vertical measurements should then be analyzed for indications of water flow direction based on frequent measurements made immediately before and after irrigation and rainfall events. Such information could be very useful for validating the model that the project seeks to develop. However, the limited quantity of data collected so far is insufficient for such a purpose.

7. REFERENCES

Akram, M., and W. D. Kemper. 1979. Infiltration of soils as affected by the pressure and water content at the time of compaction. Soil Sci. Soc. Am. J. 43:1080 -1086.

Ankeny, M. D. 1992. Methods and theory for unconfined infiltration measurements. Ch. 7. *In* Advances in measurements of soil physical properties: Bringing theory into practice. Special Publication no. 30. Soil Science Society of America, Madison WI.

Ankeny, M. D., M Ahmed, T. Kaspar, and R. Horton. 1991. Simple field method for determining unsaturated hydraulic conductivity. Soil Sci. Soc. Am. J. 55:467- 470.

Ankeny, M. D., T. C. Kaspar, and R. Horton. 1990. Characterization of tillage and traffic effects on unconfined infiltration measurements. Soil Sci. Soc. Am. J. 54:837-840.

Barley, K. P. 1954. Effects of root growth and decay on the permeability of synthetic sandy soil. Soil Sci. 78:205-210.

Boivin, P., D. Brunet, and J. O. Job. 1988. Conductivimétrie électromagnétique et cartographie automatique des sols salés: une méthode rapide et fiable, Cah. ORSTOM. Ser. Pedol. 24:39-48.

Bowman, R. S., J. M. H., Hendrickx, and S. Bulsterbaum. 1992. Las Nutrias groundwater project. *In* Proc. of New Mexico conference on the environment. Albuquerque, New Mexico.

Bradley, J. V. 1980. Non-robustness in classical tests on means and variances: A large scale sampling study. Bulletin Psychonomics Society, v. 15, No. 4.

Caravallo, H. O., D. K. Cassel, J. Hammond, and A. Bauer. 1976. Spatial variability of in situ unsaturated hydraulic conductivity of maddock sandy loam. Soil Sci. 121 (1):1-8.

Carter, M. R. 1988. Temporal variability of soil macroporosity in a fine sandy loam under moldboard ploughing and direct drilling. Soil Tillage Res. 12:37-51.

Clothier, B. E., and I. White. 1981. Measurement of sorptivity and soil water diffusivity in the field. Soil Sci. Soc. Am. J. 45:241-245.

de Jong, E., A. K. Ballantyne, D. R. Cameron, and D.W.L. Read. 1979. Measurement of apparent electrical conductivity of soils by an electromagnetic induction probe to aide salinity surveys. Soil Sci. Soc. Am. J. 43:810-812.

Elrick, D. E., W. D. Reynolds, and K. A. Tan. 1988. A new analysis for the constant head well permeameter. *In* P. J. Wierenga (ed) Proc. Int. Conf. and Workshop on the validation of flow and transport models for the unsaturated zone, Ruidoso, NM. 22-25 May.

Gardner, W. R. 1958. Some steady-state solutions of the unsaturated moisture flow equation with applications to evaporation from a water table. Soil Sci. 85:228-232.

Greenholtz, D. E., T-C Jim-Yeh, M. S. B. Nash, and P.J. Wierenga. 1988. Geostatistical analysis of soil hydraulic properties in a field plot,. Jour. Cont. Hydr. 3:227-250.

Hackett, C. 1969. Quantitative aspects of the growth of cereal root systems *In* W. J. Whittington (ed.) Root Growth. Buttersworth, London.

Hendrickx, J. M. H., B. Baerends, Z. I. Raza, M. Sadig, and M. Akram Chaudhry. 1992. Soil salinity assessment by electromagnetic induction of irrigated land. Soil Sci. Soc. Am. J. 56:1933-1941.

Hendrickx, J. M. H., Grande,C. D., A. B. Buchanan, and R. E. Bretz. 1994. Electromagnetic induction for restoration of saline environments in New Mexico. Ch. 13 *In*: ECM series on environmental management & intelligent manufacturing, R. Bhada (ed.), vol. 1, Waste-management: From risk to remediation. Dept. WERC, Las Cruces, NM.

Job, J. O., J. Y. Loyer, and M. Ailoul. 1987. Utilisation de la conductivité électromagnétique por la mésure directe de la salinité des sols. Cah. ORSTOM, Ser. Pedol. 23:123-131.

Journel, A. G., and Ch. J. Huijbregts. 1978. Mining geostatistics. Academic Press, London.

Jury, W. A., Gardner, W. A., and Gardner, W. H. 1991. Soil physics. John Wiley & Sons, Inc. New York.

McNeill, J. D. 1980a. Electrical conductivity of soils and rocks. Tech. note TN - 5, Geonics Ltd. Mississauga, Ontario.

McNeill, J. D. 1980b. Electromagnetic terrain measurement at low induction numbers. Tech. note TN-6, Geonics Ltd. Mississauga, Ontario.

McNichols, R. J., and C. B. Davis. 1988. Statistical issues and problems in ground-water detection monitoring at hazardous waste facilities. Ground-Water Monitoring and Review. Fall, 1988.

Meek, B. D., E. A. Rechel, L. M. Carter, and W. R. DeTar. 1989. Changes in infiltration under alfalfa as influenced by time and wheel traffic. Soil Sci. Soc. Am. J. 53:238-241.

Mohanty, B. P., M. D. Ankeny, R. Horton, and R. S. Kanwar. 1994. Spatial analysis of hydraulic conductivity measured using disc infiltrometer. Water Resources Research. In Press.

Mualem, Y. 1976. A new model for predicting the hydraulic conductivity of unsaturated porous media. Water Resour. Res. 12:513-522.

Nielsen, D. R., J. W. Biggar, and K. T. Erh. 1973. Spatial variability of field measured soil-water properties. Hilgardia. 42(7):215-260.

Philip, J. R. 1985. Reply to "Comments on Steady Infiltration from Spherical Cavities". Soil Sci. Soc. Am. J. 49:788-789.

Raats, P. A. C. 1975. Distribution of salts in the root zone. H. Hydrol. 27:237-248.

Rhoades, J. D., and D. L. Corwin. 1981. Determining soil electrical conductivity-depth relations using an inductive electromagnetic soil conductivity meter. Soil Sci. Soc. Am. J. 45:788-789.

Rhoades, J. D., P. J. Shouse, W. J. Alves, N. A. Manteghi, and S. M. Lesch. 1990. Determining soil salinity from soil electrical conductivity using different models and estimates. Soil Sci. Soc. Am. J. 54:46-54.

Rhoades, J. D., B. L. Waggoner, P. J. Shouse, and W. J. Alves. 1988. Determining soil salinity from soil and soil-paste electrical conductivities: Sensitivity analysis of models. Soil Sci. Soc. Am. J. 53:1368-1374.

Ross, M. S. 1987. Introduction to probability and statistics for engineers and scientists. John Wiley and Sons, New York, NY.

Roybal, F. E. 1991. Ground-water resources of Socorro County, New Mexico. Report 89-4083. 32 pp. U. S. Geological Survey, Water Resources Investigations. Albuquerque, New Mexico.

Russell, R. S. 1977. Plant root systems. McGraw-Hill Book Co., London.

Scheffé, H. 1959. The analysis of variance. John Wiley and Sons, Inc. New York, NY.

Schmidt-Petersen, R. I. 1991. Field simulation of waste impoundment seepage in the vadose zone: Horizontal spatial variability of the geologic and hydrologic properties of an alluvial fan facies. Hydrology report No.: H91-1. New Mexico Institute of Mining and Technology, Socorro, New Mexico.

Scotter, D. R. 1984. Preferential solute movement through larger soil voids: I.

Some computations using simple theory. Aust. J. Soil Res. 16:257-267.

Sheets, K. R., J.P. Taylor, and J.M.H. Hendrickx. 1994. Rapid salinity mapping by electromagnetic induction for determining riparian restoration potential. Restoration Ecology. 2:242-246.

Shirmohammadi, A., and R.W. Skaggs. 1984. Effect of surface conditions on infiltration for shallow water table soils. Transactions of the ASAE. 27(6): 1780-1787.

Siegel, A. F. 1990. Practical business statistics. Irwin Publishing. Boston, MA.

Smetten, K. R. J. 1987. Characterization of water entry into a soil with a contrasting textural class: Spatial variability of infiltration parameters and influence of macroporosity. Soil Sci. 144(3):167-174.

Trojan,M. D., and D. R. Linden. 1992. Effect of surface microrelief and rainfall intensity on water and solute movement in earthworm burrows. Soil Sci. Soc. Am. J. 56:727-733.

van Genuchten, M. Th. 1980. A closed-form equation for predicting the hydraulic conductivity of unsaturated soils. Soil Sci. Soc. Am. J. 44:892-898.

van Genuchten, M. Th., F. J. Leij, and L. J. Lund (eds.). 1991a. Proc. Int. Workshop. Indirect methods for estimating the hydraulic properties of unsaturated soils. Univ. California, Riverside. August 11 -13.

van Genuchten, M. Th., F. J. Leij, and S. R. Yates. 1991b. The RETC code for quantifying the hydraulic functions of unsaturated soils. U. S. Salinity Laboratory, USDA - ARS. Riverside, CA.

Wager, M. D., and H.P. Denton. 1989. Influence of crop and wheel traffic on soil physical properties in continuous non-till corn. Soil Sci. Soc. Am. J. 53:1206-1210.

Warner, G. S., and R. A. Young. 1991. Measurement of preferential flow beneath mature corn. *In* the Proc. of Nat. Symp. on preferential flow. T. J. Gish and A. Shirmohammadi (eds). ASAE, St. Joseph, Michigan.

White, I., and K. M. Perroux. 1987. Use of sorptivity to determine field soil hydraulic properties. Soil Sci. Soc. Am. J. 51:1343-1346.

White, I., and K. M. Perroux. 1989. Estimation of unsaturated hydraulic conductivity from field sorptivity measurements. Soil Sci. Soc. Am. J. 53:324-329.

Wooding, R. A. 1968. Steady infiltration from a shallow circular pond. Water Resour. Res. 4:1259-1273.

Yates, S. R., and M. V. Yates. 1990. Geostatistics for waste management: A user's manual for the GEOPACK (Version 1.0) geostatistical software system. Robert S. Kerr Environmental Research Laboratory, Office of Research and Development, U.S. Environmental Protection Agency, Ada, Oklahoma.

8. APPENDICES

8.1 Field Data

8.1.1 ln K(ψ) Data (cm/s)

x	y	ln K0	ln K3	ln K6	ln K15
0	65	-8.04	-7.99	-7.91	-8.49
0	50	-6.36	-6.88	-7.19	-8.38
0	38	-5.21			-9.83
0	36.5	-5.68	-7.72	-8.38	-9.75
0	35	-5.32	-6.97		
0	33.5	-5.30	-7.01	-8.37	-9.90
0	32	-6.14	-7.64	-8.39	-8.89
0	30.5			-7.92	-8.88
0	29	-5.48	-7.39	-8.31	-9.00
0	27.5	-5.86	-6.60	-7.51	-8.39
0	26	-5.51	-6.91	-7.57	-8.64
0	24.5	-5.46	-7.46	-8.47	-9.17
0	23	-4.93	-7.54	-8.55	-9.00
0	21.5	-4.81	-7.24	-8.31	-9.17
0	20	-4.72	-6.97	-8.08	-9.03
0	18.5	-4.53	-6.90	-8.09	-9.09
0	17	-6.14	-7.50	-8.45	-9.09
0	15.5	-5.71	-7.71	-8.95	-9.37
0	14	-6.57	-7.95	-9.23	-9.92
0	12.5	-6.78	-7.82	-8.70	-9.53
0	11	-6.51	-8.03	-8.98	-9.53
0	9.5	-6.51	-8.03	-8.74	-9.50
0	8	-5.90	-7.32	-8.31	-9.50
0	6.5	-5.99	-7.65	-8.72	-10.07
0	5	-5.99	-7.78	-8.76	-9.70
0	3.5	-5.99	-7.65	-8.72	-10.07
0	2	-6.51			-8.92
0	1.5			-8.06	-9.00
0	1			-7.93	-9.31
0	0.5	-6.57	-7.65	-8.62	-9.70
0	0	-7.51	-8.25	-9.30	-10.61
0	-0.5	-6.45	-8.13	-9.00	-9.70
0	-1	-6.51	-7.85	-8.98	-10.02
0	-1.5	-7.75	-8.41	-8.74	-9.50
0	-2	-6.51	-8.03	-9.27	-9.97
0	-3.5	-5.95	-8.27	-9.64	-10.02
0	-5	-6.73	-7.57	-8.35	-9.29
0	-6.5	-7.21	-7.49	-7.94	-8.89
0	-8	-5.62	-8.19	-9.35	-10.12

8.1.1 In K(ψ) Data (continued)

x	y	ln K0	ln K3	ln K6	ln K15
0	-9.5	-6.07	-7.40	-8.54	-9.70
0	-11	-5.59	-7.07	-7.82	-8.61
0	-12.5	-5.09	-7.45	-8.57	-9.09
0	-14	-6.10	-7.44	-8.35	-9.29
0	-15.5	-6.64	-7.73	-8.67	-9.44
0	-17	-6.82	-7.69	-8.45	-9.09
0	-18.5	-6.82	-7.56	-8.19	-9.15
0	-20	-6.92	-7.56	-8.29	-9.09
0	-21.5	-6.29	-7.30	-8.02	-8.78
0	-23	-6.82	-7.69	-8.45	-9.09
0	-24.5	-6.73	-7.87	-8.55	-9.00
0	-26	-6.10	-7.56	-8.82	-9.90
0	-27.5	-6.10	-7.44	-8.50	-9.44
0	-29	-6.73	-7.70	-8.47	-9.17
0	-30.5	-5.46	-7.59	-8.94	-9.33
0	-32	-6.73	-7.70	-8.63	-9.37
0	-33.5	-6.64	-7.73	-8.86	-9.92
0	-35	-5.68	-7.64	-8.70	-9.53
0	-36.5	-6.82	-7.36	-8.39	-9.53
0	-38	-6.19	-7.26	-8.33	-9.37
0	-50	-6.92	-7.56	-8.29	-9.09
0	-65		-8.27	-8.42	-9.53
15	0	-3.96	-7.28	-8.50	-9.44
-15	0	-6.24	-7.23	-8.17	-9.09
-12.728	-12.728	-6.10	-7.44	-8.50	-9.44
12.728	-12.728	-5.85	-6.98	-8.08	-9.17
-12.728	12.728	-9.41	-8.00	-8.60	-9.78
-105	0	-5.51	-7.44	-8.31	-9.17
-90	0	-5.34	-7.49	-8.39	-8.70
-75	0	-6.58	-7.31	-8.17	-9.09
-60	0	-5.78	-7.37	-8.53	-9.92
-45	0	-6.21	-7.55	-8.50	-9.44
-30	0	-7.52	-7.46	-8.06	-9.00
30	0	-6.34			-9.17
45	0	-5.50	-7.61	-8.47	-9.17
60	0	-6.18	-7.93	-8.98	-10.02
75	0	-6.74	-7.69	-8.32	-9.15
90	0	-6.53	-7.80	-8.55	-9.00
105	0	-5.52	-7.44	-8.31	-9.17
12.728	12.728	-6.76	-7.75	-8.54	-8.91
25.456	25.456	-6.50	-6.79	-7.73	-8.84
38.184	38.184	-5.71	-7.38	-8.42	-9.33
50.912	50.912	-6.20	-7.73	-8.86	-9.92
63.64	63.64	-6.35	-7.63	-8.73	-9.97
76.368	76.368	-6.71	-8.00	-8.96	-9.44

8.1.1 ln K(ψ) Data (continued)

x	y	ln K0	ln K3	ln K6	ln K15
89.096	89.096	-5.99	-7.40	-8.17	-9.00
-25.456	-25.456	-6.35	-7.74	-8.49	-9.29
-38.184	-38.184	-5.43	-7.08	-7.99	-8.78
-50.912	-50.912	-5.32	-7.45	-8.30	-8.91
-63.64	-63.64	-6.49	-8.10	-8.98	-9.53
-76.368	-76.368	-5.60	-7.62	-8.82	-9.90
-89.096	-89.096	-6.34	-7.83	-8.70	-9.53
25.456	-25.456	-7.31	-8.07	-8.74	-9.29
38.184	-38.184	-6.74	-7.69	-8.32	-9.15
50.912	-50.912	-6.20	-7.87	-8.95	-9.37
63.64	-63.64	-6.53	-7.48	-8.62	-9.97
76.368	-76.368	-5.97	-7.53	-8.22	-9.38
89.096	-89.096	-5.98	-7.55	-8.31	-9.00
-25.456	25.456	-6.73	-7.77	-8.49	-9.29
-38.184	38.184	-6.41	-7.12	-8.08	-9.17
-50.912	50.912	-6.78	-7.39	-8.21	-9.17
-63.64	63.64	-5.41	-7.31	-8.39	-9.30
-76.368	76.368	-6.07	-7.96	-8.96	-9.44
-89.096	89.096	-5.21	-7.06	-8.05	-9.03

8.1.2 EM38H Data

APPENDIX 8.1.2
Electromagnetic Induction Measurements at 0.75m Depth
(mS/m)
Grid origin located at the southwest corner of the center bench.

Grid X	Grid Y	1/13/94	2/27/94	3/22/94	4/29/94	5/30/94
0	0					58.64
0	10					55
0	20					48.16
0	30					55.44
0	40					66.36
0	50					116.96
0	60					109.92
0	70					86.12
0	80					78.8
0	90					148
0	100					129.64
0	110					44.28
0	120					45.28
0	130					92.72
0	140					136.04
0	150					155.12
0	160					122
0	170					73.84
0	180					75.44
0	190					57
0	200					41.16
10	0					138.96
10	10	47.2	79.1	80.4	99.4	105.52
10	20	26.2	38.6	42.3	58.4	67.08
10	30	32	34.1	35	49.3	87.76
10	40	20.2	29.9	31	44.8	86.04
10	50	27.4	34.6	33.3	66.7	142.12
10	60	57.9	39.1	36.5	88.9	156.76
10	70	72.3	80.6	84.2	85.9	93.48
10	80	53.5	63.5	71.9	81.2	92.24
10	90	45.6	62.9	70.6	74.4	96.4
10	100	26.2	106.2	69.6	77.6	86.44
10	110	21	116.4	128.7	129.5	144.32
10	120	54.1	31.2	41.2	44.5	47.24
10	130	47.6	34.4	44.4	41.5	46.56
10	140	101.8	60.2	77.3	104.8	121.8
10	150	76.1	126.4	111.6	128.1	151.24
10	160	32.9	109.5	100.3	128.7	148.04
10	170	53.2	68.6	106.7	122.2	136.48

8.1.2 EM38H Data (continued)

Grid X	Grid Y	1/13/94	2/27/94	3/22/94	4/29/94	5/30/94
10	180	23.9	57.5	66.8	77.1	134.76
10	190	11.4	51.1	54.2	62.3	111.16
10	200	13	27.1	26.2	29.4	36.32
20	0				900	129.16
20	10	73.4	109.8	99.2	109.3	120.28
20	20	39.8	60.6	64.8	78.5	95.4
20	30	27	57	64.1	99.7	148.64
20	40	27.8	62.9	78.4	94.7	113
20	50	26.3	55.5	64.9	69.8	98.88
20	60	49.4	100.3	123.2	134.6	153.12
20	70	71.4	128.9	122.8	129.7	140.96
20	80	40.4	58.1	66.6	69.6	76.52
20	90	61.1	61.2	64.1	66.8	73.32
20	100	37.6	65.3	77.3	88.7	113.52
20	110	43.8	60	71.9	70.8	81.56
20	120	17.4	88.8	64.1	77.9	82.44
20	130	28.7	29.9	36.7	44.8	74.16
20	140	87.6	33.4	33.8	38.1	37.68
20	150	81.1	117.1	99.4	115.6	117.96
20	160	51.3	115.2	119.7	128.3	158.76
20	170	24.4	104.3	109.5	119.1	148.72
20	180	34.3	113.4	118.4	157.1	158.88
20	190	13	67.3	99.2	122.7	125.28
20	200	14.1	39.8	44.6	49.7	50.44
30	0				900	126.16
30	10	104.3	91.3	98.8	111.3	115.6
30	20	88.3	74.4	89.5	99	117.4
30	30	56.4	72.3	68.9	85.6	90.96
30	40	50.1	78.4	80	79.4	83.72
30	50	105.3	74.4	84.3	82	79.08
30	60	62.1	59.3	61.1	64	64.08
30	70	88.7	95.3	92.9	94.1	82.92
30	80	116.7	92.6	101.4	100.8	101.08
30	90	36	43.6	66.3	74.5	81.16
30	100	54.8	46.8	70.5	69.9	78.92
30	110	23	116.3	84.2	89.7	88.84
30	120	51.7	96.1	144	157.3	168.32
30	130	39.6	35.4	114.2	159.2	162.64
30	140	15.4	44.6	48.3	51.2	55.72
30	150	59.6	22.6	59.7	54	58.84
30	160	78.4	72.9	89.6	109.9	153.12

8.1.2 EM38H Data (continued)

Grid X	Grid Y	1/13/94	2/27/94	3/22/94	4/29/94	5/30/94
30	170	87.7	118.8	124.8	162.2	164.16
30	180	73.7	128.4	134.7	147.3	160.04
30	190	30.1	117.6	122.3	141.7	142.48
30	200	10.2	82.3	78.4	86.5	96.68
40	0				900	74.88
40	10	42.4	69.5	88.8	91.7	95.56
40	20	61.1	68	78.1	77.6	71.56
40	30	43.1	67.8	69.5	78.4	81.96
40	40	69.9	72	83.4	98.1	103.88
40	50	63.7	66.5	66	64.7	62.8
40	60	58.2	63.6	68.1	73.3	75.36
40	70	56.7	52	58	59.5	62.68
40	80	49.6	73	61	69.4	70.16
40	90	78.2	68	77.4	81.6	90.32
40	100	52.8	53.1	103.8	134.7	150
40	110	43.2	51	109.1	147.7	150.84
40	120	160.1	162.9	158.3	154	144.72
40	130	96.3	139.3	149.3	158.7	157.08
40	140	18.8	93.3	159.7	154.2	161.52
40	150	26.2	24.5	27.7	30	30.68
40	160	99	83.4	64.2	58.4	43.2
40	170	106.9	124.8	113.7	120.9	113.32
40	180	82.3	132.2	144.5	154.3	158.2
40	190	47	110.9	129.9	129.3	144.72
40	200	11	90.6	36.2	29.4	43.28
50	0				900	132.64
50	10	83.6	114.3	98.7	114.1	118.88
50	20	77.5	96.1	98.8	88.1	85.92
50	30	62	74.9	79.5	79.5	100
50	40	53.3	21.9	44.7	59.6	115.8
50	50	58.3	23.9	69.9	80	123.04
50	60	61.8	176.8	94.6	101	79.48
50	70	47.1	116.2	100.3	100.9	104.16
50	80	57.9	113.4	77.5	84.9	86.8
50	90	50.2	82	124.1	129.3	139.92
50	100	66.8	81.5	114.5	119.3	132.88
50	110	70.9	46.2	88.1	90	94.52

8.1.2 EM38H Data (continued)

Grid X	Grid Y	1/13/94	2/27/94	3/22/94	4/29/94	5/30/94
50	120	72.7	47.6	73.9	75.1	140.52
50	130	110.4	55.1	93.6	119.2	162.4
50	140	94.7	50.3	113.3	144.8	152.44
50	150	145.4	62	160.8	159.8	164.96
50	160	26.5	58	58.4	69.4	91.6
50	170	19.3	61.5	49.7	51.2	46.52
50	180	79.8	54.1	100.1	87.3	135.32
50	190	90	50.6	94.9	105.6	160.24
50	200	80.4	57.5	154.2	89.6	151.48
60	0				900	136
60	10	81.5	102.7	122	129.4	130.24
60	20	82.2	68.6	88.6	98.1	102.44
60	30	57.2	48.8	74.2	79.5	86.6
60	40	42.8	50.7	66.7	68.2	68.76
60	50	41.2	67.8	77.2	79.9	87.24
60	60	44.5	90.4	94.5	95.3	98.88
60	70	45.5	66.8	88.1	89.8	95.48
60	80	40.5	64.7	77.5	89.9	95.96
60	90	41.5	69.5	79.8	104.5	109.6
60	100	43	65.4	75.3	99.9	98.88
60	110	43.7	110.5	118	104.1	98.4
60	120	93.3	93.5	97.2	112.2	116.16
60	130	96.7	72.6	94.6	122.6	129.72
60	140	111.8	94.2	150.3	159.1	160.24
60	150	18.9	164.7	145.7	162.2	145.52
60	160	16	102.9	106.3	152.8	164.8
60	170	77.2	131.4	84.3	36	25.24
60	180	67.8	70.9	80	35.6	44.16
60	190	81.3	21.9	66.4	140.3	149.08
60	200	16.8	112	100.3	150	149.32
70	0				900	143.52
70	10	91.7	112.5	119.3	137.6	144.8
70	20	85.6	92.8	91.6	99.7	115.08
70	30	105.7	78.2	78.1	84.9	88.76
70	40	64.4	62.2	68.4	66.2	74.4
70	50	65	52	59.1	61.8	67.6
70	60	51.3	51	77.6	76.4	90.8
70	70	43.4	52.8	71.6	79.8	82.64

Grid X	Grid Y	1/13/94	2/27/94	3/22/94	4/29/94	5/30/94
70	80	40.2	53.5	72.9	70	76.08
70	90	43.9	53.1	94.2	69.4	78.64
70	100	41.2	50.6	77.1	71.9	89.8
70	110	46.7	53.9	85.2	111.9	122.32
70	120	47.3	53.2	99.1	119.8	131.88
70	130	87	68.6	118.5	122.6	123.8
70	140	74.2	82.5	140	154.9	151.32
70	150	76.4	148	154.2	166.2	166.32
70	160	152.4	107.4	152.6	159.4	167.32
70	170	93.5	154.6	66	87.2	166.52
70	180	133.5	20.6	44.1	41.9	39.2
70	190	30.5	20.5	48.2	69	99.6
70	200	70.4	122	129.4	146.9	152.92
80	0				900	136.92
80	10	125.4	67.7	125.7	133.4	142.76
80	20	113.3	116	99.1	104.7	84
80	30	113.3	105	122.7	135.4	138.48
80	40	89.2	50.5	77.3	74.1	96.2
80	50	106	56.3	80.1	84.6	78.92
80	60	82.9	45.3	79.4	94.1	102.32
80	70	41.6	57.3	66.7	71.9	74.24
80	80	42.8	48.8	59.8	77.6	80.08
80	90	53.3	57.3	54.3	69.4	71.92
80	100	45.9	51.5	66.9	71.2	80.96
80	110	37.2	57.8	84.3	86.7	96
80	120	40.2	69.3	117.7	139.5	153.24
80	130	90.2	82.3	94.3	99.5	111.64
80	140	79.1	76	123.4	140.1	145.24
80	150	54.2	137.6	139.9	158.3	159.96
80	160	104.1	172.6	164.1	165.3	164.76
80	170	149.7	166.5	149.5	151	158.16
80	180	124.3	77.4	135.6	144.7	164.8
80	190	114.7	20.6	119.6	141.2	153.4
80	200	94.9	103.1	122.9	128.7	148.84
90	0				900	156.6
90	10	99.6	74.1	121	99.4	159.88
90	20	104.6	117.4	131.8	144.9	148.2
90	30	112.6	105.4	129	126.3	157.32

Grid X	Grid Y	1/13/94	2/27/94	3/22/94	4/29/94	5/30/94
90	40	84.8	68.4	95	138.4	149.56
90	50	91.8	109.8	99.7	100.1	104.16
90	60	59.6	93.7	88.7	89.4	72.64
90	70	40.1	71.9	85.1	99.1	105.76
90	80	40.5	49	89.8	91	91.44
90	90	51.3	53.1	66	73.9	72.44
90	100	42.1	49.6	59.1	67.6	68.64
90	110	31.8	46	54.9	59.3	65.64
90	120	30.4	44.5	68.4	94.5	97.96
90	130	35.6	100.4	122	129.3	128.36
90	140	34.9	109.9	113.6	119.6	121.56
90	150	35.2	94.4	90.6	101.8	119.04
90	160	58.8	127.3	133.2	158	164.36
90	170	135.7	160.5	139.9	159.4	164.92
90	180	104.7	117.2	129.3	159.1	164.28
90	190	134.3	156.5	169.4	158.3	166.4
90	200	117.4	110.3	121.9	137.9	158.08
100	0				900	151.32
100	10	54.2	129.2	141.6	149.3	154.48
100	20	53.5	120.1	140.2	120.8	140.52
100	30	92.9	69.6	101.3	140.3	142.16
100	40	90.5	133.4	125	114.6	91.6
100	50	63.6	96.7	77.1	65.4	68.28
100	60	41.8	55	64.5	63.9	66.96
100	70	32.1	43.9	71.3	75.4	77.56
100	80	34.3	61.5	77.3	89.6	92.44
100	90	46.2	50.5	71.6	79.4	68.56
100	100	40	43.9	56.2	59.4	60.16
100	110	35.8	40.5	40	41.8	62
100	120	42.5	41.4	64.9	67.8	70.4
100	130	38.5	54.2	71.5	71.3	72.6
100	140	40.6	60	79.4	84.9	80.12
100	150	55.6	48	71.3	75.4	74.76
100	160	103.8	54.3	154.9	160	161.6
100	170	119.5	124.4	150.6	166.3	166.16
100	180	105.3	162.2	174.9	162.1	156.04
100	190	123.6	154.9	165.1	159.7	161.32
100	200	109.5	138	154.9	155.5	165.92
110	0				900	143.76
110	10	48.9	133	138.2	140.3	154.36
110	20	33.2	136.4	121.6	118.3	119.76
110	30	39.2	85	129.5	138.9	138.88

Grid X	Grid Y	1/13/94	2/27/94	3/22/94	4/29/94	5/30/94
110	40	39.7	97.3	98.8	104.5	111.2
110	50	87.4	75.9	90	78.6	72.44
110	60	39.6	49.3	69.5	65.4	80.88
110	70	32.9	46.1	74.6	99.3	105.48
110	80	45.7	55.1	79.4	88.3	89.16
110	90	33	50	66.5	65.4	69.76
110	100	54.5	50.2	70.2	71.4	72.36
110	110	59.9	41.9	66.5	69.7	75.6
110	120	36.2	40	74.6	70	76.48
110	130	39	41.4	54.6	59.7	75.68
110	140	40.2	42.8	71.9	72.6	79.52
110	150	44.5	44.3	94.3	99	111.36
110	160	45.3	46.9	97.9	160.2	158.32
110	170	110.2	115	160.1	168.4	163.32
110	180	139	131.8	151.6	157.4	158
110	190	114.9	117.9	160.2	154.6	157.84
110	200	102.5	144.7	154.3	159.7	163
120	0				900	71.32
120	10	50.6	86.8	71.5	77.9	80.36
120	20	35	116.9	64	79.2	89.88
120	30	59.3	101.4	94.6	98.6	99.32
120	40	16.2	96.9	85.2	86.3	70.4
120	50	48.7	79.5	64.9	64.2	63.68
120	60	38.5	53.4	62.3	70.3	70.36
120	70	43.8	60.6	69.1	60.3	63.68
120	80	48.1	64.8	69.1	70	71.48
120	90	38.2	65	66.8	77.9	79.8
120	100	43.4	46.1	64.2	71.9	77.28
120	110	36	45.6	66.7	71.7	75.28
120	120	44	45.9	67.9	71.3	72.4
120	130	43.9	44.6	71.6	76.1	74.12
120	140	39	49.5	67.7	71.3	75
120	150	36.4	46.3	64.2	73.4	72.76
120	160	46.3	64.3	149.5	151.7	151.16
120	170	76.6	141.2	147.3	149.7	156.92
120	180	107	136.3	167.2	159.3	164.68
120	190	95.6	123.3	130	122.9	133.72
120	200	105.8	137.5	114.7	120.3	161.96
130	0				900	66.68
130	10	38	48.8	97.3	111.4	116.12
130	20	60.2	46.2	68.5	69.5	68.4

Grid X	Grid Y	1/13/94	2/27/94	3/22/94	4/29/94	5/30/94
130	30	25.7	55.2	101.4	111.3	112.84
130	40	14.9	59	96.2	69.4	70.84
130	50	66.3	50.3	79.5	61.1	63.72
130	60	43.5	40.6	53.4	89	95.96
130	70	32.9	43.7	60	65.4	77.84
130	80	34.1	43.8	64.8	65.9	70.72
130	90	38.5	50	65.9	101.3	109.92
130	100	43.6	57.3	46.1	78	78.88
130	110	39.2	48.4	45.6	71.2	72.4
130	120	41	42.6	67.3	79.1	81.28
130	130	36.1	46.8	71.3	74	72.68
130	140	46.6	47.2	66.3	71.4	75.8
130	150	68.2	53	69.7	73.4	76.64
130	160	95.6	51.5	106.7	104.7	116.32
130	170	18.7	109.8	154	159.7	161.24
130	180	96.3	140.3	155.7	167.4	165.4
130	190	83.2	137.7	121.7	125.6	124.36
130	200	81.4	82.4	158.7	162.9	164.6
140	0				900	69.2
140	10	15.5	39.1	84.2	93.4	94.36
140	20	73.3	58.3	36.4	38.7	37.44
140	30	40.7	17.6	67.8	85.1	86.16
140	40	29.4	47.2	99.8	105.1	111
140	50	24.7	74	87.1	88.6	88.16
140	60	30.7	46.8	77.9	89.7	91.36
140	70	78.8	50.5	70.7	67.3	71.96
140	80	36.3	46.9	60.6	70.4	69.04
140	90	33.9	45.4	68	71.8	79.2
140	100	36.5	48	54.3	59.8	72.2
140	110	44.7	43.7	64.7	80.6	84
140	120	44.7	47.8	81.3	80.9	88.56
140	130	39.9	60.8	46.5	70.2	74.56
140	140	43.5	46.3	69.7	75.2	78.76
140	150	38.9	44.7	69.2	89.4	83.88
140	160	56.3	52	89.3	88.5	91.84
140	170	85.6	78.1	133.2	151.8	154.12
140	180	92.6	156.1	154.7	158.3	155.84
140	190	89.3	138.7	160	153.7	153.92
140	200	120.4	130.4	151.4	150.4	153.04
150	0				900	96.84

8.1.2 EM38H Data (continued)

Grid X	Grid Y	1/13/94	2/27/94	3/22/94	4/29/94	5/30/94
150	10	20.8	60.4	42.7	49.4	50.24
150	20	22	33.9	56.2	57.6	57.44
150	30	99	21.5	33.9	41	47.6
150	40	27.3	51.1	84.7	91.4	93.68
150	50	32.7	69.4	72.4	79.6	80.76
150	60	30.6	50.7	61.7	69.8	71.92
150	70	26.7	47.9	51.7	59.3	62.36
150	80	58.2	40.5	59.8	68.1	67.08
150	90	39.4	37.3	60	66.7	68.68
150	100	41.8	40.6	59.4	61.3	68.88
150	110	43.5	41.5	66.7	69.5	71.92
150	120	51.2	49.6	67.1	63.2	73.52
150	130	59.3	59.3	70.4	69.3	70.56
150	140	42.1	47.4	74.1	74.6	75.8
150	150	51.6	50.4	68.7	69.9	69.84
150	160	58.2	47.2	101.1	105.4	104.4
150	170	50.9	81.1	140.7	129.8	140.92
150	180	94.9	110.5	154.7	158.3	157.04
150	190	100.3	131.9	144.3	152.3	152.96
150	200	103	102.4	147.6	150.1	153.56
160	0				900	122.32
160	10	22.7	67.1	54.2	57.6	57.64
160	20	51.3	33	56.7	42.9	40.96
160	30	37.5	24.8	41.9	41.5	41.12
160	40	28.8	20.9	44.9	48.2	54
160	50	28	27.9	66.7	69.2	85.36
160	60	34.7	42.4	69.8	92.6	94.32
160	70	69.8	46.8	61.4	66.3	62.44
160	80	99.3	41.5	84.3	81	66
160	90	72.8	43.4	72.4	78.1	70.28
160	100	86.7	47.7	74.9	84.3	82.32
160	110	98.4	44.6	56.7	72.4	73.28
160	120	103.5	48.4	94.5	92.3	95.8
160	130	64.7	48	61.7	63.2	68.4
160	140	59.1	43.7	77.3	82.7	82.8
160	150	107	46	72.4	78.6	76.4
160	160	102.9	48.1	91.2	97.6	98.6
160	170	62.5	79.8	135.6	142.9	143.92
160	180	96.8	113.1	139	144.1	141.16
160	190	85.9	134.1	152.6	155.5	156.56

Grid X	Grid Y	1/13/94	2/27/94	3/22/94	4/29/94	5/30/94
160	200	58.6	128.4	155.3	159.4	150.44
170	0				900	133.92
170	10	16	79	45.2	68.1	67.36
170	20	53.2	55	61.4	63.5	63.2
170	30	32.7	31.9	69.7	81.6	80.2
170	40	31	26.3	54.3	59	59.76
170	50	17.8	34.5	51.2	53.7	54.52
170	60	22.1	44.8	61.7	66.1	65
170	70	37.5	60.3	74.2	72.6	75.68
170	80	61	43.5	65.2	66.4	68.32
170	90	105.7	39.6	69.3	71.9	72.44
170	100	65.5	43.7	64.1	66.9	68
170	110	81	44.9	79.8	77.8	78.96
170	120	86.1	45	99.4	95.9	100
170	130	50.8	55.1	64.7	66.3	73.68
170	140	76.4	47.9	91.5	90	92.48
170	150	87.4	73.8	79	81.5	71.04
170	160	79.2	50.1	79.6	76.7	72.04
170	170	104.8	65.8	130.1	129.3	131.28
170	180	103.7	129.1	145.2	149.3	152.32
170	190	107.4	113.2	142.7	152	151.72
170	200	72.7	120.7	102.7	121	125.32
180	0				900	60.52
180	10	17.8	35.8	98.5	94.7	110.24
180	20	15.2	76.3	72.4	60.1	59.48
180	30	47.6	30.1	54.7	59.3	62.32
180	40	34.4	35.4	44.8	45.9	47.24
180	50	61.6	30.9	54.7	56.7	58.4
180	60	38.7	33	46.7	49.2	67.44
180	70	29.8	28.4	94.3	106.7	102
180	80	64.2	49.3	80.1	74.2	78.56
180	90	69.4	43.3	66.2	63.4	83.08
180	100	51.5	44.5	76.8	79.8	92.44
180	110	69	48.1	111.3	111.9	115.52
180	120	77.6	57.6	120	117.3	119.28
180	130	57.5	68.7	74.6	81.2	93.88
180	140	47.9	43.6	97.3	99	105.68
180	150	74.1	52.3	129.7	138.9	151.8
180	160	96.1	66.3	129.7	124.9	132.32
180	170	82.9	61.1	124.7	131	130.16
180	180	96.1	72.5	144.4	154.2	149.72
180	190	97.8	110.7	127.2	158.4	160.6
180	200	82.2	116.7	156.8	160.9	158.96

Grid X	Grid Y	1/13/94	2/27/94	3/22/94	4/29/94	5/30/94
190	0				900	70.4
190	10	15.9	38.9	61.7	99.9	100.72
190	20	12.6	55.7	61.4	49.2	54.88
190	30	15.9	28.4	37	39.4	51.08
190	40	29.8	31.3	41.4	50.1	50.92
190	50	35	38.4	47.9	44.8	48.44
190	60	40.6	37.5	79.2	94.7	96.96
190	70	26.7	63.7	84	78.5	82.6
190	80	60.2	73.4	139.6	142.3	143.84
190	90	64.8	58.7	129.7	138.4	138.68
190	100	57.6	76.5	121.3	127.3	129.8
190	110	49.5	98.7	141.3	145.8	147.12
190	120	73.8	114.4	117.6	130.1	131.08
190	130	31.8	86.4	94.5	91.3	92.52
190	140	58.4	67.4	111.9	119.5	122.52
190	150	67.9	78	140.3	137.9	141.88
190	160	73.7	115.6	161.7	159.7	154.96
190	170	78.1	103.3	126.7	119.7	124.56
190	180	82.2	68.7	144.7	149.2	158.16
190	190	84.7	110.2	151.2	151	154.68
190	200	88.1	143	91.7	107.6	157.4
200	0				900	900
200	10	10.7	67.1	14.3	19.7	50.68
200	20	11	28.9	61.4	52.7	58.88
200	30	21.1	37.7	64.7	69.7	75.32
200	40	51.3	51.9	51.3	41.9	39.36
200	50	46.7	20.8	39.5	39.6	41.28
200	60	53.1	23.7	56.4	29.7	51.24
200	70	38.3	49.6	119.7	130	125.44
200	80	59.9	67.7	149.3	157.1	154.24
200	90	59	113.3	141.8	144.4	146.12
200	100	21.6	71.5	78.3	77.7	79.76
200	110	87.8	82.9	122.4	129.3	133.64
200	120	71.2	94.8	130	134.7	138.84
200	130	30.5	83.7	91.8	94.3	94.08
200	140	36.2	58.8	81.2	88.8	90.8
200	150	21.7	93.7	125.7	135.9	136.24
200	160	38.4	101.3	155	152.4	154.52
200	170	91.4	96.8	131.7	134.8	141.52
200	180	93.9	89.5	153.6	152.2	152.64
200	190	82	112.3	160.1	158.7	157.64
200	200	100	124.3	147.9	136.7	150.72

8.1.3 EM38V Data

APPENDIX 8.1.3
Electromagnetic Induction Measurements at 1.5m Depth
(mS/m)
Grid origin located at the southwest corner of the center bench.

Grid X	Grid Y	1/13/94	2/27/94	3/22/94	4/29/94	5/30/94
0	0					55.52
0	10					47.24
0	20					43.8
0	30					57.6
0	40					61.76
0	50					139.92
0	60					118.4
0	70					94.8
0	80					96.08
0	90					148.2
0	100					143.64
0	110					47.92
0	120					53.28
0	130					78.84
0	140					134.64
0	150					123.8
0	160					93.04
0	170					60.12
0	180					70.88
0	190					59.08
0	200					34.88
10	0					146.48
10	10	62	96.1	84.3	92.6	108.84
10	20	32.3	42.4	53.4	52.3	77.64
10	30	29.6	37.7	61.2	89.5	101.4
10	40	24.6	31.7	49.9	62.4	80.48
10	50	29.8	40.4	88.7	122	136.52
10	60	75.2	49.6	96.1	102.4	147.2
10	70	84.2	175.5	122.5	118.3	101.36
10	80	73	71.3	75.3	79.8	87.2
10	90	50.3	76	84.6	98.7	113.36
10	100	38	112.1	79.8	101.1	92.04

Grid X	Grid Y	1/13/94	2/27/94	3/22/94	4/29/94	5/30/94
10	110	26.5	128	114.9	131.8	143.12
10	120	53.7	34.1	42.8	45.7	59.88
10	130	57.6	34.9	46.7	49.2	44.44
10	140	91.2	51	66.9	78.2	88.4
10	150	72.4	93	126.3	132.6	146.6
10	160	36	89.2	94	116.6	129.6
10	170	51.2	63.2	92.7	112.5	118.44
10	180	29.1	46.8	88.3	133.7	130.12
10	190	16.1	61.7	72.9	87	117.64
10	200	17.6	29.3	18.4	29.9	33.36
20	0					144.88
20	10	98.8	121.5	127	139.5	136.2
20	20	50.8	74.8	87.4	82.1	107.28
20	30	33.7	71.3	94.2	118.6	143.08
20	40	34.2	75.6	85	122.7	130
20	50	33.3	63.4	81.9	92.7	98.48
20	60	64.8	105.8	122.4	129	147.12
20	70	88.4	127	116.3	145.8	152.16
20	80	58.2	73.1	76.6	81.4	76.72
20	90	85.9	72.5	91.5	72.3	71.36
20	100	50.6	72.3	74.6	89.4	93.92
20	110	64.7	70	81.7	88.3	98.28
20	120	24	105.6	66.4	78.9	84.04
20	130	31.5	35	42.1	58.9	67.44
20	140	81.7	33.6	46.2	48.5	39.2
20	150	74.8	98.8	100.3	104.2	107.4
20	160	51.1	115.3	129.7	135.6	148.4
20	170	25.8	99.7	109	122.5	139.32
20	180	43	93.6	111.5	118.3	124.28
20	190	17.5	66.2	98.2	92.4	128
20	200	15.8	43.7	41.2	35.8	38.84
30	0					127.04
30	10	110.6	96.3	114.6	122.7	126.52
30	20	116.5	96.5	123.6	125.4	133.24
30	30	80.4	84.7	92.8	100.2	101.08
30	40	66	82.8	75.9	88.1	91.28
30	50	130.5	89.9	96	89.3	93.76

Grid X	Grid Y	1/13/94	2/27/94	3/22/94	4/29/94	5/30/94
30	60	77.3	66.1	68.9	71.4	76.4
30	70	112.9	92.1	95.2	92.5	86.44
30	80	142.1	127	137.3	129.8	130.2
30	90	46.3	51.5	62.7	80	105.32
30	100	77.8	50.1	72.3	71.4	82.48
30	110	31.5	100.6	80.8	104.7	106.64
30	120	60.3	103.2	113.7	144.6	165.88
30	130	49	41.4	125.7	132.2	144.36
30	140	21.4	47.8	39	41.3	48.24
30	150	77.9	26.3	33.7	29.9	42.48
30	160	91.4	82.4	109.3	117	125.28
30	170	94.5	132.4	128.5	133	148.36
30	180	66.8	43	55.6	72.1	125.6
30	190	31.2	103.4	99.8	100.6	115.08
30	200	14.4	88.7	62.4	66.7	68.76
40	0					94.92
40	10	69.6	88.4	106.7	92.1	124.48
40	20	82.5	76.8	78.1	81.4	89.92
40	30	62.4	90.1	90	82.9	84.28
40	40	91.2	90.4	104.2	97.6	99.12
40	50	85.5	90	84.4	88.2	68.76
40	60	68.8	74.4	79.5	72.6	78.92
40	70	61.9	61.4	63.2	66.4	73.84
40	80	49.7	71.7	69.4	65.7	78.2
40	90	89.5	89.8	92.1	87.6	99.2
40	100	69.2	63	89.3	114.1	152.72
40	110	59.2	63.1	94.8	126.2	151.72
40	120	165	166.7	139.9	151.7	147.44
40	130	101.9	146.9	125.8	133.7	158.8
40	140	25.5	71.6	92.4	132.6	152.88
40	150	31.4	26.6	42.1	31.8	28.76
40	160	94.2	90.8	96.2	89.4	44.16
40	170	96.1	122.1	89.4	102.3	82.6
40	180	77.7	116.8	122.5	121.3	126.36
40	190	48.2	102.3	99.5	106.8	114.44

Grid X	Grid Y	1/13/94	2/27/94	3/22/94	4/29/94	5/30/94
40	200	14.4	94.5	64.8	72.1	59.92
50	0					141.44
50	10	105.6	101.4	109.8	115.3	131
50	20	99.9	79.5	84.6	89.7	102.24
50	30	85.9	54.1	89.7	92.7	113.4
50	40	71.8	27.1	44.2	88.6	123.6
50	50	79	28.2	39.4	76	136.92
50	60	90.6	171.7	121.3	136.2	91.72
50	70	64.6	130.5	111.7	121.3	122.16
50	80	75.2	133	119.3	104.6	111.88
50	90	70.8	108.7	128.9	133.2	147.12
50	100	92.8	109.5	104.9	104.3	137.12
50	110	97.6	58.2	92.3	102.7	113.76
50	120	102.7	61.5	105.5	116.6	151.6
50	130	137.6	67.3	125.6	135.6	160.52
50	140	118.4	61.5	122.5	114.8	148.72
50	150	149.2	73.6	152.4	169.3	162.12
50	160	32.6	70.5	81	64.5	76.36
50	170	24.2	71.2	44.7	27.9	39.68
50	180	65.8	69	74.2	76.8	84.52
50	190	80.1	64.5	99.1	103.6	106.68
50	200	68.5	78.5	94.5	98.4	107.8
60	0					143.52
60	10	105.8	115.2	136.4	141.1	149.84
60	20	94.8	89.8	94.7	99.6	117.2
60	30	78.7	60.8	84.7	89.5	94.72
60	40	55.6	66.4	72	77.8	74
60	50	55.6	84.8	69.4	84.1	88.92
60	60	57.7	115.9	88.9	94.2	100.56
60	70	65.6	92.7	91.5	88.6	96.12
60	80	57.8	80.6	81.5	89.3	92.16
60	90	54.4	83.2	87.6	97.5	105.56
60	100	58.8	76.4	81.5	86.9	95.92
60	110	62.2	121.9	65.3	71.4	85.4
60	120	121	106.5	105.2	94.6	100.08
60	130	115.2	90.1	100.8	106.8	136.96
60	140	146.7	120.4	133.2	142.9	162.56

Grid X	Grid Y	1/13/94	2/27/94	3/22/94	4/29/94	5/30/94
60	150	38.5	169.9	152.5	146.8	146.04
60	160	19.5	112.3	134.7	129.4	161.6
60	170	87.8	149.6	72.1	68.5	34.68
60	180	66.8	70.4	75.6	58.2	37.68
60	190	69.2	25.3	35.3	84	101.48
60	200	26.2	82	79.8	74.6	108.92
70	0					146
70	10	106.8	122.4	103	135.6	145.52
70	20	112.9	105.3	119.7	126.4	122.68
70	30	118.2	92.1	102.3	99	100.52
70	40	90.3	79.7	89.2	84.6	86.04
70	50	82.1	63.8	78.5	74.6	72.08
70	60	61.8	58.9	84.2	77.5	97.16
70	70	54.3	62.3	65.3	74.8	79.76
70	80	49.1	70.4	69.5	78.1	80.8
70	90	56.8	69.5	72.1	81.1	84.92
70	100	52.4	61.7	84.6	92.9	93.24
70	110	57.8	68.4	92.3	111.6	115.32
70	120	57.8	65.3	102.8	117.6	138
70	130	108.8	73.4	89.6	99.2	124.6
70	140	85.1	96.4	142.8	144.2	150.8
70	150	78.2	158.8	149.5	154.2	164
70	160	138.8	126.3	158.6	157.2	165.56
70	170	123.5	164.2	159.4	166.5	166.36
70	180	136.5	25	49.2	39.8	44.32
70	190	35.1	24.3	68.2	62.3	78.52
70	200	77.2	107.9	110.2	94.3	115.04
80	0					151.28
80	10	127.6	92.8	132.8	142.3	149.72
80	20	133.9	127.7	119.7	125.6	104
80	30	121.9	128.7	135.3	133.9	142.64
80	40	104.8	65.6	95.6	104.3	110.88
80	50	120.4	71.6	91.5	88.1	86.84
80	60	111	55.8	112.6	109.7	119
80	70	50.3	68.6	71.2	70.9	74.04
80	80	56.4	58.2	75.4	79	88.24
80	90	68.5	67.4	68.5	71.8	78.68

Grid X	Grid Y	1/13/94	2/27/94	3/22/94	4/29/94	5/30/94
80	100	51.4	60.6	71.9	75.4	76.92
80	110	41.8	70.1	865.9	74.3	87.84
80	120	47.7	89.2	94	143	153.12
80	130	99.2	105.4	121.4	102.3	125.64
80	140	92.8	95.2	104.6	117.6	132.96
80	150	70.9	153.1	155.3	158.6	153.64
80	160	106.5	170.2	162.1	160.3	163.28
80	170	145.2	176.7	167.4	158.6	159.76
80	180	143.6	71.3	146.5	144.3	156.24
80	190	116.1	24.7	88.6	84.5	95.68
80	200	89.5	102	100.3	111.6	142.04
90	0					157.68
90	10	104	99.8	129.6	135.6	157.16
90	20	122.7	121.2	136.7	136	146.32
90	30	121.1	122.5	146.8	149.3	157.12
90	40	107.8	77.8	147.3	155.2	151.68
90	50	107.3	124.7	116.9	125.7	110.52
90	60	78.4	104.3	94.8	89.2	72.68
90	70	46.1	71.2	98.3	105.5	115.4
90	80	49.6	54.9	79.8	84.2	100.28
90	90	64.7	56.3	77.2	81.5	85.24
90	100	51.6	62.1	71.3	62.4	67.48
90	110	38.6	51.5	66.1	69.4	72.52
90	120	36.7	53.7	94.2	106.3	114.2
90	130	43.8	117.9	122.5	131.2	135.28
90	140	43.7	121	118.5	120.8	121.08
90	150	44.2	109.8	89.4	97.5	96.8
90	160	69.8	112.6	160.5	141.9	157
90	170	114.4	160.6	158.3	154.9	162.96
90	180	111.6	137.7	146.1	150.2	164.48
90	190	108.8	143.1	151	148.3	158.32
90	200	105.9	70.3	121.9	125.6	131.8
100	0					153.32
100	10	66.1	146.9	148.3	158	159.04
100	20	62.4	146.4	131.2	142.1	150.84
100	30	105.2	98	124.6	132.8	148
100	40	102.8	155.5	116.4	110.7	114.04
100	50	94	113.6	122.4	81.7	78.08

Grid X	Grid Y	1/13/94	2/27/94	3/22/94	4/29/94	5/30/94
100	60	50.9	68.6	64.5	66.7	69.96
100	70	42.8	48.5	66.7	71.3	81.28
100	80	42.8	75	81.8	88.3	97.44
100	90	67.5	63.9	71.4	75.3	82.72
100	100	48	56.8	58.6	61	65.12
100	110	44.4	45	56.2	61.3	61.56
100	120	51.1	45.5	51.2	63.9	69.24
100	130	47.7	67.5	54.3	61.8	69.6
100	140	49.9	70.7	68.7	72.4	70.04
100	150	63.9	62.7	77.3	81.6	80.72
100	160	121	64.4	134.7	141.5	151
100	170	107.9	108.5	147.9	151.7	155.6
100	180	110	156	148.2	144.2	150.12
100	190	118.1	155.7	160.4	149.4	159.52
100	200	93.8	147.3	148.7	151.6	153.16
110	0					144.68
110	10	48.3	135.6	126.4	129.8	157.28
110	20	39.8	140.2	137.5	149.8	149.08
110	30	49.1	111.5	122.4	127.6	145.48
110	40	44.6	112.2	144.7	128.6	139.24
110	50	89.6	93.6	88.5	61.5	77.48
110	60	49.5	58.3	74.7	63.2	85
110	70	42	55.2	91.7	100.1	105.76
110	80	58.7	59.3	72.8	79.4	98.48
110	90	40.6	65.3	71.4	70.5	72.16
110	100	70.6	58.9	74.6	78.9	73.12
110	110	74.2	46.1	68.2	61.7	75.92
110	120	40	42.6	59.8	71.4	77.6
110	130	45.1	46.5	64.3	71.9	80.72
110	140	47.9	49.1	64.8	71	77.6
110	150	52.7	51.4	98.4	89.7	100.56
110	160	56	58.7	74.3	149.1	152.72
110	170	114	130.8	150	161.7	158.32
110	180	122.1	138.5	152.3	159.8	154.72
110	190	107	131.3	158.1	156.7	154.2
110	200	130.2	131.5	144.6	159.4	156.04
120	0					68.92

Grid X	Grid Y	1/13/94	2/27/94	3/22/94	4/29/94	5/30/94
120	10	57.5	109.7	88.8	91.5	78.44
120	20	41.5	136.5	110.6	124.6	111.28
120	30	64.5	118.6	114.6	121.4	116.44
120	40	18.3	120	77.1	66.5	73.24
120	50	55.6	102	119.2	103.1	64.88
120	60	51	67	59.7	64.2	69.16
120	70	53.5	75	71.4	66	68.6
120	80	54.4	81.3	91.4	80.2	77.44
120	90	46.9	80.4	81.2	84.5	89.04
120	100	50	49.1	61.9	68.4	69.48
120	110	44.3	49.2	75.2	76.2	73.56
120	120	53.7	51.2	64.8	63.7	76.04
120	130	49.3	51.2	81	74.6	85.64
120	140	40.3	57.5	69.3	75.2	87.48
120	150	42.9	53.8	84.2	91.8	92.6
120	160	51.6	69.7	121.9	144.6	152
120	170	94.4	138	150.1	156.4	152.68
120	180	113.6	140.2	124.3	139.7	155.96
120	190	104.1	127.3	135.2	131.9	136.24
120	200	118.7	128.2	135.6	137.8	159.88
130	0					61.08
130	10	37.8	55.2	69.7	71.5	81.36
130	20	59.5	51.8	66	64.5	66.84
130	30	28.2	65	123.5	118.9	136.08
130	40	17.3	83	69	74.2	73.12
130	50	67.8	58.9	59.7	62.1	66.64
130	60	47.8	46.1	94.5	96.2	106.16
130	70	38.5	48.3	71.6	74.8	85.36
130	80	40.4	46	52.4	59.6	73.2
130	90	46.1	54.5	114	108.2	116.08
130	100	50.1	65.1	72.4	78.5	88.32
130	110	44	54.4	68.5	68.9	74.96
130	120	52.1	45.9	62.7	75.4	80.52
130	130	43.8	50.6	54.7	61.7	71.08
130	140	62.4	56.1	71	79.1	81
130	150	88.4	60	88.2	81.4	83.44
130	160	103.5	57.7	87.3	108.4	119.44

Grid X	Grid Y	1/13/94	2/27/94	3/22/94	4/29/94	5/30/94
130	170	90.2	125	135.8	146.8	159.16
130	180	98.4	146.1	139	144.6	147.88
130	190	93.6	134.8	129.7	128.9	129.76
130	200	90.1	106.1	151.2	158.4	159
140	0					69.8
140	10	18.3	45.1	54.2	71.6	92.52
140	20	80.9	65.2	66.7	61.2	33.68
140	30	40.8	23.1	48.9	68.1	85.12
140	40	29.3	55.2	74.6	89.7	113.24
140	50	28.5	72.9	74	82.4	87.52
140	60	38.2	59.5	78.5	94.2	101.88
140	70	90.7	65.6	67.8	69.8	71.4
140	80	44.7	53.6	54.7	58.7	68.44
140	90	39.1	54.8	74.2	68.6	81.44
140	100	43.6	54.1	59.7	74.2	71.84
140	110	49.5	51.1	88.7	94.5	91.92
140	120	60.4	54.1	82.1	98.4	90.92
140	130	48.4	62	59.6	58.4	66.76
140	140	58	46.3	54.7	64.8	67.28
140	150	50.3	48.8	62.5	69.4	74.12
140	160	73	51.8	84.7	81.6	97.12
140	170	110.8	78.9	91.4	122.6	153.68
140	180	109.2	140.8	154.3	150.3	152.12
140	190	90.8	122	126.9	138.7	155.84
140	200	122.3	124.9	148.6	152.3	150.32
150	0					93.36
150	10	23.2	62.1	64.3	66.7	50
150	20	25.8	36.9	49.7	51.2	56.96
150	30	91	22.2	36	41.6	45.92
150	40	32	49.6	88.5	84.6	91.08
150	50	33.9	95	114.1	95.3	93.2
150	60	32.6	59.6	64.5	66.7	67.84
150	70	26	57.6	54.7	66.3	64.04
150	80	56.8	45.3	48.5	51.7	61.92
150	90	45.5	44.4	66.4	67.3	71.48
150	100	50.2	49.9	68.4	71.5	76.24
150	110	47.2	49.2	66.5	74.2	71.16
150	120	55.7	53.7	63.6	71.3	78.6
150	130	66.9	71.9	81.4	74.2	70.08

Grid X	Grid Y	1/13/94	2/27/94	3/22/94	4/29/94	5/30/94
150	140	45.4	54.3	62.5	96	81.88
150	150	62.1	52.4	62.4	80.1	75.2
150	160	70.7	56.5	112.3	111.5	125.44
150	170	61.9	103.2	119.5	124.6	139.96
150	180	102.8	120	144.6	146.8	149.8
150	190	114.7	133.5	142.3	144.6	142.68
150	200	120.3	109.2	136.8	139.1	145.2
160	0					117.28
160	10	27.5	92	44.2	49.8	52.68
160	20	56.4	34.8	60.1	40.2	42.32
160	30	43.3	24.8	41.8	39.4	41.32
160	40	29.7	23.6	45.6	51.3	54.08
160	50	31.1	31.7	64.7	66.5	74.44
160	60	37.1	47.7	72	81.9	102.28
160	70	73.1	58.8	59.3	64.5	63.56
160	80	112.1	44.5	72.1	64.2	66.64
160	90	87	47	64.2	71.8	69.48
160	100	94.2	55.3	88.3	89.1	90.92
160	110	99.8	57.9	68.5	81.4	82.44
160	120	107.5	55.7	96.5	98.1	105.68
160	130	76.8	55.1	70.2	70.6	70.48
160	140	75.9	50	69.4	72.5	79.52
160	150	118.4	51.2	65.3	78.4	74.84
160	160	115.6	52.3	110.2	115.5	108.56
160	170	72.9	100.5	132.5	124.6	142.44
160	180	99.4	113.3	121.3	129.7	135.92
160	190	107	112.5	139.6	147.2	144.28
160	200	81.4	100.5	127.6	141.3	147.16
170	0					126.96
170	10	18.4	92.8	101.3	94.2	70.44
170	20	60.2	55	56.1	70.4	54.64
170	30	40	33.4	39.4	54.8	63.16
170	40	35.5	29.2	34.5	31.2	47.64
170	50	22	38.7	36.7	41.6	41.4
170	60	23.9	53.2	49.2	51.6	53.96

Grid X	Grid Y	1/13/94	2/27/94	3/22/94	4/29/94	5/30/94
170	70	46.7	78.7	74.2	79.5	74.08
170	80	69.4	49.1	63.2	63.8	65.32
170	90	117.5	45.9	69.4	71.4	71.92
170	100	79.9	50.2	71.6	65.4	71.28
170	110	107.2	55.9	75	82.3	86.68
170	120	110.5	56	68.9	90.5	100.44
170	130	66.4	62.1	74	68.9	70.36
170	140	94.8	50	92.9	94.8	100.4
170	150	110.5	64.8	100.9	92.1	75.6
170	160	100.2	50.9	84.9	88.7	75.28
170	170	105.5	74.3	122.3	128.4	130
170	180	95.7	135.5	154.2	136.8	146.64
170	190	96.4	117.9	136.7	144.2	138.88
170	200	87.6	113.3	94.9	99.7	105.52
180	0					65.12
180	10	16.5	45.9	54.2	79.8	91.92
180	20	18.4	80.3	64.7	69.1	53.12
180	30	48.9	34.8	54.7	38.2	59.64
180	40	36.8	40.4	44.5	49.5	50.56
180	50	55.3	32.6	50.1	46.9	53.08
180	60	34.5	34.3	44.4	61.3	67.04
180	70	30.3	32.8	39.6	94	113.2
180	80	61.2	63.5	74.2	79.1	89.4
180	90	81.2	53.6	79.4	61.2	86.16
180	100	60.4	56.6	88.5	97.5	105.92
180	110	70.5	57.9	126.8	114.7	115.32
180	120	99.1	75.4	113.4	126	129.36
180	130	65.5	79.5	84.3	101.8	91
180	140	57.6	53.5	104.6	102.8	112.84
180	150	91.8	63.2	154.1	127.1	151.52
180	160	92.6	79.2	125.6	131	137.76
180	170	90.8	64.9	72.5	81.4	126.92
180	180	77.2	81.7	159.6	141.3	144.28
180	190	87	128	168.2	131.5	147.68
180	200	80	125.2	154.2	112.8	136.92
190	0					73.8
190	10	16.1	47	54.2	65.3	110.84
190	20	14.5	68.2	71.2	54.5	52.24
190	30	17.9	26.4	31.6	38.1	51.44
190	40	38.3	30.4	44.2	49.5	46.8

Grid X	Grid Y	1/13/94	2/27/94	3/22/94	4/29/94	5/30/94
190	50	39.8	38.2	54.2	61.5	55.12
190	60	51.7	38.9	69.1	81.2	83.56
190	70	31.5	74.7	88.2	71	79.88
190	80	65.6	81.6	133.7	133.4	148.04
190	90	68.4	77.5	94.7	101.9	133.24
190	100	46.8	90.9	116.5	102.7	116.52
190	110	60.9	108	120.9	131.7	134.56
190	120	77	107.4	131.8	126.2	131.8
190	130	32.2	92.3	98.3	101.2	105
190	140	56	67.5	78.1	122.4	138.4
190	150	57.7	92.2	100.6	129.3	149.96
190	160	77.4	130.9	154.2	122.8	154.84
190	170	87.9	117.4	121.7	136.3	120.76
190	180	85.1	86.5	154.2	128	146.84
190	190	70.8	113	137.3	156.4	145.64
190	200	83.4	113.3	112.9	119.7	145.4
200	0					85.92
200	10	13.7	60.3	74.2	79.8	51.12
200	20	13.7	35.9	55.2	59.7	61.52
200	30	21.7	36.3	46.9	58.1	75.76
200	40	53.5	47.8	39.1	42.8	38
200	50	51.3	21.1	36.4	32.8	41.2
200	60	57.7	26.8	38.1	56.2	59.32
200	70	43.3	46.9	106.6	100.5	107.8
200	80	54.5	83.9	114	125	131.04
200	90	55.7	110	133.3	121.5	143.36
200	100	25.8	87	85.3	89.1	92.08
200	110	69	103.2	124.7	125.9	139.52
200	120	47.9	119.1	125.2	122	141.4
200	130	26.6	105.9	88.5	81.3	91.44
200	140	26.6	66.9	88.5	97.1	94.36
200	150	22	92.4	118.3	124.6	144.2
200	160	36.9	109.1	128.6	139.4	146.68
200	170	87.9	109	139.4	149.8	143.88
200	180	94	111.4	113.8	128.4	138.32
200	190	84.6	114.9	131.1	125.8	140.24
200	200	96.2	107.7	109.9	121.6	131.48

8.1.4 Differences between EM measurements at 0.75- and 1.5 m depth

Appendix 8.1.4

Differences (H-V) between EM measurements (mS/m) taken at 0.75 m and 1.5 m depth. Grid origin located at the southwest corner of the center bench.

Grid X (m)	Grid Y (m)	H-V (Jan)	H-V (Feb)	H-V (Mar)	H-V (Apr)	H-V (May)
10	10	-14.8	-17	-3.9	6.8	-3.32
10	20	-6.1	-3.8	-11.1	6.1	-10.56
10	30	2.4	-3.6	-26.2	-40.2	-13.64
10	40	-4.4	-1.8	-18.9	-17.6	5.56
10	50	-2.4	-5.8	-55.4	-55.3	5.6
10	60	-17.3	-10.5	-59.6	-13.5	9.56
10	70	-11.9	-94.9	-38.3	-32.4	-7.88
10	80	-19.5	-7.8	-3.4	1.4	5.04
10	90	-4.7	-13.1	-14	-24.3	-16.96
10	100	-11.8	-5.9	-10.2	-23.5	-5.6
10	110	-5.5	-11.6	13.8	-2.3	1.2
10	120	0.4	-2.9	-1.6	-1.2	-12.64
10	130	-10	-0.5	-2.3	-7.7	2.12
10	140	10.6	9.2	10.4	26.6	33.4
10	150	3.7	33.4	-14.7	-4.5	4.64
10	160	-3.1	20.3	6.3	12.1	18.44
10	170	2	5.4	14	9.7	18.04
10	180	-5.2	10.7	-21.5	-56.6	4.64
10	190	-4.7	-10.6	-18.7	-24.7	-6.48
10	200	-4.6	-2.2	7.8	-0.5	2.96
20	0					
20	10	-25.4	-11.7	-27.8	-30.2	-15.92
20	20	-11	-14.2	-22.6	-3.6	-11.88
20	30	-6.7	-14.3	-30.1	-18.9	5.56
20	40	-6.4	-12.7	-6.6	-28	-17
20	50	-7	-7.9	-17	-22.9	0.4
20	60	-15.4	-5.5	0.8	5.6	6
20	70	-17	1.9	6.5	-16.1	-11.2
20	80	-17.8	-15	-10	-11.8	-0.2
20	90	-24.8	-11.3	-27.4	-5.5	1.96
20	100	-13	-7	2.7	-0.7	19.6
20	110	-20.9	-10	-9.8	-17.5	-16.72
20	120	-6.6	-16.8	-2.3	-1	-1.6
20	130	-2.8	-5.1	-5.4	-14.1	6.72
20	140	5.9	-0.2	-12.4	-10.4	-1.52
20	150	6.3	18.3	-0.9	11.4	10.56
20	160	0.2	-0.1	-10	-7.3	10.36
20	170	-1.4	4.6	0.5	-3.4	9.4
20	180	-8.7	19.8	6.9	38.8	34.6
20	190	-4.5	1.1	1	30.3	-2.72

Grid X (m)	Grid Y (m)	H-V (Jan)	H-V (Feb)	H-V (Mar)	H-V (Apr)	H-V (May)
20	200	-1.7	-3.9	3.4	13.9	11.6
30	0					
30	10	-6.3	-5	-15.8	-11.4	-10.92
30	20	-28.2	-22.1	-34.1	-26.4	-15.84
30	30	-24	-12.4	-23.9	-14.6	-10.12
30	40	-15.9	-4.4	4.1	-8.7	-7.56
30	50	-25.2	-15.5	-11.7	-7.3	-14.68
30	60	-15.2	-6.8	-7.8	-7.4	-12.32
30	70	-24.2	3.2	-2.3	1.6	-3.52
30	80	-25.4	-34.4	-35.9	-29	-29.12
30	90	-10.3	-7.9	3.6	-5.5	-24.16
30	100	-23	-3.3	-1.8	-1.5	-3.56
30	110	-8.5	15.7	3.4	-15	-17.8
30	120	-8.6	-7.1	30.3	12.7	2.44
30	130	-9.4	-6	-11.5	27	18.28
30	140	-6	-3.2	9.3	9.9	7.48
30	150	-18.3	-3.7	26	24.1	16.36
30	160	-13	-9.5	-19.7	-7.1	27.84
30	170	-6.8	-13.6	-3.7	29.2	15.8
30	180	6.9	85.4	79.1	75.2	34.44
30	190	-1.1	14.2	22.5	41.1	27.4
30	200	-4.2	-6.4	16	19.8	27.92
40	0					
40	10	-27.2	-18.9	-17.9	-0.4	-28.92
40	20	-21.4	-8.8	0	-3.8	-18.36
40	30	-19.3	-22.3	-20.5	-4.5	-2.32
40	40	-21.3	-18.4	-20.8	0.5	4.76
40	50	-21.8	-23.5	-18.4	-23.5	-5.96
40	60	-10.6	-10.8	-11.4	0.7	-3.56
40	70	-5.2	-9.4	-5.2	-6.9	-11.16
40	80	-0.1	1.3	-8.4	3.7	-8.04
40	90	-11.3	-21.8	-14.7	-6	-8.88
40	100	-16.4	-9.9	14.5	20.6	-2.72
40	110	-16	-12.1	14.3	21.5	-0.88
40	120	-4.9	-3.8	18.4	2.3	-2.72
40	130	-5.6	-7.6	23.5	25	-1.72
40	140	-6.7	21.7	67.3	21.6	8.64
40	150	-5.2	-2.1	-14.4	-1.8	1.92
40	160	4.8	-7.4	-32	-31	-0.96
40	170	10.8	2.7	24.3	18.6	30.72
40	180	4.6	15.4	22	33	31.84
40	190	-1.2	8.6	30.4	22.5	30.28
40	200	-3.4	-3.9	-28.6	-42.7	-16.64

Grid X (m)	Grid Y (m)	H-V (Jan)	H-V (Feb)	H-V (Mar)	H-V (Apr)	H-V (May)
50	0					
50	10	-22	12.9	-11.1	-1.2	-12.12
50	20	-22.4	16.6	14.2	-1.6	-16.32
50	30	-23.9	20.8	-10.2	-13.2	-13.4
50	40	-18.5	-5.2	0.5	-29	-7.8
50	50	-20.7	-4.3	30.5	4	-13.88
50	60	-28.8	5.1	-26.7	-35.2	-12.24
50	70	-17.5	-14.3	-11.4	-20.4	-18
50	80	-17.3	-19.6	-41.8	-19.7	-25.08
50	90	-20.6	-26.7	-4.8	-3.9	-7.2
50	100	-26	-28	9.6	15	-4.24
50	110	-26.7	-12	-4.2	-12.7	-19.24
50	120	-30	-13.9	-31.6	-41.5	-11.08
50	130	-27.2	-12.2	-32	-16.4	1.88
50	140	-23.7	-11.2	-9.2	30	3.72
50	150	-3.8	-11.6	8.4	-9.5	2.84
50	160	-6.1	-12.5	-22.6	4.9	15.24
50	170	-4.9	-9.7	5	23.3	6.84
50	180	14	-14.9	25.9	10.5	50.8
50	190	9.9	-13.9	-4.2	2	53.56
50	200	11.9	-21	59.7	-8.8	43.68
60	0					
60	10	-24.3	-12.5	-14.4	-11.7	-19.6
60	20	-12.6	-21.2	-6.1	-1.5	-14.76
60	30	-21.5	-12	-10.5	-10	-8.12
60	40	-12.8	-15.7	-5.3	-9.6	-5.24
60	50	-14.4	-17	7.8	-4.2	-1.68
60	60	-13.2	-25.5	5.6	1.1	-1.68
60	70	-20.1	-25.9	-3.4	1.2	-0.64
60	80	-17.3	-15.9	-4	0.6	3.8
60	90	-12.9	-13.7	-7.8	7	4.04
60	100	-15.8	-11	-6.2	13	2.96
60	110	-18.5	-11.4	52.7	32.7	13
60	120	-27.7	-13	-8	17.6	16.08
60	130	-18.5	-17.5	-6.2	15.8	-7.24
60	140	-34.9	-26.2	17.1	16.2	-2.32
60	150	-19.6	-5.2	-6.8	15.4	-0.52
60	160	-3.5	-9.4	-28.4	23.4	3.2
60	170	-10.6	-18.2	12.2	-32.5	-9.44
60	180	1	0.5	4.4	-22.6	6.48
60	190	12.1	-3.4	31.1	56.3	47.6
60	200	-9.4	30	20.5	75.4	40.4
70	0					

Grid X (m)	Grid Y (m)	H-V (Jan)	H-V (Feb)	H-V (Mar)	H-V (Apr)	H-V (May)
70	10	-15.1	-9.9	16.3	2	-0.72
70	20	-27.3	-12.5	-28.1	-26.7	-7.6
70	30	-12.5	-13.9	-24.2	-14.1	-11.76
70	40	-25.9	-17.5	-20.8	-18.4	-11.64
70	50	-17.1	-11.8	-19.4	-12.8	-4.48
70	60	-10.5	-7.9	-6.6	-1.1	-6.36
70	70	-10.9	-9.5	6.3	5	2.88
70	80	-8.9	-16.9	3.4	-8.1	-4.72
70	90	-12.9	-16.4	22.1	-11.7	-6.28
70	100	-11.2	-11.1	-7.5	-21	-3.44
70	110	-11.1	-14.5	-7.1	0.3	7
70	120	-10.5	-12.1	-3.7	2.2	-6.12
70	130	-21.8	-4.8	28.9	23.4	-0.8
70	140	-10.9	-13.9	-2.8	10.7	0.52
70	150	-1.8	-10.8	4.7	12	2.32
70	160	13.6	-18.9	-6	2.2	1.76
70	170	-30	-9.6	-93.4	-79.3	0.16
70	180	-3	-4.4	-5.1	2.1	-5.12
70	190	-4.6	-3.8	-20	6.7	21.08
70	200	-6.8	14.1	19.2	52.6	37.88
80	0					
80	10	-2.2	-25.1	-7.1	-8.9	-6.96
80	20	-20.6	-11.7	-20.6	-20.9	-20
80	30	-8.6	-23.7	-12.6	1.5	-4.16
80	40	-15.6	-15.1	-18.3	-30.2	-14.68
80	50	-14.4	-15.3	-11.4	-3.5	-7.92
80	60	-28.1	-10.5	-33.2	-15.6	-16.68
80	70	-8.7	-11.3	-4.5	1	0.2
80	80	-13.6	-9.4	-15.6	-1.4	-8.16
80	90	-15.2	-10.1	-14.2	-2.4	-6.76
80	100	-5.5	-9.1	-5	-4.2	4.04
80	110	-4.6	-12.3	-781.6	12.4	8.16
80	120	-7.5	-19.9	23.7	-3.5	0.12
80	130	-9	-23.1	-27.1	-2.8	-14
80	140	-13.7	-19.2	18.8	22.5	12.28
80	150	-16.7	-15.5	-15.4	-0.3	6.32
80	160	-2.4	2.4	2	5	1.48
80	170	4.5	-10.2	-17.9	-7.6	-1.6
80	180	-19.3	6.1	-10.9	0.4	8.56
80	190	-1.4	-4.1	31	56.7	57.72
80	200	5.4	1.1	22.6	17.1	6.8
90	0					
90	10	-4.4	-25.7	-8.6	-36.2	2.72

Grid X (m)	Grid Y (m)	H-V (Jan)	H-V (Feb)	H-V (Mar)	H-V (Apr)	H-V (May)
90	20	-18.1	-3.8	-4.9	8.9	1.88
90	30	-8.5	-17.1	-17.8	-23	0.2
90	40	-23	-9.4	-52.3	-16.8	-2.12
90	50	-15.5	-14.9	-17.2	-25.6	-6.36
90	60	-18.8	-10.6	-6.1	0.2	-0.04
90	70	-6	0.7	-13.2	-6.4	-9.64
90	80	-9.1	-5.9	10	6.8	-8.84
90	90	-13.4	-3.2	-11.2	-7.6	-12.8
90	100	-9.5	-12.5	-12.2	5.2	1.16
90	110	-6.8	-5.5	-11.2	-10.1	-6.88
90	120	-6.3	-9.2	-25.8	-11.8	-16.24
90	130	-8.2	-17.5	-0.5	-1.9	-6.92
90	140	-8.8	-11.1	-4.9	-1.2	0.48
90	150	-9	-15.4	1.2	4.3	22.24
90	160	-11	14.7	-27.3	16.1	7.36
90	170	21.3	-0.1	-18.4	4.5	1.96
90	180	-6.9	-20.5	-16.8	8.9	-0.2
90	190	25.5	13.4	18.4	10	8.08
90	200	11.5	40	0	12.3	26.28
100	0					
100	10	-11.9	-17.7	-6.7	-8.7	-4.56
100	20	-8.9	-26.3	9	-21.3	-10.32
100	30	-12.3	-28.4	-23.3	7.5	-5.84
100	40	-12.3	-22.1	8.6	3.9	-22.44
100	50	-30.4	-16.9	-45.3	-16.3	-9.8
100	60	-9.1	-13.6	0	-2.8	-3
100	70	-10.7	-4.6	4.6	4.1	-3.72
100	80	-8.5	-13.5	-4.5	1.3	-5
100	90	-21.3	-13.4	0.2	4.1	-14.16
100	100	-8	-12.9	-2.4	-1.6	-4.96
100	110	-8.6	-4.5	-16.2	-19.5	0.44
100	120	-8.6	-4.1	13.7	3.9	1.16
100	130	-9.2	-13.3	17.2	9.5	3
100	140	-9.3	-10.7	10.7	12.5	10.08
100	150	-8.3	-14.7	-6	-6.2	-5.96
100	160	-17.2	-10.1	20.2	18.5	10.6
100	170	11.6	15.9	2.7	14.6	10.56
100	180	-4.7	6.2	26.7	17.9	5.92
100	190	5.5	-0.8	4.7	10.3	1.8
100	200	15.7	-9.3	6.2	3.9	12.76
110	0					
110	10	0.6	-2.6	11.8	10.5	-2.92

Grid X (m)	Grid Y (m)	H-V (Jan)	H-V (Feb)	H-V (Mar)	H-V (Apr)	H-V (May)
110	20	-6.6	-3.8	-15.9	-31.5	-29.32
110	30	-9.9	-26.5	7.1	11.3	-6.6
110	40	-4.9	-14.9	-45.9	-24.1	-28.04
110	50	-2.2	-17.7	1.5	17.1	-5.04
110	60	-9.9	-9	-5.2	2.2	-4.12
110	70	-9.1	-9.1	-17.1	-0.8	-0.28
110	80	-13	-4.2	6.6	8.9	-9.32
110	90	-7.6	-15.3	-4.9	-5.1	-2.4
110	100	-16.1	-8.7	-4.4	-7.5	-0.76
110	110	-14.3	-4.2	-1.7	8	-0.32
110	120	-3.8	-2.6	14.8	-1.4	-1.12
110	130	-6.1	-5.1	-9.7	-12.2	-5.04
110	140	-7.7	-6.3	7.1	1.6	1.92
110	150	-8.2	-7.1	-4.1	9.3	10.8
110	160	-10.7	-11.8	23.6	11.1	5.6
110	170	-3.8	-15.8	10.1	6.7	5
110	180	16.9	-6.7	-0.7	-2.4	3.28
110	190	7.9	-13.4	2.1	-2.1	3.64
110	200	-27.7	13.2	9.7	0.3	6.96
120	0					
120	10	-6.9	-22.9	-17.3	-13.6	1.92
120	20	-6.5	-19.6	-46.6	-45.4	-21.4
120	30	-5.2	-17.2	-20	-22.8	-17.12
120	40	-2.1	-23.1	8.1	19.8	-2.84
120	50	-6.9	-22.5	-54.3	-38.9	-1.2
120	60	-12.5	-13.6	2.6	6.1	1.2
120	70	-9.7	-14.4	-2.3	-5.7	-4.92
120	80	-6.3	-16.5	-22.3	-10.2	-5.96
120	90	-8.7	-15.4	-14.4	-6.6	-9.24
120	100	-6.6	-3	2.3	3.5	7.8
120	110	-8.3	-3.6	-8.5	-4.5	1.72
120	120	-9.7	-5.3	3.1	7.6	-3.64
120	130	-5.4	-6.6	-9.4	1.5	-11.52
120	140	-1.3	-8	-1.6	-3.9	-12.48
120	150	-6.5	-7.5	-20	-18.4	-19.84
120	160	-5.3	-5.4	27.6	7.1	-0.84
120	170	-17.8	3.2	-2.8	-6.7	4.24
120	180	-6.6	-3.9	42.9	19.6	8.72
120	190	-8.5	-4	-5.2	-9	-2.52
120	200	-12.9	9.3	-20.9	-17.5	2.08
130	0					
130	10	0.2	-6.4	27.6	39.9	34.76
130	20	0.7	-5.6	2.5	5	1.56

Grid X (m)	Grid Y (m)	H-V (Jan)	H-V (Feb)	H-V (Mar)	H-V (Apr)	H-V (May)
130	30	-2.5	-9.8	-22.1	-7.6	-23.24
130	40	-2.4	-24	27.2	-4.8	-2.28
130	50	-1.5	-8.6	19.8	-1	-2.92
130	60	-4.3	-5.5	-41.1	-7.2	-10.2
130	70	-5.6	-4.6	-11.6	-9.4	-7.52
130	80	-6.3	-2.2	12.4	6.3	-2.48
130	90	-7.6	-4.5	-48.1	-6.9	-6.16
130	100	-6.5	-7.8	-26.3	-0.5	-9.44
130	110	-4.8	-6	-22.9	2.3	-2.56
130	120	-11.1	-3.3	4.6	3.7	0.76
130	130	-7.7	-3.8	16.6	12.3	1.6
130	140	-15.8	-8.9	-4.7	-7.7	-5.2
130	150	-20.2	-7	-18.5	-8	-6.8
130	160	-7.9	-6.2	19.4	-3.7	-3.12
130	170	-71.5	-15.2	18.2	12.9	2.08
130	180	-2.1	-5.8	16.7	22.8	17.52
130	190	-10.4	2.9	-8	-3.3	-5.4
130	200	-8.7	-23.7	7.5	4.5	5.6
140	0					
140	10	-2.8	-6	30	21.8	1.84
140	20	-7.6	-6.9	-30.3	-22.5	3.76
140	30	-0.1	-5.5	18.9	17	1.04
140	40	0.1	-8	25.2	15.4	-2.24
140	50	-3.8	1.1	13.1	6.2	0.64
140	60	-7.5	-12.7	-0.6	-4.5	-10.52
140	70	-11.9	-15.1	2.9	-2.5	0.56
140	80	-8.4	-6.7	5.9	11.7	0.6
140	90	-5.2	-9.4	-6.2	3.2	-2.24
140	100	-7.1	-6.1	-5.4	-14.4	0.36
140	110	-4.8	-7.4	-24	-13.9	-7.92
140	120	-15.7	-6.3	-0.8	-17.5	-2.36
140	130	-8.5	-1.2	-13.1	11.8	7.8
140	140	-14.5	0	15	10.4	11.48
140	150	-11.4	-4.1	6.7	20	9.76
140	160	-16.7	0.2	4.6	6.9	-5.28
140	170	-25.2	-0.8	41.8	29.2	0.44
140	180	-16.6	15.3	0.4	8	3.72
140	190	-1.5	16.7	33.1	15	-1.92
140	200	-1.9	5.5	2.8	-1.9	2.72
150	0					
150	10	-2.4	-1.7	-21.6	-17.3	0.24
150	20	-3.8	-3	6.5	6.4	0.48
150	30	8	-0.7	-2.1	-0.6	1.68

Grid X (m)	Grid Y (m)	H-V (Jan)	H-V (Feb)	H-V (Mar)	H-V (Apr)	H-V (May)
150	40	-4.7	1.5	-3.8	6.8	2.6
150	50	-1.2	-25.6	-41.7	-15.7	-12.44
150	60	-2	-8.9	-2.8	3.1	4.08
150	70	0.7	-9.7	-3	-7	-1.68
150	80	1.4	-4.8	11.3	16.4	5.16
150	90	-6.1	-7.1	-6.4	-0.6	-2.8
150	100	-8.4	-9.3	-9	-10.2	-7.36
150	110	-3.7	-7.7	0.2	-4.7	0.76
150	120	-4.5	-4.1	3.5	-8.1	-5.08
150	130	-7.6	-12.6	-11	-4.9	0.48
150	140	-3.3	-6.9	11.6	-21.4	-6.08
150	150	-10.5	-2	6.3	-10.2	-5.36
150	160	-12.5	-9.3	-11.2	-6.1	-21.04
150	170	-11	-22.1	21.2	5.2	0.96
150	180	-7.9	-9.5	10.1	11.5	7.24
150	190	-14.4	-1.6	2	7.7	10.28
150	200	-17.3	-6.8	10.8	11	8.36
160	0					
160	10	-4.8	-24.9	10	7.8	4.96
160	20	-5.1	-1.8	-3.4	2.7	-1.36
160	30	-5.8	0	0.1	2.1	-0.2
160	40	-0.9	-2.7	-0.7	-3.1	-0.08
160	50	-3.1	-3.8	2	2.7	10.92
160	60	-2.4	-5.3	-2.2	10.7	-7.96
160	70	-3.3	-12	2.1	1.8	-1.12
160	80	-12.8	-3	12.2	16.8	-0.64
160	90	-14.2	-3.6	8.2	6.3	0.8
160	100	-7.5	-7.6	-13.4	-4.8	-8.6
160	110	-1.4	-13.3	-11.8	-9	-9.16
160	120	-4	-7.3	-2	-5.8	-9.88
160	130	-12.1	-7.1	-8.5	-7.4	-2.08
160	140	-16.8	-6.3	7.9	10.2	3.28
160	150	-11.4	-5.2	7.1	0.2	1.56
160	160	-12.7	-4.2	-19	-17.9	-9.96
160	170	-10.4	-20.7	3.1	18.3	1.48
160	180	-2.6	-0.2	17.7	14.4	5.24
160	190	-21.1	21.6	13	8.3	12.28
160	200	-22.8	27.9	27.7	18.1	3.28
170	0					
170	10	-2.4	-13.8	-56.1	-26.1	-3.08
170	20	-7	0	5.3	-6.9	8.56
170	30	-7.3	-1.5	30.3	26.8	17.04
170	40	-4.5	-2.9	19.8	27.8	12.12

Grid X (m)	Grid Y (m)	H-V (Jan)	H-V (Feb)	H-V (Mar)	H-V (Apr)	H-V (May)
170	50	-4.2	-4.2	14.5	12.1	13.12
170	60	-1.8	-8.4	12.5	14.5	11.04
170	70	-9.2	-18.4	0	-6.9	1.6
170	80	-8.4	-5.6	2	2.6	3
170	90	-11.8	-6.3	-0.1	0.5	0.52
170	100	-14.4	-6.5	-7.5	1.5	-3.28
170	110	-26.2	-11	4.8	-4.5	-7.72
170	120	-24.4	-11	30.5	5.4	-0.44
170	130	-15.6	-7	-9.3	-2.6	3.32
170	140	-18.4	-2.1	-1.4	-4.8	-7.92
170	150	-23.1	9	-21.9	-10.6	-4.56
170	160	-21	-0.8	-5.3	-12	-3.24
170	170	-0.7	-8.5	7.8	0.9	1.28
170	180	8	-6.4	-9	12.5	5.68
170	190	11	-4.7	6	7.8	12.84
170	200	-14.9	7.4	7.8	21.3	19.8
180	0					
180	10	1.3	-10.1	44.3	14.9	18.32
180	20	-3.2	-4	7.7	-9	6.36
180	30	-1.3	-4.7	0	21.1	2.68
180	40	-2.4	-5	0.3	-3.6	-3.32
180	50	6.3	-1.7	4.6	9.8	5.32
180	60	4.2	-1.3	2.3	-12.1	0.4
180	70	-0.5	-4.4	54.7	12.7	-11.2
180	80	3	-14.2	5.9	-4.9	-10.84
180	90	-11.8	-10.3	-13.2	2.2	-3.08
180	100	-8.9	-12.1	-11.7	-17.7	-13.48
180	110	-1.5	-9.8	-15.5	-2.8	0.2
180	120	-21.5	-17.8	6.6	-8.7	-10.08
180	130	-8	-10.8	-9.7	-20.6	2.88
180	140	-9.7	-9.9	-7.3	-3.8	-7.16
180	150	-17.7	-10.9	-24.4	11.8	0.28
180	160	3.5	-12.9	4.1	-6.1	-5.44
180	170	-7.9	-3.8	52.2	49.6	3.24
180	180	18.9	-9.2	-15.2	12.9	5.44
180	190	10.8	-17.3	-41	26.9	12.92
180	200	2.2	-8.5	2.6	48.1	22.04
190	0					
190	10	-0.2	-8.1	7.5	34.6	-10.12
190	20	-1.9	-12.5	-9.8	-5.3	2.64
190	30	-2	2	5.4	1.3	-0.36
190	40	-8.5	0.9	-2.8	0.6	4.12
190	50	-4.8	0.2	-6.3	-16.7	-6.68

Grid X (m)	Grid Y (m)	H-V (Jan)	H-V (Feb)	H-V (Mar)	H-V (Apr)	H-V (May)
190	60	-11.1	-1.4	10.1	13.5	13.4
190	70	-4.8	-11	-4.2	7.5	2.72
190	80	-5.4	-8.2	5.9	8.9	-4.2
190	90	-3.6	-18.8	35	36.5	5.44
190	100	10.8	-14.4	4.8	24.6	13.28
190	110	-11.4	-9.3	20.4	14.1	12.56
190	120	-3.2	7	-14.2	3.9	-0.72
190	130	-0.4	-5.9	-3.8	-9.9	-12.48
190	140	2.4	-0.1	33.8	-2.9	-15.88
190	150	10.2	-14.2	39.7	8.6	-8.08
190	160	-3.7	-15.3	7.5	36.9	0.12
190	170	-9.8	-14.1	5	-16.6	3.8
190	180	-2.9	-17.8	-9.5	21.2	11.32
190	190	13.9	-2.8	13.9	-5.4	9.04
190	200	4.7	29.7	-21.2	-12.1	12
200	0					
200	10	-3	6.8	-59.9	-60.1	-0.44
200	20	-2.7	-7	6.2	-7	-2.64
200	30	-0.6	1.4	17.8	11.6	-0.44
200	40	-2.2	4.1	12.2	-0.9	1.36
200	50	-4.6	-0.3	3.1	6.8	0.08
200	60	-4.6	-3.1	18.3	-26.5	-8.08
200	70	-5	2.7	13.1	29.5	17.64
200	80	5.4	-16.2	35.3	32.1	23.2
200	90	3.3	3.3	8.5	22.9	2.76
200	100	-4.2	-15.5	-7	-11.4	-12.32
200	110	18.8	-20.3	-2.3	3.4	-5.88
200	120	23.3	-24.3	4.8	12.7	-2.56
200	130	3.9	-22.2	3.3	13	2.64
200	140	9.6	-8.1	-7.3	-8.3	-3.56
200	150	-0.3	1.3	7.4	11.3	-7.96
200	160	1.5	-7.8	26.4	13	7.84
200	170	3.5	-12.2	-7.7	-15	-2.36
200	180	-0.1	-21.9	39.8	23.8	14.32
200	190	-2.6	-2.6	29	32.9	17.4
200	200	3.8	16.6	38	15.1	19.24

8.1.5 Estimates of average root zone salinities, EC_e, from the May, 1994 EM38 survey taken to a depth 0.75 m.

Four methods are described by Rhoades et al. (1990) for the conversion of apparent bulk soil electrical conductivity, EC_a, to average root zone conductivity, EC_e, which is often referred to as the electrical conductivity of the soil water extract. The conversions tabulated in the following appendix were executed using method IV, which only requires estimates of soil water content and percent clay of the soil being evaluated. Neither water content nor percent clay was measured at the time of the survey. However, the conversions are not sensitive to water content changes within the range of 10 to 30 volume percent (Sheets et al., 1994) and therefore, a water content of 20 volume percent was used for all calculations. Estimates of percent clay were obtained by using the U.S. Department of Agriculture textural triangle for soil textural analysis in conjunction with a soils map of the study area (Soil survey by Clarence Montoya and provided by the Socorro office of the Soil Conservation Service, 1992). As listed in the following appendix, all soils described as sandy clay loams (SCL) were assigned a clay content of 27%, all silt loams (SiL) 14%, all sandy loams (SL) 10%, all loamy sands (SL) 7%, all silty clay loams (SCL) 33%, and all clay loams (CL) 35%. Each of these values lies near the center of corresponding boundaries on the textural triangle.

The calculated values listed in the following appendix range from 1.46 dS/m to 10.5 dS/m and the mean value is 5.58 dS/m. At the time that the aerial photograph (Figure 16c) of the field site was taken, field corn was the crop. According to the Soil Conservation Service Technical Guide of Toxic Salt Reduction Specifications, EC_e values of approximately 6 dS/m are associated with a 50% reduction in yield of field corn. Comparable reductions are illustrated by the aerial photograph. The current crop at the field site is alfalfa. The technical guide states that 50% reductions in the yield of alfalfa are associated with EC_e values of approximately 8 dS/m. Therefore the landowner can expect a significant increase in alfalfa yield relative to the yield of field corn.

Appendix 8.1.5

Grid X	Grid Y	ECa (mS/m)	Soil Type	~% Clay	EC$_e$ (dS/m)
0	0	58.64	SCL	27	2.83
0	10	55	SCL	27	2.65
0	20	48.16	SiL	14	2.80
0	30	55.44	SiL	14	3.22
0	40	66.36	SiL	14	3.86
0	50	116.96	SiL	14	6.82
0	60	109.92	SCL	27	5.31
0	70	86.12	SCL	27	4.16
0	80	78.8	SCL	27	3.80
0	90	148	SCL	27	7.16
0	100	129.64	SL	10	8.11
0	110	44.28	SiL	14	2.57
0	120	45.28	SiL	14	2.63
0	130	92.72	SiL	14	5.40
0	140	136.04	SL	10	8.51
0	150	155.12	SL	10	9.71
0	160	122	SL	10	7.63
0	170	73.84	LS	7	4.89
0	180	75.44	LS	7	5.00
0	190	57	LS	7	3.77
0	200	41.16	LS	7	2.72
10	0	138.96	SCL	27	6.72
10	10	105.52	SCL	27	5.10
10	20	67.08	SiL	14	3.90
10	30	87.76	SiL	14	5.11
10	40	86.04	SiL	14	5.01
10	50	142.12	SiL	14	8.29
10	60	156.76	SiL	14	9.14
10	70	93.48	SCL	27	4.52
10	80	92.24	SCL	27	4.46
10	90	96.4	SL	10	6.03
10	100	86.44	SL	10	5.40
10	110	144.32	SiL	14	8.42
10	120	47.24	SiL	14	2.75
10	130	46.56	SiL	14	2.71
10	140	121.8	SL	10	7.62
10	150	151.24	SL	10	9.46
10	160	148.04	SL	10	9.26
10	170	136.48	LS	7	9.05
10	180	134.76	LS	7	8.93
10	190	111.16	LS	7	7.37
10	200	36.32	LS	7	2.40
20	0	129.16	SCL	27	6.25
20	10	120.28	SCL	27	5.82
20	20	95.4	SCL	27	4.61
20	30	148.64	SCL	27	7.19

Grid X	Grid Y	ECa (mS/m)	Soil Type	~% Clay	EC$_e$ (dS/m)
20	40	113	SiL	14	6.59
20	50	98.88	SiL	14	5.76
20	60	153.12	SiL	14	8.93
20	70	140.96	SiL	14	8.22
20	80	76.52	SiL	14	4.46
20	90	73.32	SiL	14	4.27
20	100	113.52	SiL	14	6.62
20	110	81.56	SiL	14	4.75
20	120	82.44	SiL	14	4.80
20	130	74.16	SL	10	4.63
20	140	37.68	SL	10	2.35
20	150	117.96	SiL	14	6.88
20	160	158.76	SiL	14	9.26
20	170	148.72	SiL	14	8.68
20	180	158.88	LS	7	10.53
20	190	125.28	LS	7	8.30
20	200	50.44	LS	7	3.34
30	0	126.16	SCL	27	6.10
30	10	115.6	SCL	27	5.59
30	20	117.4	SCL	27	5.68
30	30	90.96	SCL	27	4.39
30	40	83.72	SiL	14	4.88
30	50	79.08	SiL	14	4.61
30	60	64.08	SiL	14	3.73
30	70	82.92	SiCL	33	3.73
30	80	101.08	SiCL	33	4.56
30	90	81.16	SiL	27	3.92
30	100	78.92	SiL	27	3.81
30	110	88.84	SiL	27	4.29
30	120	168.32	SiL	27	8.15
30	130	162.64	SL	10	10.18
30	140	55.72	SL	10	3.48
30	150	58.84	SiL	14	3.42
30	160	153.12	SiL	14	8.93
30	170	164.16	SiL	14	9.58
30	180	160.04	SiL	14	9.34
30	190	142.48	LS	7	9.45
30	200	96.68	LS	7	6.41
40	0	74.88	SCL	27	3.61
40	10	95.56	SiL	14	5.57
40	20	71.56	SiL	14	4.17
40	30	81.96	SCL	27	3.96
40	40	103.88	SiL	14	6.06
40	50	62.8	SiL	14	3.65
40	60	75.36	SiL	14	4.39

Appendix 8.1.5 (Continued)

Grid X	Grid Y	ECa (mS/m)	Soil Type	~% Clay	EC_e (dS/m)
40	70	62.68	SiCL	33	2.82
40	80	70.16	SiCL	33	3.16
40	90	90.32	SiCL	33	4.07
40	100	150	SiL	14	8.75
40	110	150.84	SiL	14	8.80
40	120	144.72	SiL	14	8.44
40	130	157.08	SiL	14	9.16
40	140	161.52	SiL	14	9.42
40	150	30.68	SiL	14	1.78
40	160	113.32	SiL	14	6.61
40	170	158.2	SiL	14	9.23
40	180	144.72	SiL	14	8.44
40	190	43.28	LS	7	2.86
40	200	132.64	SiL	14	7.74
50	0	118.88	SiL	14	6.93
50	10	85.92	SiL	14	5.01
50	20	100	SiL	14	5.83
50	30	115.8	SiL	14	6.75
50	40	123.04	SiL	14	7.17
50	50	79.48	SiL	14	4.63
50	60	104.16	SiL	14	6.07
50	70	86.8	SiL	14	5.06
50	80	139.92	SiCL	33	6.31
50	90	132.88	SiL	14	7.75
50	100	94.52	SiL	14	5.51
50	110	140.52	SiCL	33	6.34
50	120	162.4	SiL	14	9.47
50	130	152.44	SiL	14	8.89
50	140	164.96	SiL	14	9.62
50	150	91.6	SiL	14	5.34
50	160	46.52	SL	10	2.90
50	170	135.32	SL	10	8.47
50	180	160.24	SL	10	10.03
50	190	151.48	SiL	14	8.84
50	200	136	SiL	14	7.93
60	0	130.24	SiL	14	7.60
60	10	102.44	SiL	14	5.97
60	20	86.6	SiL	14	5.05
60	30	68.76	SiL	14	4.00
60	40	87.24	SiL	14	5.08
60	50	98.88	SiL	14	5.76
60	60	95.48	SiL	14	5.56
60	70	95.96	SiL	14	5.59
60	80	109.6	SiL	14	6.39
60	90	98.88	SiCL	33	4.46
60	100	98.4	SiCL	33	4.43

116

Grid X	Grid Y	ECa (mS/m)	Soil Type	~% Clay	EC$_e$ (dS/m)
60	110	116.16	SiCL	33	5.24
60	120	129.72	SiL	14	7.56
60	130	160.24	SiL	14	9.35
60	140	145.52	SiL	14	8.49
60	150	164.8	SiL	14	9.61
60	160	25.24	SiL	14	1.46
60	170	44.16	SiL	14	2.57
60	180	149.08	SL	10	9.33
60	190	149.32	SL	10	9.34
60	200	143.52	SiL	14	8.37
70	0	144.8	SiL	14	8.45
70	10	115.08	SiL	14	6.71
70	20	88.76	SiL	14	5.17
70	30	74.4	SiL	14	4.33
70	40	67.6	SiL	14	3.94
70	50	90.8	SiL	14	5.29
70	60	82.64	SiL	14	4.81
70	70	76.08	SiL	14	4.43
70	80	78.64	SCL	27	3.80
70	90	89.8	SCL	27	4.34
70	100	122.32	SCL	27	5.92
70	110	131.88	SCL	27	6.38
70	120	123.8	SiL	14	7.22
70	130	151.32	SiL	14	8.83
70	140	166.32	SiL	14	9.70
70	150	167.32	SiL	14	9.76
70	160	166.52	SiL	14	9.72
70	170	39.2	SiL	14	2.28
70	180	99.6	SiL	14	5.80
70	190	152.92	SL	10	9.57
70	200	136.92	SiL	14	7.99
80	0	142.76	SiL	14	8.33
80	10	84	SiL	14	4.89
80	20	138.48	SiL	14	8.08
80	30	96.2	SiL	14	5.61
80	40	78.92	SiL	14	4.60
80	50	102.32	SiL	14	5.96
80	60	74.24	SiL	14	4.32
80	70	80.08	SiL	14	4.66
80	80	71.92	SiL	14	4.19
80	90	80.96	SCL	27	3.91
80	100	96	SCL	27	4.64
80	110	153.24	SCL	27	7.42
80	120	111.64	SiL	14	6.51
80	130	145.24	SiL	14	8.47
80	140	159.96	SiL	14	9.33
80	150	164.76	SiL	14	9.61

Grid X	Grid Y	ECa (mS/m)	Soil Type	~% Clay	EC_e (dS/m)
80	160	158.16	SiL	14	9.23
80	170	164.8	SiL	14	9.61
80	180	153.4	SiL	14	8.95
80	190	148.84	SL	10	9.31
80	200	156.6	SiL	14	9.14
90	0	159.88	SiL	14	9.33
90	10	148.2	SiL	14	8.64
90	20	157.32	SiCL	33	7.10
90	30	149.56	SiCL	33	6.75
90	40	104.16	SiCL	33	4.69
90	50	72.64	SiCL	33	3.27
90	60	105.76	SiCL	33	4.77
90	70	91.44	SiL	14	5.33
90	80	72.44	SiL	14	4.22
90	100	68.64	SiL	14	4.00
90	110	65.64	SiL	14	3.82
90	120	97.96	SCL	27	4.73
90	130	128.36	SCL	27	6.21
90	140	121.56	CL	35	5.37
90	150	119.04	SiL	14	6.94
90	160	164.36	SiL	14	9.59
90	170	164.92	SiL	14	9.62
90	180	164.28	SiL	14	9.58
90	190	166.4	SiL	14	9.71
90	200	158.08	SiL	14	9.22
100	0	151.32	SiL	14	8.83
100	10	154.48	SiL	14	9.01
100	20	140.52	SiCL	33	6.34
100	30	142.16	SiCL	33	6.41
100	40	91.6	SiCL	33	4.13
100	50	68.28	SiCL	33	3.07
100	60	66.96	SiCL	33	3.01
100	70	77.56	SiCL	33	3.49
100	80	92.44	SiCL	33	4.16
100	90	68.56	SiCL	33	3.08
100	100	60.16	SiCL	33	2.70
100	110	62	SiCL	33	2.79
100	120	70.4	SCL	27	3.40
100	130	72.6	SCL	27	3.50
100	140	80.12	CL	35	3.53
100	150	74.76	SiL	14	4.35
100	160	161.6	SiL	14	9.43
100	170	166.16	SiL	14	9.69
100	180	156.04	SiL	14	9.10
100	190	161.32	SCL	27	7.81
100	200	165.92	SCL	27	8.03
110	0	143.76	SiL	14	8.39

Grid X	Grid Y	ECa (mS/m)	Soil Type	~% Clay	EC_e (dS/m)
110	10	154.36	SiCL	33	6.97
110	20	119.76	SiL	14	6.98
110	30	138.88	SiL	14	8.10
110	40	111.2	SiL	14	6.48
110	50	72.44	SiL	14	4.22
110	60	80.88	SiCL	33	3.64
110	70	105.48	SiCL	33	4.75
110	80	89.16	SiCL	33	4.02
110	90	69.76	SiCL	33	3.14
110	100	72.36	SiCL	33	3.25
110	110	75.6	SiCL	33	3.40
110	120	76.48	SCL	27	3.69
110	130	75.68	CL	35	3.33
110	140	79.52	SiL	14	4.63
110	150	111.36	SiL	14	6.49
110	160	158.32	SiL	14	9.24
110	170	163.32	SiL	14	9.53
110	180	158	SiCL	33	7.13
110	190	157.84	SCL	27	7.64
110	200	163	SiL	14	9.51
120	0	71.32	SiCL	33	3.21
120	10	80.36	SiCL	33	3.62
120	20	89.88	SiCL	33	4.05
120	30	99.32	SiL	14	5.79
120	40	70.4	SiL	14	4.10
120	50	63.68	SiL	14	3.71
120	60	70.36	CL	35	3.10
120	70	63.68	CL	35	2.80
120	80	71.48	CL	35	3.15
120	90	79.8	CL	35	3.52
120	100	77.28	CL	35	3.40
120	110	75.28	CL	35	3.31
120	120	72.4	CL	35	3.19
120	130	74.12	CL	35	3.26
120	140	75	CL	35	3.30
120	150	72.76	SiCL	33	3.27
120	160	151.16	SiCL	33	6.82
120	170	156.92	SiCL	33	7.08
120	180	164.68	SiL	14	9.61
120	190	133.72	SiL	14	7.80
120	200	161.96	SiL	14	9.45
130	0	66.68	CL	35	2.93
130	10	116.12	SiCL	33	5.24
130	20	68.4	SiCL	33	3.08
130	30	112.84	SiCL	33	5.09
130	40	70.84	SiL	14	4.12
130	50	63.72	SiL	14	3.71

Grid X	Grid Y	ECa (mS/m)	Soil Type	~% Clay	EC$_e$ (dS/m)
130	60	95.96	CL	35	4.23
130	70	77.84	CL	35	3.43
130	80	70.72	CL	35	3.11
130	90	109.92	CL	35	4.85
130	100	78.88	CL	35	3.47
130	110	72.4	CL	35	3.19
130	120	81.28	CL	35	3.58
130	130	72.68	CL	35	3.20
130	140	75.8	CL	35	3.34
130	150	76.64	CL	35	3.38
130	160	116.32	SiCL	33	5.24
130	170	161.24	SiCL	33	7.28
130	180	165.4	SiCL	33	7.47
130	190	124.36	SiL	14	7.25
130	200	164.6	SiL	14	9.60
140	0	69.2	CL	35	3.05
140	10	94.36	CL	35	4.16
140	20	37.44	CL	35	1.64
140	30	86.16	CL	35	3.80
140	40	111	SiCL	33	5.00
140	50	88.16	CL	35	3.89
140	60	91.36	CL	35	4.03
140	70	71.96	CL	35	3.17
140	80	69.04	CL	35	3.04
140	90	79.2	CL	35	3.49
140	100	72.2	CL	35	3.18
140	110	84	CL	35	3.70
140	120	88.56	CL	35	3.90
140	130	74.56	CL	35	3.28
140	140	78.76	CL	35	3.47
140	150	83.88	CL	35	3.70
140	160	91.84	SiCL	33	4.14
140	170	154.12	SiCL	33	6.96
140	180	155.84	SiCL	33	7.03
140	190	153.92	SiL	14	8.98
140	200	153.04	SiL	14	8.93
150	0	96.84	CL	35	4.27
150	10	50.24	CL	35	2.21
150	20	57.44	CL	35	2.52
150	30	47.6	CL	35	2.09
150	40	93.68	CL	35	4.13
150	50	80.76	CL	35	3.56
150	60	71.92	CL	35	3.17
150	70	62.36	CL	35	2.74
150	80	67.08	CL	35	2.95
150	90	68.68	CL	35	3.02
150	100	68.88	CL	35	3.03

Grid X	Grid Y	ECa (mS/m)	Soil Type	~% Clay	EC$_e$ (dS/m)
150	110	71.92	CL	35	3.17
150	120	73.52	CL	35	3.24
150	130	70.56	CL	35	3.11
150	140	75.8	CL	35	3.34
150	150	69.84	CL	35	3.07
150	160	104.4	SiCL	33	4.71
150	170	140.92	SiCL	33	6.36
150	180	157.04	SiCL	33	7.09
150	190	152.96	SiCL	33	6.90
150	200	153.56	SiL	14	8.96
160	0	122.32	CL	35	5.40
160	10	57.64	CL	35	2.53
160	20	40.96	CL	35	1.79
160	30	41.12	CL	35	1.80
160	40	54	SCL	27	2.60
160	50	85.36	CL	35	3.76
160	60	94.32	CL	35	4.16
160	70	62.44	CL	35	2.75
160	80	66	CL	35	2.90
160	90	70.28	SiCL	14	4.09
160	100	82.32	SiCL	14	4.80
160	110	73.28	CL	35	3.23
160	120	95.8	CL	35	4.22
160	130	68.4	CL	35	3.01
160	140	82.8	CL	35	3.65
160	150	76.4	SiL	14	4.45
160	160	98.6	SiCL	33	4.44
160	170	143.92	SiCL	33	6.49
160	180	141.16	SiCL	33	6.37
160	190	156.56	SiCL	33	7.07
160	200	150.44	SiCL	33	6.79
170	0	133.92	SCL	27	6.48
170	10	67.36	CL	35	2.96
170	20	63.2	CL	35	2.78
170	30	80.2	CL	35	3.53
170	40	59.76	SCL	27	2.88
170	50	54.52	SCL	27	2.63
170	60	65	CL	35	2.86
170	70	75.68	CL	35	3.33
170	80	68.32	SiCL	33	3.07
170	90	72.44	SiCL	33	3.26
170	100	68	SiCL	33	3.06
170	110	78.96	SiL	14	4.60
170	120	100	SiL	14	5.83
170	130	73.68	SiL	14	4.29
170	140	92.48	SiL	14	5.39
170	150	71.04	SiL	14	4.14

Grid X	Grid Y	ECa (mS/m)	Soil Type	~% Clay	EC_e (dS/m)
170	160	72.04	SiL	14	4.19
170	170	131.28	SiL	14	7.66
170	180	152.32	SiCL	33	6.87
170	190	151.72	SiCL	33	6.85
170	200	125.32	SiCL	33	5.65
180	0	60.52	CL	35	2.66
180	10	110.24	CL	35	4.86
180	20	59.48	CL	35	2.61
180	30	62.32	CL	35	2.74
180	40	47.24	SCL	27	2.27
180	50	58.4	SCL	27	2.81
180	60	67.44	CL	35	2.97
180	70	102	SiCL	33	4.60
180	80	78.56	SiCL	33	3.54
180	90	83.08	SiCL	33	3.74
180	100	92.44	SiL	14	5.39
180	110	115.52	SiL	14	6.74
180	120	119.28	SiCL	33	5.38
180	130	93.88	SiL	14	5.47
180	140	105.68	SiL	14	6.16
180	150	151.8	SiL	14	8.85
180	160	132.32	SiL	14	7.72
180	170	130.16	SiL	14	7.59
180	180	149.72	SiL	14	8.73
180	190	160.6	SiL	14	9.37
180	200	158.96	SiL	14	9.27
190	0	70.4	CL	35	3.10
190	10	100.72	CL	35	4.44
190	20	54.88	SiCL	33	2.46
190	30	51.08	SiCL	33	2.29
190	40	50.92	SCL	27	2.45
190	50	48.44	SCL	27	2.33
190	60	96.96	SiCL	33	4.37
190	70	82.6	SiCL	33	3.72
190	80	143.84	SiCL	33	6.49
190	90	138.68	SiL	14	8.09
190	100	129.8	SiL	14	7.57
190	110	147.12	SiCL	33	6.64
190	120	131.08	SiCL	33	5.91
190	130	92.52	SiCL	33	4.17
190	140	122.52	SiL	14	7.14
190	150	141.88	SiL	14	8.28
190	160	154.96	SiL	14	9.04
190	170	124.56	SiL	14	7.26
190	180	158.16	SiL	14	9.23
190	190	154.68	SiL	14	9.02
190	200	157.4	SiL	14	9.18

Appendix 8.1.5 (Continued)

Grid X	Grid Y	ECa (mS/m)	Soil Type	~% Clay	EC$_e$ (dS/m)
200	10	50.68	SCL	27	2.44
200	20	58.88	SiCL	33	2.64
200	30	75.32	SiCL	33	3.39
200	40	39.36	SiCL	33	1.76
200	50	41.28	SCL	27	1.98
200	60	51.24	SCL	27	2.47
200	70	125.44	SCL	27	6.07
200	80	154.24	SCL	27	7.46
200	90	146.12	SiL	14	8.52
200	100	79.76	SiCL	33	3.59
200	110	133.64	SiCL	33	6.03
200	120	138.84	SiL	14	8.10
200	130	94.08	SiL	14	5.48
200	140	90.8	SiL	14	5.29
200	150	136.24	SiL	14	7.95
200	160	154.52	SiL	14	9.01
200	170	141.52	SiL	14	8.25
200	180	152.64	SiL	14	8.90
200	190	157.64	SiL	14	9.20
200	200	150.72	SiL	14	8.79

8.2 Data from Laboratory Experiments

8.2.1 Bulk Density and Porosity Data

APPENDIX 8.2.1
Bulk Density (g/cm^3) and Saturated Water Content (cm^3/ cm^3)

Station I.D.	ρ_b	θsat	Station I.D.	ρ_b	θsat	Station I.D.	ρ_b	θsat
N-65.0	1.22	0.541	S-0.5	1.32	0.503	E-30.0	1.35	0.492
N-50.0	1.31	0.504	S-1.0	1.34	0.494	E-60.0	1.4	0.471
N-38.0	1.32	0.503	S-1.5	1.22	0.541	E-75.0	1.3	0.508
N-36.5	1.21	0.543	S-2.0	1.32	0.5	E-90.0	1.33	0.498
N-35.0	1.23	0.535	S-3.5	1.3	0.508	W-15.0	1.29	0.512
N-33.5	1.25	0.527	S-5.0	1.27	0.521	W-30.0	1.4	0.471
N-32.0	1.24	0.534	S-6.5	1.42	0.465	W-45.0	1.33	0.498
N-30.5	1.33	0.499	S-8.0	1.34	0.493	W-60.0	1.26	0.523
N-29.0	1.33	0.497	S-9.5	1.35	0.491	W-75.0	1.35	0.491
N-27.5	1.22	0.541	S-11.0	1.23	0.537	NE-18.0	1.16	0.563
N-26.0	1.3	0.509	S-12.5	1.22	0.54	NE-36.0	1.17	0.557
N-24.5	1.31	0.504	S-14.0	1.39	0.476	NE-54.0	1.19	0.55
N-23.0	1.31	0.504	S-15.5	1.33	0.497	NE-72.0	1.33	0.499
N-21.5	1.34	0.495	S-17.0	1.27	0.522	NE-90.0	1.41	0.469
N-20.0	1.38	0.479	S-18.5	1.37	0.485	NE-108.0	1.32	0.5
N-18.5	1.28	0.517	S-20.0	1.32	0.503	NE-126.0	1.26	0.524
N-17.0	1.27	0.521	S-21.5	1.28	0.515	SE-18.0	1.15	0.565
N-15.5	1.32	0.501	S-23.0	1.23	0.536	SE-36.0	1.18	0.555
N-14.0	1.3	0.508	S-24.5	1.33	0.498	SE-54.0	1.26	0.526
N-12.5	1.26	0.525	S-26.0	1.33	0.498	SE-72.0	1.23	0.535
N-11.0	1.31	0.506	S-27.5	1.19	0.552	SE-90.0	1.3	0.509
N-9.5	1.27	0.52	S-29.0	1.26	0.525	SE-108.0	1.26	0.526
N-8.0	1.25	0.527	S-30.5	1.37	0.484	SE-126.0	1.29	0.512
N-6.5	1.22	0.54	S-32.0	1.31	0.506	SW-18.0	1.27	0.52
N-5.0	1.26	0.526	S-33.5	1.24	0.534	SW-36.0	1.21	0.545
N-3.5	1.3	0.508	S-35.0	1.21	0.543	SW-90.0	1.28	0.517
N-2.0	1.27	0.52	S-36.5	1.24	0.533	SW-126.0	1.29	0.513
N-1.5	1.22	0.54	S-38.0	1.19	0.551	NW-18.0	1.33	0.498
N-1.0	1.28	0.516	S-50.0	1.2	0.548	NW-36.0	1.2	0.549
N-0.5	1.3	0.51	S-65.0	1.29	0.513	NW-54.0	1.31	0.505
N-0.0	1.3	0.511	E-15.0	1.22	0.54	NW-72.0	1.26	0.526
						NW-108.0	1.15	0.567

8.2.2 Water Retention Data

Appendix 8.2.2

Water retention data from hanging column experiment.
See section 3.2.2 for details of experimental methods.

Sample	SW54	W90	SW108	SW72	NW90	S38	E45	W105	E105
ψ(cm)	θ_v	θ_v	θ_v	θ_v	θ_v	θ_v	θ_v	θ_v	θ_v
0	0.440	0.483	0.510	0.441	0.492	0.517	0.515	0.447	0.542
2	0.433	0.477	0.502	0.420	0.484	0.514	0.510	0.441	0.526
3	0.432	0.475	0.500	0.420	0.483	0.511	0.509	0.441	0.524
4	0.432	0.474	0.500	0.420	0.483	0.509	0.506	0.441	0.522
6	0.432	0.474	0.500	0.420	0.483	0.508	0.504	0.440	0.522
10	0.432	0.474	0.499	0.419	0.482	0.505	0.501	0.437	0.522
15	0.432	0.469	0.495	0.419	0.481	0.503	0.500	0.435	0.520
20	0.432	0.464	0.465	0.418	0.480	0.499	0.499	0.435	0.517
30	0.431	0.445	0.441	0.417	0.471	0.499	0.499	0.417	0.487
40	0.421	0.428	0.419	0.410	0.438	0.492	0.496	0.397	0.455
50	0.395	0.401	0.402	0.398	0.418	0.464	0.490	0.371	0.428
60	0.371	0.380	0.388	0.384	0.413	0.450	0.486	0.349	0.407
70	0.353	0.361	0.373	0.364	0.396	0.450	0.483	0.331	0.390
80	0.332	0.344	0.361	0.344	0.391	0.434	0.482	0.311	0.386
90	0.320	0.329	0.349	0.325	0.389	0.430	0.477	0.287	0.386
100	0.310	0.316	0.347	0.314	0.383	0.428	0.472	0.273	0.386
110	0.300	0.305	0.346	0.299	0.382	0.426	0.448	0.258	0.351
120	0.292	0.294	0.345	0.288	0.380	0.425	0.343	0.246	0.345
130	0.286	0.286	0.344	0.279	0.378	0.424	0.334	0.236	0.339
140	0.280	0.279	0.343	0.271	0.377	0.422	0.328	0.229	0.334
150	0.274	0.272	0.342	0.263	0.374	0.394	0.321	0.220	0.328
160	0.272	0.265	0.341	0.255	0.373	0.337	0.316	0.215	0.323
170	0.270	0.260	0.340	0.250	0.370	0.310	0.310	0.210	0.320

8.3 Summary of Other Data Collected at the Las Nutrias Project Site

APPENDIX 8.3.1
Observation Well and Piezometer Data
(Meters above arbitrary datum)

Water levels in the observation wells and piezometers were measured regularly with an electric sounder. This appendix contains recordings of these measurements since February of 1994. Each level was measured with respect to an arbitrary datum which is located 100 m below a rod fixed to the fence in the extreme southwest corner of the west bench. Well locations are illustrated in Figure 2. The well number 1A refers to location number one, with the A referring to the type and depth of the well. The letter A indicates an observation well (all observation wells are 2 m deep). The letters B, C, and E indicate piezometers installed to nominal depths of 3 m, 5 m, and 7 m, respectively.

Well	2-14-94	2-28-94	3-17-94	3-25-94	4-01-94	4-11-94	4-18-94	5-04-94	5-14-94	5-25-94	6-01-94
1A	98.811	98.793	98.847	99.033	99.148	99.483	99.273	99.321	99.232	99.233	99.138
2A	98.808	98.800	98.891	99.048	99.251	99.431	99.283	99.305	99.256	99.283	99.163
3A	98.490	98.486	98.513	98.992	99.356	99.299	99.257	99.378	99.189	99.213	99.084
4A	98.827	98.832	98.927	99.098	99.235	99.518	99.325	99.401	99.292	99.252	99.203
5A	98.779	98.693	98.773	98.993	99.353	99.196	99.193	99.340	99.164	99.155	99.067
6A	98.892	98.885	99.095	99.082	99.235	99.454	99.274	99.356	99.237	99.215	99.165
7A	98.789	98.785	98.901	98.994	99.229	99.275	99.179	99.267	99.161	99.139	99.077
8A	98.808	98.792	98.838	98.961	99.290	99.149	99.142	99.305	99.115	99.107	99.027
9A	98.847	98.841	98.861	99.060	99.213	99.425	99.255	99.332	99.229	99.181	99.140
10A	98.815	98.784	98.815	99.020	99.226	99.309	99.117	99.293	99.201	99.152	99.096
11A	98.777	98.759	98.884	98.933	99.159	99.204	99.112	99.212	99.095	99.083	99.016
12A	98.837	98.789	98.844	98.955	99.227	99.195	99.133	99.232	99.112	99.102	99.039
13A	98.843	98.839	98.951	98.973	99.261	99.180	99.116	99.218	99.107	99.100	99.027
14A	98.495	98.491	98.545	98.914	99.193	99.135	99.091	99.203	99.071	99.048	98.982
15A	98.513	98.518	98.604	98.937	99.252	99.147	99.124	99.257	99.113	99.044	99.006
16A	98.624	98.616	98.693	98.939	99.261	99.125	99.116	99.283	99.087	99.071	98.995
17A	98.768	98.773	98.803	99.032	99.209	99.311	99.202	99.279	99.180	99.179	99.112
18A	98.810	98.793	98.859	98.922	99.223	99.084	99.053	99.200	99.030	99.047	98.958
19A	98.917	98.911	98.981	99.001	99.219	99.271	99.132	99.201	99.134	99.151	99.075
20A	98.852	98.827	98.877	98.943	99.218	99.176	99.069	99.149	99.073	99.117	99.020
21A	98.779	98.775	98.954	98.889	99.178	99.094	99.009	99.094	99.012	99.062	98.957
22A	98.871	98.872	98.980	98.915	99.213	99.103	99.025	99.120	99.032	99.082	98.972
23A	98.850	98.835	98.967	98.919	99.233	99.093	99.024	99.110	99.039	99.082	98.967
24A	98.872	98.846	98.961	98.970	99.288	99.144	99.082	99.173	99.077	99.132	99.010
25A	98.810	98.813	98.849	98.882	99.319	99.025	98.985	99.098	98.980	99.039	98.929
26A	98.755	98.769	98.866	98.876	99.380	99.004	98.976	99.083	98.958	99.074	98.910
27A	97.914	97.910	98.192	97.966	99.179	99.253	99.111	99.186	99.099	99.140	99.044
28A	98.790	98.785	98.920	98.917	---------	99.125	99.034	99.126	99.052	99.100	98.984
30A	98.446	98.439	98.578	98.830	99.211	99.183	99.059	99.125	99.076	99.107	99.034
32A	98.624	98.604	98.699	98.733	98.833	98.846	98.831	98.871	98.847	98.917	98.826
33A	98.451	98.446	98.541	98.583	98.736	98.678	98.669	98.718	98.686	98.778	98.658
34A	98.350	98.318	98.478	98.487	98.660	98.566	98.577	98.663	98.594	98.679	98.566

APPENDIX 8.3.1 (continued)
Observation Well and Piezometer Data
(Meters above arbitrary datum)

Well	2-14-94	2-28-94	3-17-94	3-25-94	4-01-94	4-11-94	4-18-94	5-04-94	5-14-94	5-25-94	6-01-94
1B	98.857	98.838	98.900	99.067	99.174	99.519	99.300	99.361	99.254	99.234	99.165
3B	98.480	98.474	98.504	99.011	99.382	99.307	99.167	99.404	99.216	99.231	99.101
11B	98.815	98.807	98.906	98.910	99.235	99.275	99.177	99.286	99.181	99.137	99.079
14B	98.704	98.683	98.733	98.987	99.269	99.216	99.166	99.278	99.188	99.132	99.058
21B	98.921	98.913	99.015	99.025	99.316	99.235	99.142	99.233	99.148	99.199	99.089
24B	98.724	98.720	98.857	98.910	99.217	99.082	99.011	99.118	99.005	99.065	98.954
32B	98.568	98.564	98.647	98.679	98.788	98.792	98.825	98.822	98.797	98.873	98.765
34B	98.281	98.278	98.310	98.448	98.626	98.533	98.660	98.575	98.544	98.629	98.525
1C	98.993	98.984	99.080	99.183	99.284	99.630	99.419	99.478	99.374	99.358	99.282
3C	98.478	98.484	98.536	98.991	99.366	99.297	99.239	99.392	99.203	99.205	99.087
11C	98.866	98.859	98.930	99.046	99.275	99.323	99.217	99.321	99.217	99.183	99.124
21C	98.735	98.736	98.841	98.845	99.136	99.053	98.965	99.061	98.975	99.020	98.910
24C	98.643	98.293	98.346	98.823	99.132	98.995	98.929	99.034	98.925	98.809	98.866
32C	98.557	98.538	98.632	98.668	98.772	98.784	98.856	98.803	98.783	98.860	98.754
34C	98.391	98.379	98.482	98.542	98.711	98.634	98.623	98.660	98.640	98.731	98.613
1E	99.004	98.992	99.089	99.228	99.335	99.670	99.459	99.515	99.410	99.393	99.323
3E	98.523	98.501	98.551	99.039	99.332	99.221	99.240	99.365	99.207	99.222	99.102
11E	98.970	98.869	99.128	99.085	99.208	99.248	99.155	99.255	99.137	99.113	99.056
14E	98.653	98.649	98.708	98.884	99.162	99.110	99.062	99.175	99.048	99.030	98.955
21E	98.035	98.030	98.171	98.935	99.221	99.140	99.047	99.137	99.058	99.102	98.998
24E	98.643	98.634	98.678	98.835	99.149	99.016	98.941	99.054	98.946	98.994	98.888
32E	98.508	98.492	98.571	98.631	98.731	98.744	98.735	98.777	98.756	98.825	98.714
34E	98.593	98.582	98.683	98.702	98.869	98.795	98.789	98.726	98.806	98.895	98.780

Well	6-07-94	6-09-94	7-7-94	7-19-94	9-7-94	9-12-94	9-24-94	10-4-94	10-23-94	11-6-94	12-4-94	12-17-94
1A	99.422	99.464	99.309	99.580	99.141	99.112	99.076	99.124	99.033	99.028	98.980	98.947
2A	99.339	99.436	99.375	99.540	99.169	99.124	99.073	99.116	99.021	99.010	98.923	98.901
3A	99.419	99.337	99.237	99.472	99.091	99.019	98.989	99.018	98.932	98.912	98.834	98.788
4A	99.370	99.563	99.362	99.649	99.222	99.175	99.153	99.171	99.102	99.098	99.029	99.016
5A	99.156	99.285	99.192	99.343	99.081	99.005	99.003	99.004	98.918	98.912	98.835	98.793
6A	99.334	99.546	99.307	99.564	99.200	99.137	99.127	99.148	99.065	99.081	99.023	99.002
7A	99.169	99.424	99.226	99.366	99.099	99.031	99.029	99.061	98.954	98.954	98.898	98.864
8A	99.088	99.291	99.145	99.282	99.034	98.963	98.958	98.966	98.873	98.885	98.806	98.770
9A	99.293	99.519	99.378	99.530	99.175	99.096	99.092	99.136	99.029	99.037	98.975	98.945
10A	99.207	99.450	99.239	99.403	99.110	99.043	99.042	99.057	98.963	98.974	98.900	98.873
11A	99.106	99.366	99.159	99.295	99.902	98.966	98.952	98.980	98.880	98.889	98.819	98.787
12A	99.113	99.391	99.180	99.300	99.045	98.981	98.974	99.010	98.903	98.919	98.842	98.803
13A	99.098	99.382	99.165	99.317	99.035	98.966	98.965	98.996	98.891	98.904	98.828	98.788
14A	99.042	99.306	99.116	99.233	98.990	98.920	98.927	98.948	98.841	98.851	98.783	98.736
15A	99.076	99.307	99.129	99.257	99.017	98.948	98.947	98.971	98.857	-------	98.798	98.752
16A	99.059	99.273	99.122	99.252	-------	-------	98.949	98.973	98.859	98.867	-------	98.751
17A	99.340	99.533	99.264	99.396	99.137	99.068	99.086	99.083	98.993	99.024	98.955	98.916
18A	99.032	99.312	99.100	99.190	98.968	98.870	98.909	98.901	98.808	98.816	98.754	98.708
19A	99.443	99.530	99.234	99.255	99.087	99.009	99.081	99.022	98.940	98.983	98.896	98.860
20A	99.186	99.546	99.179	99.192	100.027	98.943	99.005	98.954	98.876	98.914	98.834	98.797
21A	99.073	99.498	99.117	99.123	99.032	98.915	98.932	98.901	98.804	98.835	98.759	98.721
22A	99.055	99.546	99.145	99.151	98.982	98.891	98.940	98.855	98.822	98.860	98.783	98.742
23A	99.056	99.594	99.160	99.155	98.984	98.984	98.944	98.919	98.824	98.856	98.779	98.739
24A	99.105	99.574	99.182	99.198	99.028	98.921	98.978	98.951	98.866	98.889	98.829	98.784
25A	98.983	99.614	99.151	99.104	98.950	98.827	98.886	98.864	88.773	98.802	98.736	98.696
26A	98.964	99.608	99.189	99.108	99.047	98.836	98.871	98.855	98.757	98.785	98.723	98.674
27A	99.438	99.516	99.221	99.239	99.071	98.982	99.059	99.007	98.926	98.959	98.882	98.843
28A	99.110	-------	99.156	99.159	99.083	98.908	98.961	98.924	98.839	-------	98.791	98.754
30A	99.255	99.539	99.226	99.116	99.031	98.959	99.090	98.965	98.894	98.931	98.859	98.827
32A	98.990	98.998	98.906	98.686	98.711	98.675	98.755	98.648	98.650	98.633	98.640	98.641
33A	98.720	99.071	98.768	98.539	98.561	98.505	98.542	98.511	98.492	98.485	98.484	98.475
34A	98.573	99.040	98.663	98.443	98.466	98.449	98.438	98.414	98.394	98.385	98.382	98.380
1B	99.341	99.489	99.337	99.602	99.162	99.124	99.097	99.141	99.052	99.041	98.789	98.962
3B	99.422	99.353	99.256	99.493	99.115	99.033	99.010	99.035	98.947	98.922	98.838	98.802
11B	99.169	99.420	99.228	99.366	99.096	99.023	99.023	99.056	98.948	98.943	98.878	98.848
14B	99.124	99.376	99.189	99.318	99.052	98.994	98.996	99.049	98.917	98.919	98.853	98.811
21B	99.220	99.631	99.248	99.260	99.096	98.888	99.071	99.025	98.941	98.977	98.899	98.863
24B	99.029	99.502	99.120	99.138	98.960	98.862	98.927	98.901	98.802	98.829	98.744	98.720
32B	98.927	98.937	98.845	98.626	98.650	98.468	98.690	98.598	98.587	98.579	98.572	98.576
34B	98.533	99.032	-------	98.418	98.432	98.524	98.410	98.381	98.353	98.345	98.337	98.333
1C	99.468	99.631	99.466	99.730	99.287	99.247	99.223	99.258	99.177	99.102	99.083	99.084
3C	99.407	99.342	99.238	99.477	99.095	99.015	98.992	99.020	98.928	98.900	98.820	98.786
11C	99.217	99.463	99.268	99.406	99.136	99.061	99.064	99.087	98.993	98.986	98.931	98.907
21C	99.034	99.460	99.062	99.077	98.915	98.892	98.883	98.850	98.754	98.792	98.705	98.670
24C	98.944	99.405	99.033	99.406	98.870	98.873	98.827	98.784	98.709	98.734	98.666	98.627
32C	98.915	98.917	98.828	98.612	98.638	98.520	98.684	98.574	98.574	98.559	98.557	98.564
34C	98.605	99.074	98.720	98.498	98.514	98.522	98.489	98.461	98.441	98.030	98.429	98.426
1E	99.509	99.643	99.495	99.754	99.322	99.284	99.256	99.291	99.214	99.196	99.123	99.127
3E	99.337	99.383	99.275	99.468	99.108	99.040	99.022	99.079	98.960	98.921	98.846	98.813
11E	99.147	99.399	99.199	99.336	99.073	98.999	98.996	99.030	98.850	98.913	98.899	98.831
14E	99.022	99.277	99.088	99.206	98.958	98.879	98.877	98.918	98.805	98.814	98.729	98.701
21E	99.112	99.533	99.152	99.167	99.000	98.905	98.971	98.940	98.841	98.882	98.204	98.763
24E	98.957	99.418	99.057	99.063	98.890	98.068	98.846	98.833	98.727	98.757	98.682	98.650
32E	98.885	98.881	98.792	98.576	98.600	98.473	98.641	98.538	98.537	98.529	98.517	98.525
34E	98.787	99.241	98.879	98.661	98.678	98.536	98.647	98.630	98.606	97.999	98.593	98.588

APPENDIX 8.3.2

Tile Drain Discharge Data
West Manhole
Rates expressed in liters per minute (lpm)

Tile drain discharge rates were measured in a simple fashion. The west manhole outlet was closed and water was pumped from the west manhole until the water level in the manhole was at a steady level. At this time it was assumed that the pumping rate was equal to the flow rate from the tile drain into the manhole. The water being pumped was then captured in a large graduated cylinder during a specific time period and thus the rates listed below were calculated.

Date	Flow Rate (lpm)
07-Jan-94	12
18-Jan-94	7
11-Feb-94	6.8
28-Feb-94	6.5
09-Mar-94	6.6
11-Mar-94	60
25-Mar-94	120
24-Apr-94	130
11-Mar-94	52
25-Mar-94	100
24-Apr-94	100
16-May-94	54

8.3.3 Irrigation Measurements

The weir used to estimate irrigation flow rates consisted of a 10-in outer diameter pipe installed axially inside a trapezoidal irrigation canal with 45° side slopes. The presence of the pipe reduced the cross-sectional area of the flow, creating a critical-flow condition. A gage was installed at the upstream side of the pipe to measure the depth of the water upstream of the critical flow section. The reading on the gage is directly related to the rate. The algorithm for calculating flow rates is described in an article entitled, "Measuring Water In Trapezoidal Canals", by Zohrab Samani, which was published in the Journal of Irrigation and Drainage Engineering, Vol. 119, No. 1, January/February, 1993. A computer model was developed for the calibration of the circular weir. The calibration model was based on parameters measured in the laboratory and was tested using data from flumes installed in the field.

APPENDIX 8.3.3
Irrigation Measurements
(Water depths measured at upstream circular weir gauge)
(Total gallons applied shown in bold)

Irrigation Date: June 8, 1994						
time	depth (cm)	flow rate (gpm)	elapsed time (min)	increment flow (gal)	cumulative flow (gal)	cumulative %
10:57	23.6	632	1	632	632	0.1
11:01	42.5	2553	4	10214	10846	1.0
11:03	45.8	3061	2	6122	16968	1.6
11:04	47.7	3379	1	3379	20347	1.9
11:05	48.5	3518	1	3518	23865	2.2
11:06	49.4	3680	1	3680	27545	2.5
11:07	49.6	3716	1	3716	31261	2.9
11:09	51.0	3977	2	7955	39215	3.6
11:11	51.5	4073	2	8146	47361	4.3
11:12	51.5	4073	1	4073	51435	4.7
11:13	51.5	4073	1	4073	55508	5.1
11:14	51.5	4073	1	4073	59581	5.4
11:15	51.5	4073	1	4073	63654	5.8
11:18	51.7	4112	3	12336	75990	7.0
11:19	51.9	4151	1	4151	80141	7.3
11:20	52.1	4190	1	4190	84331	7.7
11:22	51.9	4151	2	8302	92633	8.5
11:26	51.9	4151	4	16604	109237	10.0
11:30	51.9	4151	4	16604	125840	11.5
11:45	52.1	4190	5	20951	146791	13.4
12:00	52.1	4190	15	62852	209643	19.2
12:15	52.2	4210	15	63147	272790	25.0
12:30	52.0	4170	15	62557	335348	30.7
12:45	52.2	4210	15	63147	398495	36.5
13:00	52.3	4230	15	63443	461938	42.3
13:15	52.3	4230	15	63443	525382	48.1
13:30	52.6	4289	15	64337	589719	53.9
13:40	52.4	4249	10	42494	632213	57.8
13:47	52.1	4190	7	29331	661543	60.5
14:10	52.1	4190	23	96373	757916	69.3
14:15	52.2	4210	5	21049	778966	71.3
14:30	52.4	4249	15	63741	842706	77.1
14:45	52.3	4230	15	63443	906150	82.9
15:00	52.0	4170	15	62557	968707	88.6
15:15	51.8	4131	15	61971	1030678	94.3
15:30	52.0	4170	15	62557	**1093235**	100.0

130

APPENDIX 8.3.3 (continued)
Irrigation Measurements
(Water depths measured at circular weir upstream gauge)
(Total gallons applied shown in bold)

time	depth (cm)	flow rate (gpm)	elapsed time (min)	increment flow (gal)	cumulative flow (gal)	cumulative %
Irrigation Date: June 27, 1994
12:00	45.3	2980	1	2980	2980	0.2
12:15	45.8	3061	15	45912	48892	4.1
12:30	45.8	3061	15	45912	94805	7.9
12:45	45.8	3061	15	45912	140717	11.7
13:00	45.6	3028	15	45427	186143	15.5
13:15	45.4	2996	15	44945	231088	19.2
13:30	44.7	2885	15	43282	274370	22.8
13:45	44.3	2823	15	42348	316718	26.3
14:00	44.0	2777	15	41657	358375	29.8
14:15	43.3	2671	15	40070	398444	33.1
14:30	45.9	3077	15	46156	444600	36.9
14:45	44.0	2777	15	41657	486257	40.4
15:00	43.6	2716	15	40745	527002	43.8
15:15	43.6	2716	15	40745	567747	47.1
15:30	43.5	2701	15	40519	608266	50.5
15:45	43.5	2701	15	40519	648785	53.9
16:00	44.0	2777	15	41657	690442	57.3
16:15	44.0	2777	15	41657	732099	60.8
16:30	44.2	2808	15	42117	774216	64.3
16:45	44.2	2808	15	42117	816333	67.8
17:00	44.2	2808	15	42117	858450	71.3
17:15	44.2	2808	15	42117	900567	74.8
17:30	44.7	2885	15	43282	943849	78.4
17:45	44.7	2885	15	43282	987130	82.0
18:00	44.7	2885	15	43282	1030412	85.6
18:15	44.7	2885	15	43282	1073693	89.2
18:30	44.8	2901	15	43517	1117210	92.8
18:45	44.8	2901	15	43517	1160727	96.4
19:00	44.8	2901	15	43517	**1204244**	100.0

Irrigation Measurements
(Water depths measured at circular weir upstream gauge)
(Total gallons applied shown in bold)

Irrigation Date: August 8, 1994						
time	depth (cm)	flow rate (gpm)	elapsed time (min)	increment flow (gal)	cumulative flow (gal)	cumulative %
11:53	46.4	3159	1	3159	3159	0.2
12:00	53.8	4533	8	36260	39420	2.9
12:15	54.0	4574	15	68609	108029	8.0
12:30	54.1	4595	15	68921	176949	13.1
12:45	54.4	4657	15	69860	246810	18.3
13:00	54.3	4636	15	69546	316356	23.5
13:15	54.2	4616	15	69233	385589	28.6
13:30	53.8	4533	15	67988	453577	33.7
13:45	54.6	4699	15	70491	524069	38.9
14:00	53.7	4512	15	67679	591748	43.9
14:15	54.2	4616	15	69233	660981	49.1
14:30	54.6	4699	15	70491	731472	54.3
14:45	53.8	4533	15	67988	799461	59.4
15:00	53.0	4369	15	65541	865001	64.2
15:15	52.1	4190	15	62852	927853	68.9
15:30	51.6	4093	15	61388	989241	73.5
15:45	51.0	3977	15	59659	1048900	77.9
16:00	50.8	3939	15	59089	1107989	82.3
16:15	50.4	3864	15	57960	1165949	86.6
16:30	49.8	3753	15	56291	1222239	90.8
16:45	50.0	3790	15	56844	1279083	95.0
17:00	43.8	2747	15	41199	1320282	98.0
17:15	30.8	1181	15	36359	**1356642**	99.8

Irrigation Measurements
(Water depths measured at circular weir upstream gauge)
(Total gallons applied shown in bold)

September 28, 1994						
time	depth (cm)	flow rate	elapsed time	increment flow	cumulative	cumulative %
11:35	35.0	1601	5	8005	8005	0.5
11:38	39.0	2075	3	6226	14230	0.9
11:40	41.0	2341	2	4682	18913	1.2
11:43	42.0	2481	3	7444	26357	1.7
11:45	43.0	2627	2	5253	31610	2.0
11:55	45.5	3012	5	15062	46672	3.0
12:00	47.0	3259	5	16297	62969	4.1
12:10	47.5	3344	10	33444	96413	6.2
12:15	48.5	3518	15	52776	149188	9.6
12:30	49.8	3753	15	56291	205479	13.2
12:45	50.5	3883	15	58241	263720	17.0
13:00	51.5	4073	15	61098	324817	20.9
13:15	51.5	4073	15	61098	385915	24.9
13:30	51.5	4073	15	61098	447013	28.8
13:45	51.5	4073	15	61098	508110	32.7
14:00	51.0	3977	15	59659	567769	36.6
14:15	51.0	3977	15	59659	627428	40.4
14:30	51.0	3977	15	59659	687087	44.3
14:45	51.0	3977	15	59659	746745	48.1
15:00	51.0	3977	15	59659	806404	51.9
15:15	51.5	4073	15	61098	867502	55.9
15:30	51.5	4073	15	61098	928599	59.8
15:45	51.5	4073	15	61098	989697	63.8
16:00	51.5	4073	15	61098	1050795	67.7
16:15	51.5	4073	15	61098	1111892	71.6
16:30	52.0	4170	15	62557	1174450	75.7
16:45	52.0	4170	15	62557	1237007	79.7
17:00	52.0	4170	15	62557	1299565	83.7
17:15	50.5	3883	15	58241	1357805	87.5
17:30	48.5	3518	15	52776	1410581	90.9
17:45	47.0	3259	15	48891	1459472	94.0
18:00	46.0	3093	15	46401	1505872	97.0
18:15	37.0	1829	15	27431	1533303	98.8
18:20	30.5	1154	5	5770	1539073	99.1
18:25	26.0	793	5	3963	1543036	99.4
18:30	22.0	538	5	2688	1545724	99.6
18:35	19.0	384	5	1921	1547645	99.7
18:40	17.0	299	5	1494	1549139	99.8
18:45	15.0	226	5	1129	1550268	99.9
18:50	13.0	165	5	824	1551091	99.9
18:55	12.0	138	5	692	1551783	100.0
19:00	11.0	115	5	573	**1552356**	100.0

8.3.4 Precipitation Measurements

Measurements in Appendix 8.3.4 represent rainfall that occurred on the date listed in the table. Gauges were located at each of the manholes and at the north end of the center bench.

APPENDIX 8.3.4
Precipitation

Date	Gauge Location		
	North (mm)	West (mm)	East (mm)
08-Mar-94	8.4	5.4	7.0
11-Mar-94	6.4	6.2	6.2
22-Mar-94	2.4	2.3	2.2
29-Mar-94	1.4	1.4	1.4
11-May-94	12.2	11.8	12.5
22-May-94	1.2	1.2	1.2
23-May-94	11.2	11.0	11.3
28-May-94	5.8	5.6	6.0
02-Jun-94	1.4	1.6	1.2
25-Jul-94	2.8	3.2	3.2
27-Jul-94	16.0	15.7	16.1
29-Jul-94	10.6	11.0	10.5
01-Aug-94	4.0	4.2	4.0
03-Aug-94	0.6	0.5	0.4
15-Aug-94	38.4	38.4	38.2
30-Aug-94	19.1	16.8	20.5
31-Aug-94	16.4	19.8	4.4
03-Sep-94	29.9	27.6	27.6
07-Sep-94	17.1	17.7	17.1
11-Sep-94	0.3	0.3	0.3
17-Sep-94	7.8	7.3	6.5
21-Sep-94	0.2	0.2	0.2
15-Oct-94	23.7	24.6	23.2
04-Oct-94	0.2	1.6	1.4
04-Dec-94	27.4	27.0	23.0
17-Dec-94	21.0	22.3	20.6

8.4 FORTRAN Code for the Analysis of Infiltration Data

```
integer ndata,n

    real Qdata(150,4),K0,K1a,K1b,K2a,K2b,K3,a,b

    open(unit=30,file='inrate.dat')

    open(unit=31,file='inrate.out')

    ndata=1

    do while(.true.)

        read(30,*,end=15) Qdata(ndata,1),Qdata(ndata,2),

    +    Qdata(ndata,3),Qdata(ndata,4)

        ndata=ndata+1

    enddo

15 continue

    close(30)

    ndata=ndata-1

    print*,ndata,' data points in file '

    do n=1,ndata

        call picard(Qdata(n,1),Qdata(n,2),a,b,3.)

        K0=a

        K1a=b

        call Picard(Qdata(n,2),Qdata(n,3),a,b,3.)

        K1b=a

        K2a=b

        call Picard(Qdata(n,3),Qdata(n,4),a,b,9.)
```

```fortran
      K2b=a

      K3=b

      write(31,5) K0,K1a,K1b,K2a,K2b,K3
c        write(*,5)  K0,K1a,K1b,K2a,K2b,K3

      enddo

    5 format(6E10.3)

      print*,ndata,' data locations'

      end



      subroutine picard(Q0,Q1,K0,K1,dY)

      integer n

      real Q0,Q1,K0,K0old,K1,K1old,A,r,pi,dY,tmp1,tmp2

      pi=4*atan(1)

      A=1

      n=1

      r=4.1

      K0old=0

      K1old=0
C     print*,'enter data as Q0,Q1,Y0,Y1'

C     read(*,*) Q0,Q1,Y0,Y1

      if(Q0.eq.Q1) then

        print*,'*******'

        K0=777
```

```fortran
          K1=777

          return

        endif

10    continue

          K0=Q0/(pi*r**2+4*r/A)

          K1=Q1/(pi*r**2+4*r/A)

          A=2*(K0-K1)/(dY*(K0+K1))

          n=n+1

          tmp1=abs(K0-K0old)

          tmp2=abs(K1-K1old)

          K0old=K0

          K1old=K1
c         print*,tmp1,tmp2

          if(tmp1.gt.1E-7.or.tmp2.gt.1E-7) go to 10
c     print*,'converged in ',n,'iterations'
c     print*,'K0 = ',K0
c     print*,'K1 = ',K1

        return

        end
```